

**DAMPING ENHANCEMENT OF MULTIMACHINE
POWER SYSTEM THROUGH STATCOM CONTROL**

BY

SYED FAIZULLAH FAISAL

A Thesis Presented to the
DEANSHIP OF GRADUATE STUDIES

KING FAHD UNIVERSITY OF PETROLEUM & MINERALS
DHAHRAN, SAUDI ARABIA

In Partial Fulfillment of the
Requirements for the Degree of

MASTER OF SCIENCE

In

ELECTRICAL ENGINEERING

MARCH, 2005

KING FAHD UNIVERSITY OF PETROLEUM AND MINERALS
DHAHRAN 31261, SAUDI ARABIA

DEANSHIP OF GRADUATE STUDIES

This thesis, written by SYED FAIZULLAH FAISAL under the direction of his Thesis Advisor and approved by his Thesis Committee, has been presented to and accepted by the Dean of Graduate Studies, in partial fulfillment of the requirements for the degree of **MASTER OF SCIENCE IN ELECTRICAL ENGINEERING.**

Thesis Committee

A. H. Rahim

Dr. Abu Hamed M. Abdur-Rahim (Chairman)

[Signature]

Dr. Samir A. Al - Baiyat (Member)

J. M. Bakhshwain

Dr. Jamil M. Bakhshwain (Member)

[Signature]

Dr. Ibrahim M. El - Amin (Member)

[Signature]

Dr. Mohammad A. Abido (Member)

J. M. Bakhshwain

Dr. Jamil M. Bakhshwain
Department Chairman

[Signature]

Dr. Mohammed Abdul Aziz Al-Ohali
Dean of Graduate Studies

10 July 2005

Date



Dedicated
to
My Father, Mother
and
Brothers, Sisters

ACKNOWLEDGMENTS

In the name of Allah, Most Gracious, Most Merciful.

“Read! In the name of your lord and Cherisher, Who has created (all that exists). He has created man from a clot (a piece of thick coagulated blood). Read! And your Lord is the Most Generous. Who has taught (the writing) by the pen. Taught man that which he knew not. Nay! Verily, man does transgress (in disbelief and evil deed). Because he considers himself self – sufficient. Surely, unto your lord is the return.” (Surah 96. Al-’Alaq. The Holy Quran)

All praise and glory be to Almighty Allah subhanhowa tala who gave me the courage and patience to carry out this work, and peace and blessings of Allah be upon his last prophet Mohammed.

I am deeply indebted to my thesis advisor Dr. Abu Hamed Abdur-Rahim for his constant support, guidance, encouragement and constructive criticism through out the course of this research. I will always revere his patience, expert guidance and ability to solve intricate problems. He made my pursuit of higher education a truly enjoyable and unforgettable experience. At the later stages he helped me a lot in writing my thesis.

I would also like to thank my committee members Dr. Samir A. Al-Baiyat, Dr. Jamil M. Bakhawain, Dr. Ibrahim, El-Amin and Dr. M. A. Abido for their

encouragement, cooperation and for spending their time reading my thesis and for their constructive comments and suggestions.

I am thankful to Dr. Samir A. Al-Baiyat, Dean, College of engineering sciences, for taking out time from his busy schedule to explain me the concepts of model reduction.

I am thankful to Dr. Jamil M. Bakhashwain, Chairman EE dept, for providing an excellent environment of research in the department.

Acknowledgement is due to King Fahd University of Petroleum & Minerals for supporting my M.S. studies and this research work.

A special thanks goes to Mr. M. Baber Abbas whom I have known for more than eight years now and who showed to be a kind, mostly helpful and trustful friend. I am also thankful to my friends Ahmed Aleemuddin, Masood Ali, Amer Baig, Riyaz Ali, Anees Ahmed, Abdul Hameed, Kashif, Ismail, Siraj, Ayub, Khaja, Awes, Abbas, Baba, Aleem, Mazher, Waseem, Ilyas, Farooq, Hafeez, Gayazullah, Fareed, Mayowa, Moosa, and my 92 Ma-tam members. I am thankful to Mr. Fareed Kandlawala, lecturer EE dept for his help and support. Thanks are also due to Indo-kfupm community which made me feel at home.

Lastly but not the least, thanks must go out to my parents, brothers and sisters for their tireless support, encouragement and prayers in all my endeavors. Their knowledge, sacrifice and love, has helped me achieve all my goals to date.

TABLE OF CONTENTS

Acknowledgements	iii
List of Tables.....	ix
List of Figures	x
Nomenclature	xiv
Thesis Abstract	xvii
Thesis Abstract (Arabic)	xviii
Chapter 1	1
INTRODUCTION.....	1
1.1 Power system stability.....	1
1.2 FACTS devices.....	4
1.2.1 First generation of FACTS devices.....	6
1.2.2 Second Generation of FACTS devices.....	7
1.3 Damping enhancement through STATCOM	8
1.4 Scope of the thesis.....	9
Chapter 2	11
LITERATURE SURVEY	11
2.1 STATCOM for power system	11
2.2 STATCOM modeling for stability studies.....	14

2.3	STATCOM controller design for damping of system oscillation	15
2.4	Location of FACTS devices for damping enhancement	17
2.5	STATCOM in multi-machine system.....	19
Chapter 3		21
POWER SYSTEM MODEL WITH STATCOM		21
3.1	The single machine infinite bus system	22
	3.1.1 Synchronous generator and its excitation system	22
	3.1.2 The STATCOM system	24
3.2	The linearized equations	26
3.3	A multimachine power system	29
	3.3.1 The network equations	31
3.4	Linearized model of multimachine power system with STATCOM	39
	3.4.1 Linearized of the Synchronous Machine Model	39
	3.4.2 Linearization of exciter model	43
	3.4.3 Linearization of STATCOM model	45
Chapter 4		47
ROBUST CONTROL DESIGN BY GRAPHICAL AND PSO BASED LOOP-SHAPING TECHNIQUE		47
4.1	The robust controller design through graphical loop-shaping	48
	4.1.1 Uncertainty modeling	49

4.1.2	Robust stability and performance.....	50
4.1.3	Graphical loop-shaping technique.....	53
4.1.4	The Algorithm.....	54
4.2	The particle swarm optimization	56
4.2.1	The Algorithm.....	58
4.3	Robust control design through PSO based loop-shaping.....	59
4.3.1	The Algorithm.....	60
Chapter 5	63
SIMULATION RESULTS: SINGLE MACHINE CASE.....		63
5.1	Robust loop-shaping design using PSO	71
Chapter 6	79
SIMULATION RESULTS: MULTI MACHINE POWER SYSTEM.....		79
6.1	Reduced order model: manual graphical loop-shaping	81
6.2	Reduced order system: PSO based loop shaping	89
6.3	Detailed model: PSO based loop-shaping.....	98
6.4	Coordinated Design.....	109
Chapter 7	112
CONCLUSIONS AND FUTURE WORK.....		112
7.1	Recommendations for future research.....	114
APPENDIX A	115

APPENDIX B.....	119
APPENDIX C.....	137
APPENDIX D.....	156
REFERENCES.....	160

LIST OF TABLES

TABLE	Page
5.1 PSO Parameters	72
6.1 Nominal operating points for generator	82
6.2 Nominal loadings	82
6.3 PSO Parameters	89
6.4 Generator loadings	95
6.5 Loads	95
A.1 Nominal operating points for generator	116
A.2 Nominal loadings	117
A.3 Generator data for multimachine system	117
A.4 STATCOM data for multimachine system	118

LIST OF FIGURES

Figure	Page
2.1 General arrangement of STATCOM	13
3.1 STATCOM installed in SMIB power system	22
3.2 Block diagram of excitation system	23
3.3 Block diagram of the linearized system installed with STATCOM	28
3.4 Reduced multimachine system configuration showing the generators and STATCOMS	29
3.5 Two frames of reference for phasor quantities for a voltage V_{ti}	33
3.6 Configuration of the i -th generator in n – machine system	35
4.1 Unity feedback plant with controller	51
4.2 Feed back loop with uncertainty representation	52
4.3 Feed back loop in standard reduced form	52
4.4 Flow chart for robust control design by graphical method.....	55
4.5 Flow chart for the proposed PSO based loop-shaping.....	62
5.1 STATCOM installed in SMIB power system	64
5.2 Collapsed block diagram for robust C controller	65
5.3 Nominal and perturbed plant transfer functions for robust speed feedback system	67
5.4 The uncertainty profile and W_2	68

5.5	Graphical Loop-Shaping plots relating W_1 , W_2 and L	69
5.6	Robust and nominal performance criteria (graphical loop-shaping)	69
5.7	Rotor angle with robust controller for a disturbance of 50% Torque pulse for 0.1s	70
5.8	D.C. voltage variations corresponding to Fig. 5.7	71
5.9	PSO based Loop-Shaping plots relating W_1 , W_2 and L	73
5.10	Robust and nominal performance criteria (PSO based loop-shaping)	74
5.11	Comparison of generator rotor angle variations following a 50% input torque pulse (solid line is for graphical method and dotted line for automatic loop-shaping)	75
5.12	D.C. capacitor voltage variations of the STATCOM corresponding to Fig 5.11	76
5.13	Comparison of generator rotor angle variations following a 6 cycle 3 phase fault at remote bus	77
5.14	D.C. voltage corresponding to Fig. 5.13.....	78
6.1	Multimachine power system	80
6.2	Magnitude plots for original and reduced order systems	83
6.3	Phase plots for original and reduced order systems	83
6.4	Nominal and perturbed plants	85
6.5	Uncertainty profile	85
6.6	Loop-Shaping plots relating W_1 , W_2 and L (graphical method).....	86
6.7	Robust and nominal performance criteria (graphical method)	86
6.8	Relative speed deviations for 50% torque pulse on generator 2	87

6.9	Relative angles for 50% torque pulse on generator 2	88
6.10	Loop-Shaping plots relating W_1 , W_2 and L (PSO based loop-shaping).....	90
6.11	Robust and nominal performance criteria (PSO based loop-shaping)	91
6.12	Relative speed deviations for 50% torque pulse on generator 2	92
6.13	Relative angles for 50% torque pulse on generator 2	93
6.14	D.C. capacitor voltage corresponding to Fig. 6.12	94
6.15	Relative speed deviations for 50% torque pulse on generator 2	96
6.16	Relative angles for 50% torque pulse on generator 2	97
6.17	Loop-Shaping plots relating W_1 , W_2 and L (PSO based loop-shaping).....	99
6.18	Robust and nominal performance criteria (PSO based loop-shaping)	100
6.19	Relative speed deviations for 50% torque pulse on generator 2	101
6.20	Relative rotor angles for 50% torque pulse on generator 2	102
6.21	Relative speed deviations for 6 cycle 3 phase fault at network bus of generator 2	104
6.22	Relative rotor angles for 6 cycle 3 phase fault at network bus of generator 2	105
6.23	D.C. capacitor voltage for 6 cycle 3 phase fault at network bus of generator 2 ...	106
6.24	Relative speed deviations for 6 cycle 3 phase fault at network bus of generator 2	107
6.25	Relative rotor angles for 6 cycle 3 phase fault at network bus of generator 2	108
6.26	Multimachine power system installed with two STATCOM	109
6.27	Relative speed variations for generators 1 and 2 for cases a,b,c and uncontrolled case.....	110

6.28	Relative speed variations for generators 2 and 3 for cases a,b,c and uncontrolled case.....	111
6.29	Relative speed variations for generators 2 and 4 for cases a,b,c and uncontrolled case.....	111
A.1	Multimachine power system	116
C.1	Reduced multimachine system configuration showing the generators and STATCOMS.....	138
C.2	Configuration of the i-th generator in n – machine system.....	139

NOMENCLATURE

Symbols

X	Transmission line reactance
H	Inertia constant
M	Inertia coefficient, $M = 2H$
D	Damping coefficient
p.u.	Per unit quantities
pf	Power factor
P_e	Electrical power output from the machine
e_q	Internal voltage across x_q
V_t	Machine terminal voltage
P_m	Mechanical power output to the machine
ψ	Phase angle of the mid-bus voltage
m	Magnitude voltage of STATCOM control
e'_q	Internal voltage on q-axis proportional to field flux linkage
e'_d	Internal voltage on d-axis proportional to field flux linkage
E_{fd}	Generator field voltage
δ	Angle between q-axis and the infinite busbar

T'_{do}	Direct axis open-circuit field time constant
T'_{qo}	Quadrature axis open-circuit field time constant
K_A	Exciter gain
T_A	Exciter time constant
x_q	Quadrature axis reactance
x'_q	Quadrature axis transient reactance
x_d	Direct axis reactance
x'_d	Direct axis transient reactance
ω_o	Radian frequency
I_d, I_q	Armature current (I_t), direct and quadrature axis component
I_{sd}, I_{sq}	STATCOM current (I_s), direct and quadrature axis component
V_d, V_q	Armature voltage, direct and quadrature axis component
V_B	Infinite busbar voltage
V_L	STATCOM bus voltage or mid-bus voltage
\dot{g}	Derivative of g

Abbreviations

AC	Alternating current
DC	Direct current
FACTS	Flexible AC transmission system
SVC	Static var compenstor
TCSC	Thyristor controlled series capacitor
STATCOM	Static synchronous compensator
SSSC	Static synchronous series compensator
UPFC	Unified power flow controller
PID	Proportional-integral-derivative
PWM	Pulse width modulation
PSS	Power system stabilizer
GTO	Gate turn-off thyristor
VSC	Voltage-sourced converter
SMIB	Single machine infinite bus

THESIS ABSTRACT

Name: SYED FAIZULLAH FAISAL
Title: DAMPING ENHANCEMENT OF MULTIMACHINE POWER
SYSTEM THROUGH STATCOM CONTROL
Degree: MASTER OF SCIENCE
Major Field: ELECTRICAL ENGINEERING
Date of Degree: MARCH 2005

A static synchronous compensator (STATCOM) is a shunt connected FACTS device, which is capable of enhancing the power system damping by exchanging reactive power with the system. In this thesis, robust STATCOM controls have been investigated for power system damping improvement. Non-linear and linear models of a single machine infinite bus (SMIB) system as well as multimachine systems installed with STATCOM have been derived. The method of multiplicative uncertainty has been employed in the robust design to model the variations of the operating points. A graphical method termed as loop-shaping is used to select a suitable open loop-transfer function from which the robust controller is constructed. Improvement in the graphical method is proposed by embedding a computational technique called the particle swarm optimization (PSO) in the original loop-shaping method. The high order multimachine models have been simplified for control design through model reduction techniques. Linear and non-linear models of both single machine as well as multimachine system have been simulated including the PSO embedded robust controllers. A four machine test system is used to test controllers considering small as well as large disturbances including three phase symmetrical faults. Results indicate that the proposed robust design provides extremely good damping over a wide range of operating conditions.

Keywords: STATCOM, FACTS, Multimachine System, Robust Controller, Uncertainty Modeling, Loop shaping, PSO, Model reduction.

Master of Science Degree

King Fahd University of Petroleum & Minerals, Dhahran.

March 2005

ملخص الرسالة

اسم الطالب: سيد فيض الله فيصل

عنوان الرسالة: تعزيز توهين ذبذبات نظام القدرة الكهربائية لعدة ماكينات من خلال نظام

(STATCOM)التحكم

التخصص: هندسة كهربائية

تاريخ التخرج: مارس / 2005م

عبارة هن جهاز قاطع موصول (STATCOM) المعادل التزامني السكوني ، والذي بإمكانه تعزيز توهين ذبذبات نظام القدرة الكهربائية بواسطة تغيير القدرة (FACTS) لتحسين توهين (STATCOM)النشطة مع النظام. في هذه الرسالة يتم بحث أنظمة تحكم ثابتة ذبذبات نظام القدرة الكهربائية. يتم اشتقاق نماذج رياضية خطية وغير خطية لنظام الموصل إضافة لأنظمة الماكينات المتعددة المركبة مع نظام التحكم (SMIB) اللامتناهي لماكنية مفردة . يتم توظيف طريقة عدم التأكد المضاعف في التصميم الثابت لنمذجة تغيرات نقاط (STATCOM) التشغيل. تستعمل طريقة بيانية، عنوانها تشكيل الدارة، لاختيار اقتران النقل للدارة المفتوحة الملائم والذي من خلاله يتم بناء المتحكم الثابت. تحسين الطريقة البيانية يتم بإدراج تقنية حسابية تدعى تعظيم في طريقة تشكيل الدارة الأصلية. يتم تبسيط النماذج الرياضية للماكينات (PSO) اندفاع الجزئي المتعددة ذات الدرجة العالية لتصميم نظام التحكم من خلال تقنيات إنقاص درجة النموذج الرياضي. النماذج الخطية وغير الخطية لكل من نظامي الماكينة المفردة والماكينات المتعددة تتم محاكاتها حيث الثابتة المدرجة. يتم استعمال نظام اختبار مكون من أربع ماكينات لاختبار (PSO)تضم أجهزة تحكم أجهزة التحكم مع وجود اضطرابات صغيرة وكبيرة تضم أخطاء متماثلة ذات ثلاثة أطوار. تشير النتائج إلى أن التصميم الذي تم تقديمه يعطي توهيناً للذبذبات فائق الجودة ضمن مدى واسع من الظروف التشغيلية.

الكلمات المفتاحية: STATCOM، FACTS، نظام متعدد الماكينات، المتحكم الثابت، نمذجة عدم الدقة، تشكيل الدارة، PSO ، إنقاص النموذج.

CHAPTER 1

INTRODUCTION

1.1 POWER SYSTEM STABILITY

Modern electric power system is a complex network of synchronous generators, transmission lines and loads. The characteristics of the system vary with changes in load and generation schedules. Electric utilities first grew as isolated systems, and then gradually neighboring utilities began to join forming highly interconnected systems. This enabled the utilities to draw on each other's generation reserves during the time of need. The overall reliability has improved through interconnection but disturbances in such systems propagate through, leading to system instability and possible black-outs. Systems which have long transmission distances between the load centers and generating stations

may exhibit poorly damped or even negatively damped oscillations. If the magnitude of disturbance is large, such as a three phase fault, major line or load switching, the system could even become transiently unstable. A good power system should possess the ability to regain its normal operating condition after a disturbance. Since ability to supply uninterrupted electricity determines the quality of electric power supplied to the load, stability is regarded as one of the important topics of power system research [1, 2, 3].

Power system stability can be defined by the ability of synchronous machines to remain in synchronism with each other. The capability of power system to remain in synchronism in the event of possible disturbance such as line faults, generator and line outages and load switching etc., is characterized by its stability. Depending on the order of magnitude and type of disturbances, power system stability can be classified as steady state stability, transient stability and slowly growing stability [4, 5, 6].

Following unbalances in the system, a power system may experience sustained oscillations. These oscillations may be local to a single generator or they may involve a number of generators widely separated geographically (inter-area oscillations). Local oscillations can occur, for example, when a fast exciter is used on the generator. Inter area oscillations may appear as the system loading is increased across the weak transmission links. If not controlled, these oscillations may lead to partial or total power interruption [7, 8, 9].

Damping the oscillations is not only important in increasing the transmission capability but also for stabilization of power system conditions after critical faults. If the

net damping of the system is negative, then the system may lose synchronism. Extra damping has to be provided to the system in order to avoid this. Powerful damping in the system has a two fold advantage of both decreasing the amplitude of first swing and the ratio of each successive swing to the preceding one, thus resulting in overall improvement of stability margin of the system [10, 11].

The major methods of damping of power system oscillations are:

1. Governor control: Control of input power P_m can stabilize a power system following a disturbance. Though governor control has shown some good results in damping control, it is not accepted by power utilities.
2. Excitation control: Among the various methods of damping, excitation control is one of the most common and economical method. Excitation controllers are referred to as power system stabilizers (PSS). PSSs have been thought to improve power system damping by generator voltage regulation depending on system dynamic response [12, 13].
3. Braking Resistors: Braking resistors prevent transient instability by immediately absorbing the real power that would otherwise be used in accelerating the generator. These are very effective to damp the first power system swing.
4. Control of the rotor angle (δ): The electrical power output P_e can also be altered by varying the angle δ . Phase shifters can be employed to perform this job.
5. Load shedding: This is the least considered option and is adopted as a last measure.

6. Control of the line reactance X : From (1.2), the electrical power output P_e can be controlled by controlling the line reactance X . Reactance (or X) control can be achieved by series or shunt compensation. Traditionally these compensators have been fixed, and switched in and out of the system at low rates. Developments in power electronics have allowed dynamic control of these static shunt and series compensators. Electronically controlled FACTS devices, discussed in the next section are now being widely used in the power system.

1.2 FACTS DEVICES

Flexible AC transmission systems (FACTS) devices are power electronic based controllers that regulate the power flow and transmission voltage through rapid control action. The concept of FACTS was proposed by N.G.Hingorani, of Electric Power Research Institute (EPRI) in late 1980's [17, 18, 19]. Before the FACTS technology was introduced, power system control was focused on the generator control, because controlling ability of transmission network was very weak. FACTS devices have the capability of controlling the transmission parameters like series impedance, shunt impedance, phase angle etc. FACTS technology is not a single high power controller but rather a collection of controllers that can be applied individually or collectively to control these parameters [17, 18, 19, 20].

Some of the functions of FACTS devices are,

- Regulation of power flows in prescribed transmission routes.
- Secure loadings of lines near their thermal limits.
- Prevention of cascading outages by contributing to emergency control.
- Damping of oscillations which can threaten security or limit the usable line capacity and improve system stability in general.

From control point of view, FACTS controllers can be classified into the following four types [15].

- a) Series controllers: These can be variable impedance such as capacitor, reactor etc., or a power electronic based variable source of main frequency, sub-synchronous or harmonic frequencies placed in series in the transmission lines. In principle, series controllers inject voltage in series with the line.
- b) Shunt controllers: The shunt controllers may be variable impedance, variable source or a combination of these. In principle, shunt controllers inject current into the system at the point of connection.
- c) Combined series-series controllers: These could be a combination of separate series controllers which are controlled in a coordinated manner in a multi-line transmission system.
- d) Combined – series shunt controllers: These could be a combination of separate series and shunt controller, which are controlled in a coordinated manner.

1.2.1 First generation of FACTS devices

Power electronics based controllers were in use in power systems before N.G.Hingornani's use of the terminology, FACTS. These first generation FACTS devices have a common characteristic that is the necessary reactive power required for the compensation is generated or absorbed by traditional capacitor or reactor banks, and thyristor switches are used for control of the combined reactive impedance these banks present to the system during successive periods of voltage application. Consequently, conventional thyristor controlled compensator present a variable reactive admittance to the transmission network [15,21].

Some of the first generation FACTS devices are,

- 1 Thyristor switched series capacitor (TSSC): A capacitive reactance compensator which consists of series capacitor bank shunted by a thyristor switched reactor to provide a stepwise control of series capacitive reactance.
- 2 Thyristor controlled series capacitor (TCSC): A capacitive reactance compensator which consists of a series capacitive bank shunted by a thyristor controlled reactor in order to provide smooth variation of series capacitive reactance.
- 3 Thyristor switched capacitor (TSC): Consists of a thyristor switched capacitor whose effective reactance is varied in stepwise manner by a thyristor valve. It is a shunt connected device.

- 4 Static VAR compensator (SVC): Consists of thyristor controlled reactors (TCR) in parallel with thyristor switched capacitor (TSC). It is a shunt connected device. SVC units are dynamic reactive power compensation devices conventionally used for voltage control through reactive power modulation. SVC can also be used for improving static power transfer capability of long transmission lines and thus can also be used for increasing stability limits.

1.2.2 Second Generation of FACTS devices

The second generation of FACTS controllers is based on voltage source converter, which use turn off devices like GTOs. These controllers require lower ratings of passive elements (inductors and capacitors) and the voltage source characteristics present several advantages over conventional variable impedance controllers. Some of the FACTS controllers belonging to this category are

1. Static synchronous series compensator (SSSC): It is a voltage –sourced converter based series compensator and was proposed by Gyugi [15] in 1989.
2. Static synchronous compensator (STATCOM): STATCOM, previously known as STATCON or static condenser, is an advanced static Var compensator (SVC) using voltage source converters with capacitors connected on DC side. STATCOM resembles in many respects a rotating synchronous condenser used for voltage control and reactive power compensation. As compared to conventional

SVC, STATCOM does not require expensive large inductors, moreover it can also operate as reactive power sink or source flexibly, which makes STATCOM more attractive [48]. Because of its several advantages over conventional SVC, it is expected to play a major role in the optimum and secure operation of AC transmission system in future.

3. Unified power flow controller (UPFC): UPFC concept was proposed by Gyugi [15]. It consists of back to back voltage source converter arrangement, one converter of the back to back arrangement is in series and other is in shunt with the transmission line.

1.3 DAMPING ENHANCEMENT THROUGH STATCOM

A STATCOM plays an important role in reactive power provision and voltage support because of its attractive steady state performance and operating characteristics. A number of studies have been performed about the dynamic behavior of STATCOM and its application to improve the transient performance of power systems [29, 32, 35, 36]. However, proper control strategies are necessary in order to achieve full utilization of STATCOM. Some of the controllers designed are simple lag-lead controllers [33,52], conventional PI controllers [20, 37, 58], controllers designed by the phase compensation method [49], the linear quadratic regulators [53, 54], pole assignment [55], etc. Fuzzy controllers for STATCOM have also been reported recently [56, 57]. Selection of input signal is one of the important items in designing a controller. Some of the auxiliary input

signals used for STATCOM controllers are delivered active power, the STATCOM bus voltage, computed internal voltage, synthesized remote phasor, driving point reactance seen from STATCOM location, etc [35, 51, 52]. A comprehensive literature search covering the details of these issues has been included in the next chapter.

Most of the controllers' designed for STATCOM are based on linearized model of the power system and hence are suitable for particular operating points. Changes in operation in the system occur because of the load changes as well as for unpredictable disturbances. A controller designed for operation at certain operating condition may not perform satisfactorily at other operating points. A controller that is designed to operate over a set of perturbed operating points can circumvent the mentioned problem of uncertainty of power system operation. Such a controller is known as robust controller. Thus designing a robust controller which will operate efficiently over a range of operating conditions is highly desirable [20, 21, 22].

1.4 SCOPE OF THE THESIS

The objective of this work is to investigate the performance of power system with STATCOM controllers. Design of robust STATCOM controls has been investigated for single machine as well as multimachine power systems. A graphical robust control design has been explored, and improvement of the algorithm by embedding a particle swarm optimization (PSO) technique has been investigated. The high order multimachine models

have been simplified for control design through model reduction techniques. Both single machine and multimachine systems have been simulated for the robust control study including the PSO based controllers. Specifically, this research proposes to address the following:

- Determination of damping properties of a single machine system vis-à-vis the location of STATCOM.
- Selection of an appropriate robust control technique for single machine system and its evaluation.
- Development of a multimachine powers system program for dynamic study with STATCOM controller.
- Designing and testing of a robust controller for multimachine system
 - Retaining the original order,
 - Reduced order model obtained through balanced realization technique
- Designing Robust STATCOM controller through PSO based Loop-Shaping technique for
 - Single machine infinite bus system,
 - Multimachine power system (Both reduced and detailed model)

CHAPTER 2

LITERATURE SURVEY

This chapter presents a comprehensive literature search on STATCOM – its modeling, ability to damp system oscillations and impact of its location on dynamic performance, application of STATCOM to multimachine system etc.

2.1 STATCOM FOR POWER SYSTEM CONTROL

The new generations of FACTS controllers are based on voltage source converter, which use turn off devices like GTOs. The main advantages of these types of controllers are that they require lower ratings of passive elements (inductor and capacitors) and the voltage

source characteristics present advantages over conventional variable impedance controllers [20]].

The STATCOM resembles in many respects a synchronous condenser but without inertia. The basic electronic block of a STATCOM is the voltage source converter (VSC), which in general, converts an input dc voltage into a three phase ac output voltage at fundamental frequency, with rapidly controllable amplitude and phase angle. In addition to this, the controller has a coupling transformer and dc capacitor. The control system can be designed to maintain the magnitude of the bus voltage constant by controlling the amplitude and / or the phase shift of the VSC output voltage [7].

The general arrangement of STATCOM is shown in Fig 2.1. The static compensator (STATCOM) provides shunt compensation in a similar way to static var compensators (SVC) but utilizes a voltage source converter rather than shunt capacitors and reactors [23]. The basic principle of operation of STATCOM is generation of a controllable AC voltage source behind a transformer leakage reactance by a voltage source converter connected to a DC capacitor. The voltage difference across the reactance produce active and reactive power exchanges between the STATCOM and power system.

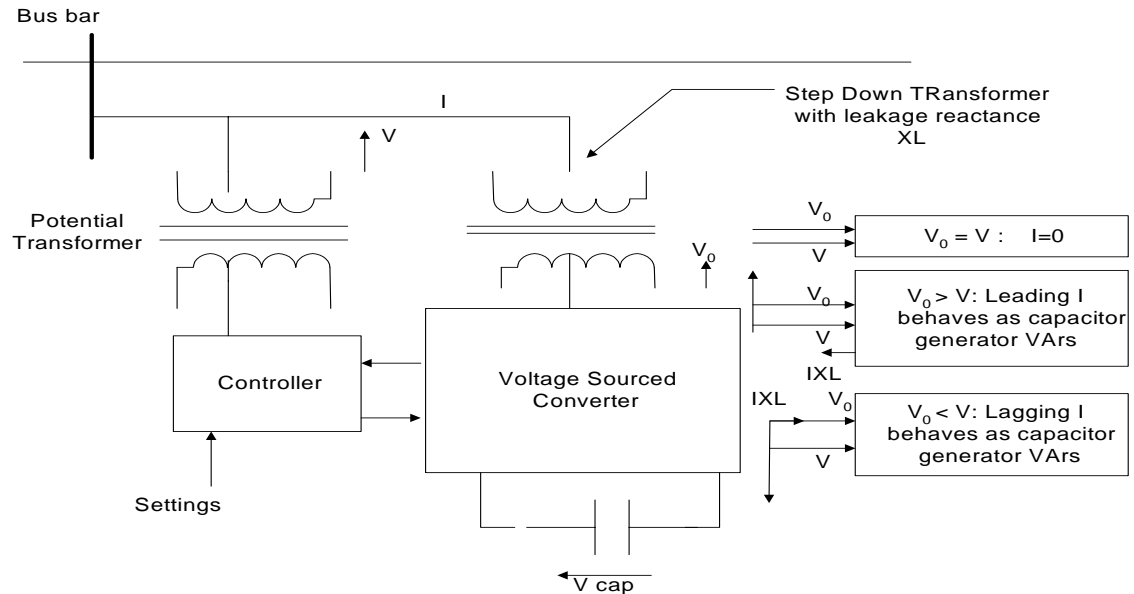


Figure 2.1 General arrangement of STATCOM

The main advantages of STATCOM over the conventional SVC are [20, 21, 22, 24].

- Significant size reduction due to reduced number of passive elements.
- Ability to supply required reactive power even at low voltages.
- Greater reactive power current output capability at depressed voltages.
- STATCOM exhibits faster response and better control stability.
- With proper choice of design ratings and thermal design, STATCOM can have short time overload capability. This is not possible in SVC due to its inherent susceptance limit support.
- The ability of STATCOM to produce full capacitive output current at low system voltage also make it highly effective in improving the transient (first swing) stability.
- The transient stability margin obtained with STATCOM is significantly greater than attainable with SVC of identical rating. This means that transmittable power

can be increased if the shunt compensation is provided by STATCOM rather than SVC. This means that for same stability STATCOM has lower rating than that of SVC.

2.2 STATCOM MODELING FOR STABILITY STUDIES

Since the first STATCOM installation in USA nearly a decade ago, there is an ever growing interest in STATCOM modeling owing to its many advantages over conventional SVC controllers. Several distinct models have been proposed to represent STATCOM in static and dynamic analysis. In [16] STATCOM is modeled as parallel connected current source; where in the controllable parameter is assumed to be current magnitude. In [26] the authors proposed different models for transient stability and steady state stability analysis of the power system with STATCOM. However, the models were based on the assumptions that voltages and currents are sinusoidal, balanced and operate near fundamental frequency, hence could not be applied to systems under the impact of large disturbance that have voltage and/or current with high harmonic content. In [25] the author proposes a per unit STATCOM model; which is suitable for study the performance of STATCOM under unbalanced distorted system voltage. A comparative study is carried out for dynamic operation of different models of STATCOM and their performance in [27]. In [29] the author proposes a third order dynamic model of the power system to incorporate STATCOM in the system to study its damping properties.

2.3 STATCOM CONTROLLER DESIGN FOR DAMPING OF SYSTEM OSCILLATIONS

Though it is a costly option when compared to the use of PSS for oscillation control, there are additional benefits of STATCOM controllers. Besides oscillation control, STATCOMs' local voltage control capabilities allow an increase in system loadability, which is not at all possible with PSS.

In [20] comparative study for different combinations of PID controller is presented for STATCOM controller. It is reported that two control inputs are identified, one in the speed loop (i.e. the input signal to controller is the speed deviations of the machine) and the other in the voltage loop. The control in voltage loop alone is not effective in damping control but its presence is found to be necessary for the voltage regulation. A controller in the speed loop has effective control over the electrical and electro- mechanical transients. It is found that for nominal unity gain in the voltage, a PD controller in the speed loop gave reasonably good damping characteristic. It is concluded that PID control was not generally found satisfactory in terms of both steady state and transient performance.

In [20, 21, 22] a novel method of designing robust damping control strategies for STATCOM controller is proposed for both the approximate and detailed models. The controller designed was tested for a number of disturbance conditions including symmetrical three phase faults. The robust controller was found to be effective for a range of operating conditions of the power system. The proposed robust controller was found to be superior to the conventional PI controller.

Design of non-linear controller for STATCOM based on differential algebra theory is presented in [31]. The controller designed by this method allows linearizing the

compensator and controlling directly the capacitor voltage output and reactive power of STATCOM.

In [33] a simple lead lag controller whose time constants were tuned at the frequency of critical swing mode to be damped is used for STATCOM. The authors proposes the local voltage compensated by the reactive current output of the STATCOM and the driving point reactance seen from STATCOM location as the input signal for the damping controller because of its favorable observability and lower self interaction gain.

Design of STATCOM multivariable sampled regulator is proposed in [33]. The authors have observed a case of negative interaction when two separate controllers are assigned for AC and DC voltage control of a STATCOM installed in power system. They proposed a decoupled multivariable sampled regulator for the coordinated control of STATCOM AC and DC voltage so as to overcome a potential negative interaction.

Fuzzy logic controllers have also been proposed for FACTS in interconnected systems to improve the dynamic behavior of the system [34]

STATCOM controllers can also be used for damping of sub-synchronous oscillations in EHV series compensated systems [35]. It is observed that STATCOM with voltage controller alone is not sufficient to damp unstable modes to a good stability margin. Thus a need was felt for an additional control signal along with STATCOM voltage controller. Additional control signal proposed is the computed internal voltage (CIV) which involves the computation of internal voltage of remotely located generator utilizing locally measurable STATCOM bus voltage and transmission line current signals.

Dynamic controller design for SVC and STATCOM is the topic of recent research for steady state, transient and eigen value studies [36].

A comparative study is performed in [37] between the damping characteristic of PID PSS and PID STATCOM. The authors concluded that under a severe three phase short circuit fault, the response of a system with proposed STATCOM damping controller have rendered better damping effects than the ones of the system with PSS.

2.4 LOCATION OF FACTS DEVICES FOR DAMPING ENHANCEMENT

Many articles deal with the optimal location of FACTS devices to damp system oscillations. In [7] the authors state that for damping system oscillations the FACTS controller should be located such that they brings the critical eigen values in the open left half plane. This location might not correspond to the best placement to increase system loadability and improve voltage regulation.

A non-linear controller is proposed in [38] whose performance depends on the location of fault and on the location of the STATCOM.

There exists a contradiction between the voltage control and damping control of STATCOM. More emphasis on voltage control would decrease the damping torque while increasing the synchronizing torque. This is the reason why damping control can stabilize the system oscillations but produces slight oscillations in the voltage and that is why too much voltage control will weaken the damping effects by enhancing the oscillation amplitude. However the best installation position of STATCOM for damping system oscillations in single machine infinite bus system (SMIB) according to [29] is the midpoint of the line where the damping torque coefficients will be maximum.

Reduced order method of model analysis is used in [39] for determining the best location of SVC (Static Var Compensator). It is especially very useful method for large power system. It is shown in the paper that the computation burden is reduced by as much as ten times when compared to using the full order system matrix. Since STATCOM and SVC work on the same principle, this method can apply to STATCOM as well.

In reference [40], the authors state that the damping effect of FACTS devices is strongly influenced by their location and control system. They propose a location index to determine the optimal location of FACTS devices in a large power system. The optimization algorithm also determines the optimal control parameters for FACTS in addition to the optimal solution.

Power system stability index approach has also been implemented in determining the number and location of TCSC (a FACTS device) in multimachine power system. The paper uses power system stability for evaluation of TCSC allocations. Once the locations are determined a robust controller is designed by the H_∞ control and the time response against a disturbance is assessed [41, 42].

In [9], the authors performed an exhaustive study on different control strategies to assess the most appropriated auxiliary signal and best location of the SVC for achieving good damping of electromechanical oscillations for single machine infinite bus system. The paper gives a contradictory location compared to most of the papers for the location of SVC to damp system oscillations. It says generator bus is the best location for SVC for both damping of system oscillation and voltage regulation; when active power P_e is used as the auxiliary control signal. Based on the same argument as stated earlier that

STATCOM and SVC operates on similar principle, this finding can also be extended to STATCOM.

Analytical techniques based on modal analysis and study of controllability and observability measure to place multiple power system controllers for power oscillation damping are presented in reference [43]. The authors concluded that modal bus voltage calculations can be helpful in identifying suitable locations for adding voltage control devices such as SVC; further it was emphasized that modal power flow can indicate transmission paths through which energy flow is highly observable. This could help in ascertaining operating condition that might aggregate damping of critical modes.

In [44] the author proves that the shunt FACTS devices like SVC and STATCOM need to be placed slightly off centre when installed on a long transmission line to get the best performance in terms of both power transfer capability and system stability.

Sensitivity based approach is developed in [45] for determining the optimal location for TCSC in power system. In reference [46] the authors used genetic algorithm to optimally locate multi-type FACTS devices in power system. Optimizations are performed on three parameters: location of the devices, their types and their values.

2.5 STATCOM IN MULTI-MACHINE SYSTEM

STATCOM has attracted attention of many researchers because of its several advantages over conventional SVC controllers; though a good amount of work has been reported for the SMIB very limited work on damping control in multimachine system is available.

Fuzzy controllers for STATCOM installed in multi-machine power system are reported in recent publications [56, 57]. In [56] the authors propose a variable structure

fuzzy controller with the control signal obtained from a combination of generator speed deviation and STATCOM bus voltage deviation. The parameters of fuzzy reactive current controller were adapted using a sliding surface. The fuzzy controller designed was applied to SMIB as well as four generator multi-machine system. Fuzzy controllers, designed for both main and supplementary controllers of the STATCOM are presented in [57]. The fuzzy main control is designed to provide the voltage support on the tie lines of interconnected power system. The fuzzy supplementary control (SC) is designed for inter area power oscillation and enhancing dynamic stability of interconnected power system. Look up table method is used for both main and SC. The authors claim that results support the application of fuzzy controller in power system and also the controllers are robust over a wide range of power system operating conditions.

In ref [58], the author develops dynamic models for STATCOM installed in both SMIB and multi-machine power systems. STATCOM performance was tested by designing a conventional PI controller. The author observes that PI controllers designed provide stabilizing controls when the AC and DC voltage regulators are designed independently. However, it was observed that the joint operation of the two leads to system instability due to the interaction of the two controllers.

In [60] the authors perform eigen value analysis to study the effectiveness of the controller and the location of STATCOM that would give best damping. Simulations are carried out on four generator multi-machine power system. It is found that, with Thevinin's voltage as the input signal, the best location for the STATCOM is the sending end of the tie line.

CHAPTER 3

POWER SYSTEM MODEL WITH STATCOM

Controller design for power system stability studies requires proper and adequate mathematical representation of power system so as to include all significant components of the power system. Dynamic models, both non-linear and linearized, for single machine infinite bus as well as multimachine systems installed with STATCOM are presented in this chapter.

3.1 THE SINGLE MACHINE INFINITE BUS SYSTEM

A single machine infinite bus (SMIB) system is shown in Fig. 3.1. The STATCOM is connected at the middle of transmission line. The dynamic models for the various components of the system are given in the following.

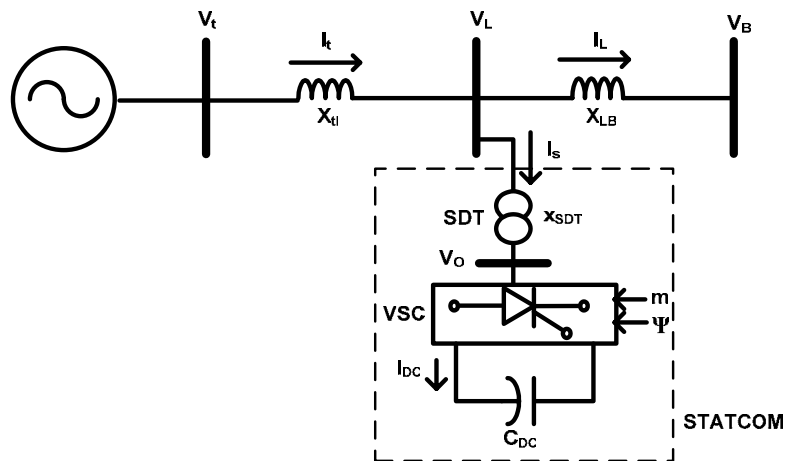


Fig. 3.1 STATCOM installed in SMIB power system

3.1.1 Synchronous generator and its excitation system

The synchronous generator is modeled through q-axis component of transient voltage and electromechanical swing equation representing motion of the rotor.

The internal voltage equation of the generator is written as,

$$\dot{e}'_q = \left[E_{fd} - e'_q - (x_d - x'_d) I_d \right] \frac{1}{T'_{do}} \quad (3.1)$$

where, e'_q subscript d and q represents the direct and quadrature axis of the machine. x_d , x'_d and T_{do} are the d-axis synchronous reactance, transient reactance and open circuit field constants, respectively. I_d is the current along the d-axis and e'_q is the voltage behind the transient reactance.

The electromechanical swing equation is broken into two first order differential equations and is written as,

$$\begin{aligned}\dot{\omega} &= \frac{1}{2H} [P_m - P_e - K_D \omega] \\ \dot{\delta} &= \omega_o \omega\end{aligned}\quad (3.2)$$

where, the electrical power output is,

$$P_e = v_d I_d + v_q I_q$$

v_d and v_q are components of generator terminal voltage (V_t). P_m is the mechanical power input. H is the inertia constant in seconds, ($2H = M$). ω_o is the synchronous speed.

The IEEE type ST is used for the voltage regulator excitation. The block diagram of the excitation system is shown in Fig. 3.2.

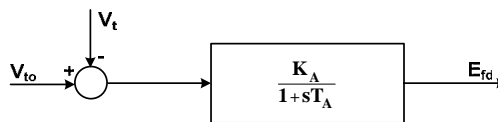


Fig. 3.2 Block diagram of excitation system

The dynamic model of the excitation system is,

$$\dot{E}_{fd} = -\frac{1}{T_A} E_{fd} + \frac{K_A}{T_A} (V_{to} - V_t) \quad (3.3)$$

where, K_A and T_A are the gain and time constant of exciter, respectively. V_{to} represents the steady state (reference) value of terminal voltage.

3.1.2 The STATCOM system

The STATCOM system shown in Fig. 3.1 consists of a step down transformer (SDT) with leakage reactance X_{SDT} , a three phase GTO based voltage source converter (VSC) and a DC capacitor. The VSC generates a controller AC voltage $\bar{V}_o = V_o \sin(\omega t - \psi)$ behind the leakage reactance. The voltage difference between the STATCOM bus voltage V_o and the bus voltage V_L produces active and reactive power exchange between STATCOM and the power system, which can be controlled by adjusting the magnitude V_o and phase ψ .

The voltage current relationship in the STATCOM are expressed as [58],

$$\dot{V}_{DC} = \frac{I_{DC}}{C_{DC}} = \frac{m}{C_{DC}} (I_{sd} \cos \psi + I_{sq} j \sin \psi) \quad (3.4)$$

where,

$$m = ek$$

$$k = \frac{AC \text{ Voltage}}{DC \text{ Voltage}}$$

e = modulation ratio defined by PWM

ψ = phase angle defined by PWM

I_{sd} and I_{sq} are components of STATCOM current.

The relationship between STATCOM AC voltage V_o and V_{DC} is

$$V_o = mV_{DC} \angle \psi$$

The components of generator and STATCOM currents can be expressed in the form,

$$I_d = \frac{\left(1 + \frac{X_{LB}}{X_{SDT}}\right) e'_q - \frac{X_{LB}}{X_{SDT}} mV_{DC} \sin \psi - V_B \cos \delta}{X_{tL} + X_{LB} + \frac{X_{tL}}{X_{SDT}} + \left(1 + \frac{X_{LB}}{X_{SDT}}\right) x'_d} \quad (3.5)$$

$$I_q = \frac{\left[\frac{X_{LB}}{X_{SDT}}\right] mV_{DC} \cos \psi + V_B \sin \delta}{\left[X_{tL} + X_{LB} + \frac{X_{tL} X_{LB}}{X_{SDT}}\right] + \left[1 + \frac{X_{LB}}{X_{SDT}}\right] x_q}$$

$$I_{sd} = \frac{e'_q}{X_{SDT}} - \frac{(x'_d + X_{tL}) I_q}{X_{SDT}} - \frac{mV_{DC} \sin \psi}{X_{SDT}} \quad (3.6)$$

$$I_{sq} = \frac{mV_{DC} \cos \psi}{X_{SDT}} - \frac{(x_q + X_{tL}) I_q}{X_{SDT}}$$

The symbols used are given in nomenclature. The set of equations (3.1), (3.2), (3.3) and (3.4) form the non-linear model of SMIB system with STATCOM. This can be written as

$$\dot{x} = f(x, u) \quad (3.7)$$

where, x is the vector of state variables, $\left[e'_q, \omega, \delta, E_{fd}, V_{DC}\right]^T$ and u is the vector of control

variables, $\left[m, \psi\right]^T$.

3.2 THE LINEARIZED EQUATIONS

The linearized model for SMIB with STATCOM is obtained by perturbing the set of equations (3.7) around a nominal operating point. The linearized system equations are written as,

$$\begin{aligned}
 \Delta \dot{e}'_q &= \left[\Delta E_{fd} - \Delta e'_q - (x_d - x'_d) \Delta I_d \right] \frac{1}{T_{do}} \\
 \Delta \dot{\omega} &= -\frac{1}{2H} [\Delta P_e + K_D \Delta \omega] \\
 \Delta \dot{\delta} &= \omega_o \Delta \omega \\
 \Delta \dot{E}_{fd} &= -\frac{1}{T_A} \Delta E_{fd} - \frac{K_A}{T_A} \Delta V_t \\
 \Delta \dot{V}_{dc} &= \frac{1}{C_{DC}} \left[(I_{sdo} \cos \psi_o + I_{sqo} \sin \psi_o) \Delta m + m_o (-I_{sdo} \sin \psi_o + I_{sqo} \cos \psi_o) \Delta \psi + \right. \\
 &\quad \left. m_o (\cos \psi_o \Delta I_{sdo} + \sin \psi_o \Delta I_{sqo}) \right]
 \end{aligned} \tag{3.8}$$

where,

$$\begin{aligned}
 \Delta P_e &= K_1 \Delta \delta + K_2 \Delta e'_q + K_{pDC} \Delta V_{DC} + K_{pc} \Delta m + K_{p\psi} \Delta \psi \\
 \Delta e_q &= K_3 \Delta e'_q + K_4 \Delta \delta + K_{q\psi} \Delta \psi + K_{qc} \Delta m + K_{qDC} \Delta V_{DC} \\
 \Delta V_t &= K_5 \Delta \delta + K_6 \Delta e'_q + K_{VDC} \Delta V_{DC} + K_{Vm} \Delta m + K_{V\psi} \Delta \psi
 \end{aligned} \tag{3.9}$$

Arranging the state equations in matrix form gives,

$$\begin{aligned}
\begin{bmatrix} \Delta \dot{\delta} \\ \Delta \dot{\omega} \\ \Delta \dot{e}'_q \\ \Delta \dot{E}_{fd} \\ \Delta \dot{V}_{DC} \end{bmatrix} &= \begin{pmatrix} 0 & \omega_o & 0 & 0 & 0 \\ -\frac{K_1}{M} & -\frac{D}{M} & -\frac{K_2}{M} & 0 & -\frac{K_{pDC}}{M} \\ -\frac{K_4}{T_{do'}} & 0 & -\frac{K_3}{T_{do'}} & \frac{1}{T_{do'}} & -\frac{K_{qDC}}{T_{do'}} \\ -\frac{K_A K_5}{T_A} & 0 & -\frac{K_A K_6}{T_A} & -\frac{1}{T_A} & -\frac{K_A K_{VDC}}{T_A} \\ K_7 & 0 & K_8 & K_9 & 0 \end{pmatrix} \begin{bmatrix} \Delta \delta \\ \Delta \omega \\ \Delta e'_q \\ \Delta E_{fd} \\ \Delta V_{DC} \end{bmatrix} + \\
&+ \begin{pmatrix} 0 & 0 \\ -\frac{K_{pm}}{M} & -\frac{K_{p\psi}}{M} \\ -\frac{K_{qm}}{T_{do'}} & -\frac{K_{q\psi}}{T_{do'}} \\ -\frac{K_A K_{Vm}}{T_A} & -\frac{K_A K_{V\psi}}{T_A} \\ K_{DC} & K_{d\psi} \end{pmatrix} \begin{bmatrix} \Delta m \\ \Delta \psi \end{bmatrix} \quad (3.10)
\end{aligned}$$

or,

$$\dot{x} = Ax + Bu \quad (3.11)$$

Here, x is the perturbation of the states in (3.8) and u is the vector of control, $[\Delta m \ \Delta \psi]^T$.

Detailed derivations are given in Appendix B. Fig. 3.3 shows the block diagram of linearized model of SMIB system with STATCOM.

3.3 A MULTIMACHINE POWER SYSTEM

The model of a multimachine power system containing the dynamics of synchronous generator, its excitation system, the loads etc, is presented in the following. It is assumed that each generator is connected to the network through its transmission network. The STATCOM is considered to be connected at the middle of transmission lines as shown in Fig. 3.4.

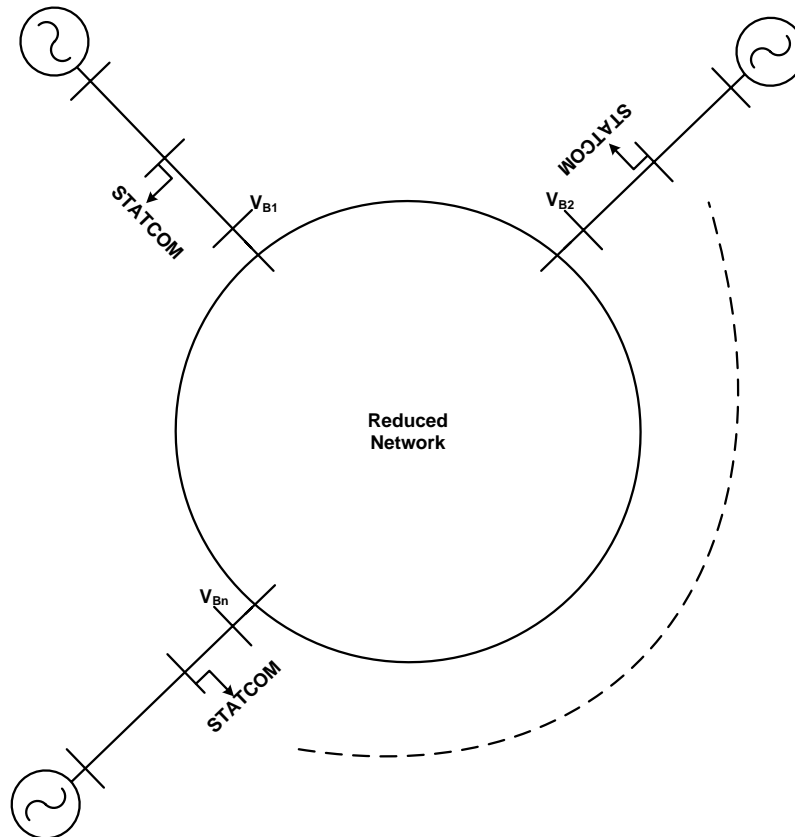


Fig. 3.4 Reduced multimachine system configuration showing the generators and STATCOMS

The following assumptions are made to simplify the mathematical model which describes the non-linear dominant dynamic behavior of a multimachine power system.

1. Transient saliency of the generator is neglected (i.e. $x'_d = x'_q$).
2. Governor and turbine dynamics are neglected. This results in constant input mechanical power.
3. The network is in quasi-static state (no transmission line dynamics included).
4. The loads are represented by constant impedance loads. The load buses are eliminated and the network voltage current relationship between the terminal buses of generators is expressed through a reduced bus admittance matrix (Y_b).

The multimachine power system configuration with the loads eliminated is shown in Fig.

3.4

The non-linear dynamics for the i -th machine of the n -machine power system of Fig. 3.4, including STATCOM can be written similar to (3.1), (3.2), (3.3) and (3.4) as,

$$\begin{aligned}
\dot{e}'_{di} &= \left[-e'_{di} + (x_{qi} - x'_{di}) I_{qi} \right] \frac{1}{T'_{qoi}} \\
\dot{e}'_{qi} &= \left[E_{fdi} - e'_{qi} - (x_{di} - x'_{di}) I_{di} \right] \frac{1}{T'_{doi}} \\
\dot{\omega}_i &= -\frac{1}{2H_i} [P_{mi} - P_{ei} - K_{Di} \omega_i] \\
\dot{\delta}_i &= \omega_o \omega_i \\
\dot{E}_{fdi} &= -\frac{1}{T_{Ai}} E_{fdi} - \frac{K_{Ai}}{T_{Ai}} (V_{toi} - V_{ti}) \\
\dot{V}_{DCi} &= \frac{m_i}{C_{DCi}} [I_{sdi} \cos \psi_i + I_{sqi} \sin \psi_i]
\end{aligned} \tag{3.12}$$

The symbols in (3.12) are exactly the same as in case of single machine system. The variations in d-q internal voltage dynamics have been included in this analysis inline with Anderson's work [3].

The non-linear model of (3.12) for the i-th machine can be expressed in the form,

$$\dot{x} = f(x, u, I_{di}, I_{qi}, I_{sdi}, I_{sqi}) \tag{3.13}$$

where, x_i is the state vector for the i-th machine, $[e'_{di}, e'_{qi}, \omega_i, \delta_i, E_{fdi}, V_{DCi}]^T$ and the only control u_i is m_i .

3.3.1 The network equations

The non-linear model of the synchronous generator-STATCOM system contains generator and STATCOM currents which are non-state variables. These non-state variables are eliminated by including the voltage-current relationship of the network.

From Fig. 3.4,

$$I_L = Y_b V_B \quad (3.14)$$

Here, I_L is the vector of injected currents to the network $[I_{L1}, I_{L2}, \dots, I_{Ln}]^T$; V_B is the vector of network bus voltages $[V_{B1}, V_{B2}, \dots, V_{Bn}]^T$ and Y_b is the reduced bus admittance matrix.

The currents and voltages in (3.14) are complex quantities and when broken up into real and imaginary parts, they will be along the natural common frame of reference, called the D-Q coordinates. The state equations in (3.13) for each generator are along their individual di – qi frames of references. In order to combine the network equations (3.14) with the machine equation a transformation of variables is needed. The following two transformations are reported in the literature [3],

- a) Transforming generator quantities to common reference frame.
- b) Transforming network equations to individual generator reference frames.

In this thesis the second transformation is used; the advantage is that the generator quantities remain unchanged thus making control design somewhat simpler.

Consider the phasor diagram shown in Fig. 3.5. Here, D – Q is the common network reference frame and di – qi is the reference frames of individual machines.

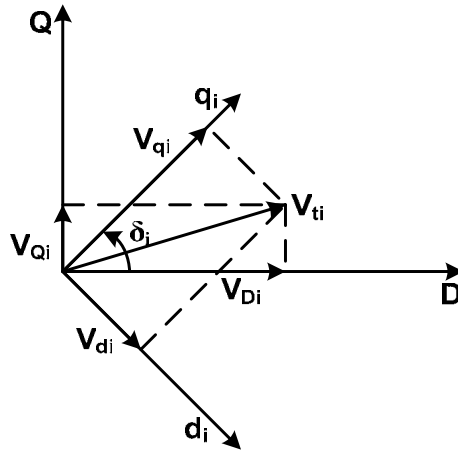


Fig. 3.5 Two frames of reference for phasor quantities for a voltage V_{ti}

Let δ_i (the rotor angle for i -th synchronous machine) be the angle between D and q_i . It can be shown from Fig. 3.5 that,

$$\begin{aligned} V_{Di} &= V_{di} \sin \delta_i + V_{qi} \cos \delta_i \\ V_{Qi} &= -V_{di} \cos \delta_i + V_{qi} \sin \delta_i \end{aligned} \quad (3.15)$$

or,

$$\begin{aligned} V_{Di} + jV_{Qi} &= (V_{di} \sin \delta_i + V_{qi} \cos \delta_i) + j(-V_{di} \cos \delta_i + V_{qi} \sin \delta_i) \\ V_{ti D-Q} &= e^{j\left(\delta_i - \frac{\pi}{2}\right)} V_{ti d-q} \end{aligned} \quad (3.16)$$

Here, $V_{ti D-Q}$ is the terminal voltage on common reference frame $D-Q$ and $V_{ti d-q}$ the terminal voltage $d-q$ frame of machine i .

(3.16) can be written as,

$$V_{t D-Q} = T_r V_{t d-q} \quad (3.17)$$

or,

$$V_{t \, d-q} = T_r^{-1} V_{t \, D-Q} \quad (3.18)$$

where,

$$T_r = \begin{pmatrix} e^{j\left(\delta_1 - \frac{\pi}{2}\right)} & & & \\ & \ddots & & \\ & & \ddots & \\ & & & e^{j\left(\delta_n - \frac{\pi}{2}\right)} \end{pmatrix}, \quad V_{t \, D-Q} = \begin{bmatrix} V_{D1} + jV_{Q1} \\ V_{D2} + jV_{Q2} \\ \vdots \\ V_{Dn} + jV_{Qn} \end{bmatrix}$$

$$V_{t \, d-q} = \begin{bmatrix} V_{d1} + jV_{q1} \\ V_{d2} + jV_{q2} \\ \vdots \\ V_{dn} + jV_{qn} \end{bmatrix}$$

Similarly the currents on the network frame can be written as

$$I_{D-Q} = T_r I_{d-q} \quad (3.19)$$

I_L and V_B in (3.14) are in network frame (D – Q) which can be transformed to d – q frame using (3.17) and (3.19) as,

$$T_r I_{L \, d-q} = Y_b T_r V_{B \, d-q}$$

Pre – multiplying by T_r^{-1} yields,

$$I_{L \, d-q} = (T_r^{-1} Y_b T_r) V_{B \, d-q} \quad (3.20)$$

or,

$$I_{L \, d-q} = Y_m V_{B \, d-q} \quad (3.21)$$

where, $Y_m = (T_r^{-1} Y_b T_r)$ is the reduced admittance matrix transferred to generator coordinates.

For convenience the subscript d – q in (3.21) is dropped from now onwards and is to be assumed that all the variables are referred to generator side unless mentioned otherwise.

The non state variables in (3.13) are eliminated by breaking (3.21) in d – q components as,

$$I_{Ld} + jI_{Lq} = (G_m + jB_m)(V_{Bd} + jV_{Bq}) \quad (3.22)$$

Referring to Fig. 3.6, it can be seen that the multimachine case is similar to SMIB case except that the currents, voltages, STATCOM voltage phase angles (ψ) and m are all vectors and all the reactances are expressed as diagonal matrices.

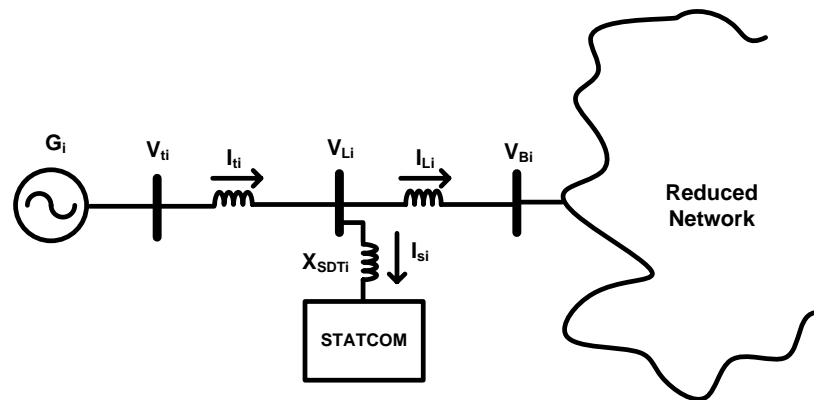


Fig. 3.6 Configuration of the i-th generator in n – machine system

The vector of generator currents of the multimachine system installed with STATCOM can be written as,

$$I_d = \frac{\left(I + \frac{X_{LB}}{X_{SDT}} \right) e'_q - \frac{X_{LB}}{X_{SDT}} mV_{DC} \sin \psi - V_{Bq}}{X_{iL} + X_{LB} + \frac{X_{iL} X_{LB}}{X_{SDT}} + \left(I + \frac{X_{LB}}{X_{SDT}} \right) x'_d} \quad (3.23)$$

$$I_q = \frac{-\left[\frac{X_{LB}}{X_{SDT}} \right] e'_d + \frac{X_{LB}}{X_{SDT}} mV_{DC} \cos \psi + V_{Bd}}{\left[X_{iL} + X_{LB} + \frac{X_{iL} X_{LB}}{X_{SDT}} \right] + \left[I + \frac{X_{LB}}{X_{SDT}} \right] x'_d} \quad (3.24)$$

From (3.23) and (3.24) V_{Bd} and V_{Bq} can be written as

$$V_{Bd} = \left[I + \frac{X_{LB}}{X_{SDT}} \right] e'_d - \frac{X_{LB}}{X_{SDT}} mV_{DC} \cos \psi + \left[X_{iL} + X_{LB} + \frac{X_{iL} X_{LB}}{X_{SDT}} + \left(I + \frac{X_{LB}}{X_{SDT}} \right) x'_d \right] I_q \quad (3.25)$$

$$V_{Bq} = \left[\frac{X_{LB}}{X_{SDT}} \right] e'_q - \frac{X_{LB}}{X_{SDT}} mV_{DC} \sin \psi - \left[X_{iL} + X_{LB} + \frac{X_{iL} X_{LB}}{X_{SDT}} + \left(I + \frac{X_{LB}}{X_{SDT}} \right) x'_d \right] I_d \quad (3.26)$$

The currents injected into the network can be expressed as,

$$I_L = \left(I + \frac{X_{LB}}{X_{SDT}} \right) I_t + j \frac{V_t}{X_{SDT}} - j \frac{V_o}{X_{SDT}} \quad (3.27)$$

Breaking (3.27) in d – q components and solving for I_{Ld} and I_{Lq} gives,

$$I_{Ld} = Z_2 I_d - \frac{e'_q}{X_{SDT}} + \frac{mV_{DC} \sin \psi}{X_{SDT}} \quad (3.28)$$

$$I_{Lq} = Z_3 I_q + \frac{e'_d}{X_{SDT}} - \frac{mV_{DC} \cos \psi}{X_{SDT}} \quad (3.29)$$

From (3.25) and (3.28), V_{Bd} can be written as,

$$V_{Bd} = A_{1d} e'_d + A_3 V_{DC} \cos \psi + N_3 I_{Lq} \quad (3.30)$$

While from (3.26) and (3.29), V_{Bq} can be written as,

$$V_{Bq} = A_1 e'_q + A_2 V_{DC} \sin \psi - N_2 I_{Ld} \quad (3.31)$$

Substituting (3.30) and (3.31) in (3.32) and solving for I_{Ld} and I_{Lq} gives,

$$I_{Ld} = K_4^{-1} K_1^{-1} \left\{ [K_3 B_m A_{1d} + G_{m1} A_{1d}] e'_d + [K_3 G_m A_1 - B_m A_1] e'_q \right. \\ \left. + [K_3 B_m A_3 + G_m A_3] V_{DC} \cos \psi + [K_3 G_m A_2 - B_m A_2] V_{DC} \sin \psi \right\} \quad (3.32)$$

$$I_{Lq} = K_2^{-1} \left\{ B_m A_{1d} e'_d + B_m A_3 V_{DC} \cos \psi + G_m A_1 e'_q + G_m A_2 V_{DC} \sin \psi - G_m N_2 I_{Ld} \right\} \quad (3.33)$$

The non state variable STATCOM current I_s can be expressed as

$$I_s = \frac{V_L - V_o}{jX_{SDT}} \quad (3.34)$$

where,

$$V_o = mV_{DC} (\cos \psi + j \sin \psi) \\ V_L = V_B + jX_{LB} I_L \quad (3.35)$$

Breaking (3.35) in d – q components gives,

$$V_{Ld} + jV_{Lq} = jX_{LB} (I_{Ld} + jI_{Lq}) (V_{Bd} + jV_{Bq}) \quad (3.36)$$

Substituting (3.30) – (3.33) in (3.36) and expressing (3.36) as

$$V_{Ld} = R_{L1}e'_d + R_{L2}e'_q + R_{L3}mV_{DC} \sin \psi + R_{L4}m \cos \psi \quad (3.37)$$

$$V_{Lq} = R_{L5}e'_d + R_{L6}e'_q + R_{L7}mV_{DC} \sin \psi + R_{L8}m \cos \psi \quad (3.38)$$

Substituting (3.37), (3.38) in (3.34) and expressing I_s in d – q components

$$I_{sd} = R_{s1}e'_d + R_{s2}e'_q + R_{s3}mV_{DC} \sin \psi + R_{s4}m \cos \psi \quad (3.39)$$

$$I_{sq} = R_{s5}e'_d + R_{s6}e'_q + R_{s7}mV_{DC} \sin \psi + R_{s8}m \cos \psi \quad (3.40)$$

Finally the generator currents can be expressed as $I_t = I_L + I_s$ or,

$$I_d + jI_q = (I_{Ld} + jI_{Lq}) + (I_{sd} + jI_{sq}) \quad (3.41)$$

Substituting (3.32), (3.33) and (3.39), (3.40) in (3.41) and expressing in terms of d-q components yields,

$$I_d = R_{d1}e'_d + R_{d2}e'_q + R_{d3}mV_{DC} \sin \psi + R_{d4}mV_{DC} \cos \psi \quad (3.42)$$

$$I_q = R_{d5}e'_d + R_{d6}e'_q + R_{d7}mV_{DC} \sin \psi + R_{d8}mV_{DC} \cos \psi \quad (3.43)$$

Equations (3.39) – (3.40) and (3.41) – (3.43) together with (3.13) give the complete non-linear model of multi-machine system with STATCOM.

3.4 LINEARIZED MODEL OF MULTIMACHINE POWER SYSTEM WITH STATCOM

The process of obtaining the system matrices of a non-linear system essentially comprises of obtaining the linearized equations of the entire system and then eliminating the non state variables in terms of state variables.

Linearized equations for the synchronous generator, exciter, STATCOM and the network currents are derived in the following sections.

3.4.1 Linearized of the Synchronous Machine Model

The non-linear model (3.12) of the i-th synchronous machine is linearized around an operating point and expressed in the following perturbed form.

$$\begin{bmatrix} \Delta \dot{e}'_{qi} \\ \Delta \dot{e}'_{di} \\ \Delta \dot{\omega}_i \\ \Delta \dot{\delta}_i \end{bmatrix} = \begin{bmatrix} c_{1i} & 0 \\ 0 & c_{3i} \\ \frac{-e_{doi}}{M_i} & \frac{-e_{qoi}}{M_i} \\ 0 & 0 \end{bmatrix} \begin{bmatrix} \Delta i_{di} \\ \Delta i_{qi} \end{bmatrix} + \begin{pmatrix} c_{2i} & 0 & 0 & 0 \\ 0 & c_{4i} & 0 & 0 \\ \frac{-i_{qoi}}{M_i} & \frac{-i_{doi}}{M_i} & \frac{-k_{Di}}{M_i} & 0 \\ 0 & 0 & 1 & 0 \end{pmatrix} \begin{bmatrix} \Delta e'_{qi} \\ \Delta e'_{di} \\ \Delta \omega \\ \Delta \delta \end{bmatrix} + \begin{bmatrix} c_{2i} \\ 0 \\ 0 \\ 0 \end{bmatrix} \Delta E_{fdi} \quad (3.44)$$

where,

$$\begin{aligned} c_{1i} &= \frac{-(x_{di} - x'_i)}{T'_{doi}} & c_{2i} &= -\frac{1}{T'_{doi}} \\ c_{3i} &= \frac{x_{qi} - x'_i}{T'_{qoi}} & c_{4i} &= -\frac{1}{T'_{qoi}} \end{aligned} \quad (3.45)$$

For 'n' machine system (3.44) can be written as,

$$\Delta \dot{X}_g = [H_t] \Delta I_{tl} + [D] \Delta X_g + [B_e] \Delta E_{fd} \quad (3.46)$$

where,

$$[H_t] = \begin{pmatrix} [H_{t1}] & & \\ & \ddots & \\ & & [H_{tn}] \end{pmatrix}, \quad [D] = \begin{pmatrix} [D_1] & & \\ & \ddots & \\ & & [D_n] \end{pmatrix}, \quad [B_e] = \begin{pmatrix} [B_{e1}] & & \\ & \ddots & \\ & & [B_{en}] \end{pmatrix}$$

$$\begin{aligned} \Delta X_g &= [\Delta e'_{q1} \Delta e'_{d1} \Delta \omega_1 \Delta \delta_1 \cdots \Delta \delta_n]' \\ \Delta I_{tl} &= [\Delta I_{d1} \Delta I_{q1} \Delta I_{d2} \Delta I_{q2} \cdots \Delta I_{qn}]' \\ \Delta E_{fd} &= [\Delta E_{fd1} \Delta E_{fd2} \cdots \Delta E_{fdn}]' \end{aligned}$$

It is now required to express the non state variable ΔI_t in terms of state variables. This can be achieved by Linearising (3.22) as,

$$\Delta I_L = [Y_{mo}] \Delta V_B + [\Delta Y_m] V_{Bo} \quad (3.47)$$

It is worth mentioning here that the reduced admittance matrix Y_m is no longer constant as it has the state δ embedded in it.

Breaking (3.47) in d – q components yields,

$$\begin{aligned} \Delta I_{Ld} + j \Delta I_{Lq} &= (G_{mo} + jB_{mo}) (\Delta V_{Bd} + j \Delta V_{Bq}) \\ &+ \left\{ -j (\Delta \delta (G_{mo} + jB_{mo})) - (G_{mo} + jB_{mo}) \Delta \delta \right\} (V_{Bdo} + j V_{Bqo}) \end{aligned} \quad (3.48)$$

Linearizing (3.25) – (3.26) and substituting in (3.48) gives,

$$\begin{aligned}
\Delta I_{Ld} + j\Delta I_{Lq} = & (G_{mo} + jB_{mo}) \left\{ \left[A_{1d}\Delta e'_d + A_3\Delta m V_{DCo} + A_3m_o\Delta V_{DC} + N_3\Delta I_{Lq} \right] + \right. \\
& \left. j \left[A_1\Delta e'_q + A_2m CV_{DCo} + A_2m_o\Delta V_{DC} - N_2\Delta I_{Ld} \right] \right\} + \\
& \left\{ -j \left[\Delta\delta (G_{mo} + jB_{mo}) - (G_{mo} + jB_{mo})\Delta\delta \right] (V_{Bdo} + jV_{Bqo}) \right\}
\end{aligned} \tag{3.49}$$

Breaking in d-q components in (3.49) and solving for ΔI_{Ld} and ΔI_{Lq} gives,

$$\begin{aligned}
\Delta I_{Ld} &= Y_{L1}\Delta e'_d + Y_{L2}\Delta e'_q + Y_{L3}\Delta V_{DC} + Y_{L4}\Delta m + Y_{L5}\Delta\delta \\
\Delta I_{Lq} &= Y_{L6}\Delta e'_d + Y_{L7}\Delta e'_q + Y_{L8}\Delta V_{DC} + Y_{L9}\Delta m + Y_{L10}\Delta\delta
\end{aligned} \tag{3.50}$$

now consider to obtain expression for generator currents in terms of state variables the Eq. (3.41) is linearized as,

$$\Delta I_t = \Delta I_s + \Delta I_L \tag{3.51}$$

where, ΔI_s is obtained by linearizing (3.34) and (3.35) and is written in terms of d – q components as,

$$\begin{aligned}
\Delta I_{sd} &= Y_{L01}\Delta e'_d + Y_{L02}\Delta e'_q + Y_{L03}\Delta V_{DC} + Y_{L04}\Delta m + Y_{L05}\Delta\delta \\
\Delta I_{sq} &= Y_{L06}\Delta e'_d + Y_{L07}\Delta e'_q + Y_{L08}\Delta V_{DC} + Y_{L09}\Delta m + Y_{L010}\Delta\delta
\end{aligned} \tag{3.52}$$

Arranging the (3.52) in matrix form as,

$$\Delta I_s = [Y_{LON}] \Delta e'_N + [Y_{LOV}] \Delta V_{DC} + [Y_{LOC}] \Delta m + [Y_{LOD}] \Delta\delta \tag{3.53}$$

where,

$$\begin{aligned}
\Delta e'_N &= \left[\Delta e'_{d1} \quad \Delta e'_{q1} \quad \Delta e'_{d2} \quad \Delta e'_{q2} \quad \cdots \quad \Delta e'_{qn} \right]^T \\
\Delta I_s &= \left[\Delta I_{sd1} \quad \Delta I_{sq1} \quad \cdots \quad \Delta I_{sqn} \right]^T
\end{aligned}$$

Substituting (3.50) and (3.52) in (3.51) and expressing ΔI_t in d – q components yields,

$$\begin{aligned}
\Delta I_{id} &= Y_1 \Delta e'_d + Y_2 \Delta e'_q + Y_3 \Delta V_{DC} + Y_4 \Delta m + Y_5 \Delta \delta \\
\Delta I_{iq} &= Y_6 \Delta e'_d + Y_7 \Delta e'_q + Y_8 \Delta V_{DC} + Y_9 \Delta m + Y_{10} \Delta \delta
\end{aligned} \tag{3.54}$$

Arranging the (3.54) in matrix form as,

$$\Delta I_t = [Y_N] \Delta e'_N + [Y_{NV}] \Delta V_{DC} + [Y_{NC}] \Delta m + [Y_{ND}] \Delta \delta \tag{3.55}$$

where,

$$\Delta I_t = [\Delta I_{id1} \quad \Delta I_{iq1} \quad \dots \quad \Delta I_{iqn}]'$$

(3.55) gives the required generator current variations in terms of state variables.

Substituting (3.55) in (3.45) gives,

$$\begin{aligned}
\Delta \dot{X}_g &= [H] \{ [Y_N] \Delta e'_N + [Y_{NV}] \Delta V_{DC} + [Y_{NC}] \Delta m + [Y_{ND}] \Delta \delta \} \\
&\quad + [D] \Delta X_g + [B_e] \Delta E_{fd}
\end{aligned} \tag{3.56}$$

since $\Delta e'_N$ and $\Delta \delta$ are subsets of ΔX_g , by proper matrix manipulation (3.56) can be written as,

$$\Delta \dot{X}_g = [A_m] \Delta X_g + [A_V] \Delta V_{DC} + [B_e] \Delta E_{fd} + [B_{C1}] \Delta m \tag{3.57}$$

Once the equations for exciter and STATCOM are added, ΔE_{fd} and ΔV_{DC} form a part of the state vector.

3.4.2 Linearization of exciter model

The linearized differential equation for the exciter of i-th synchronous machine is obtained from (3.3) as,

$$\Delta \dot{E}_{fdi} = -\frac{K_{Ai}}{T_{Ai}} \Delta V_{ti} - \frac{1}{T_{Ai}} \Delta E_{fdi} \quad (3.58)$$

In (3.58) the change in terminal voltage ΔV_{ti} has to be expressed in terms of the state variables. This can be accomplished using,

$$V_{ti}^2 = V_{di}^2 + V_{qi}^2 \quad (3.59)$$

Linearizing (3.59) gives,

$$\Delta V_{ti} = \frac{V_{doi}}{V_{toi}} \Delta V_{di} + \frac{V_{qoi}}{V_{toi}} \Delta V_{qi} \quad (3.60)$$

Substituting (3.60) in (3.58) and expressing in matrix form gives,

$$\Delta \dot{E}_{fdi} = -\frac{1}{T_{Ai}} \Delta E_{fdi} + \begin{bmatrix} -\frac{K_{Ai} V_{doi}}{T_{Ai} V_{toi}} & -\frac{K_{Ai} V_{qoi}}{T_{Ai} V_{toi}} \end{bmatrix} \begin{bmatrix} \Delta V_{di} \\ \Delta V_{qi} \end{bmatrix} \quad (3.61)$$

For 'n' machine system (3.61) can be written as,

$$\Delta \dot{E}_{fd} = [A_E] \Delta E_{fd} + [E] \Delta V_N \quad (3.62)$$

where,

$$[A_E] = \begin{pmatrix} [A_{E1}] & & \\ & \ddots & \\ & & [A_{En}] \end{pmatrix} \quad [E] = \begin{pmatrix} [E_1] & & \\ & \ddots & \\ & & [E_n] \end{pmatrix}$$

$$\Delta \mathbf{E}_{fd} = [\Delta E_{fd1} \quad \Delta E_{fd2} \quad \dots \quad \Delta E_{fdn}]'$$

$$\Delta \mathbf{V}_N = [\Delta V_{d1} \quad \Delta V_{q1} \quad \dots \quad \Delta V_{qn}]'$$

$\Delta \mathbf{V}_N$ for 'n' machine system can be expressed as,

$$\Delta \mathbf{V}_N = [\mathbf{Z}_A] \Delta \mathbf{I}_t + \Delta \mathbf{e}'_N \quad (3.63)$$

where,

$$[\mathbf{Z}_A] = \begin{pmatrix} \begin{pmatrix} 0 & x'_{d1} \\ -x'_{d1} & 0 \end{pmatrix} & & \\ & \ddots & \\ & & \begin{pmatrix} 0 & x'_{dn} \\ -x'_{dn} & 0 \end{pmatrix} \end{pmatrix}$$

Substituting (3.63) in (3.62) gives,

$$\Delta \dot{\mathbf{E}}_{fd} = [\mathbf{A}_E] \Delta \mathbf{E}_{fd} + [\mathbf{E}] \{ [\mathbf{Z}_A] \Delta \mathbf{I}_t + \Delta \mathbf{e}'_N \} \quad (3.64)$$

Substituting (3.55) in (3.64) and after proper matrix manipulations the linearized model of excitation system can be written as,

$$\Delta \dot{\mathbf{E}}_{fd} = [\mathbf{A}_{me}] \Delta \mathbf{X}_g + [\mathbf{A}_E] \Delta \mathbf{E}_{fd} + [\mathbf{A}_{ve}] \Delta V_{DC} + [\mathbf{B}_{c2}] \Delta m \quad (3.65)$$

3.4.3 Linearization of STATCOM model

The non-linear model of STATCOM for the i -th machine can be written as,

$$\dot{V}_{DCi} = \frac{m_i}{C_{Dci}} \{ F_{di} I_{sdi} + F_{qi} I_{sqi} \} \quad (3.66)$$

Linearizing (3.66) and writing in matrix form as,

$$\Delta \dot{V}_{DCi} = \begin{bmatrix} \frac{F_{doi}}{C_{Dci}} & \frac{F_{qoi}}{C_{Dci}} \end{bmatrix} \begin{bmatrix} \Delta I_{sdi} \\ \Delta I_{sqi} \end{bmatrix} \quad (3.67)$$

For 'n' machine system (3.67) can be written as,

$$\Delta \dot{V}_{DC} = [Y_{Lo}] \Delta I_s \quad (3.68)$$

where,

$$[Y_{Lo}] = \begin{pmatrix} \begin{bmatrix} \frac{F_{do1}}{C_{Dc1}} & \frac{F_{qo1}}{C_{Dc1}} \end{bmatrix} & & \\ & \ddots & \\ & & \begin{bmatrix} \frac{F_{don}}{C_{Dcn}} & \frac{F_{qon}}{C_{Dcn}} \end{bmatrix} \end{pmatrix}$$

$$\Delta I_s = [\Delta I_{sd1} \quad \Delta I_{sq1} \quad \cdots \quad \Delta I_{sqn}]$$

Substituting (3.53) in (3.68) and after proper matrix manipulations, the linearized model for STATCOM is given by,

$$\Delta \dot{V}_{DCi} = [A_{Lom}] \Delta X_g + [A_{Lom}] \Delta V_{DC} + [B_{c3}] \Delta m \quad (3.69)$$

The linearized model of multimachine power system with STATCOM can be obtained by combining (3.57), (3.65) and (3.69) and is given by,

$$\Delta\dot{X} = [A_{matrix}] \Delta X + [B_{matrix}] \Delta C \quad (3.70)$$

where,

$$A_{matrix} = \begin{pmatrix} A_m & B_e & A_v \\ A_{me} & A_e & A_{ve} \\ A_{LOm} & 0 & A_{LOv} \end{pmatrix}$$

$$B_{matrix} = \begin{bmatrix} B_{c1} \\ B_{c2} \\ B_{c3} \end{bmatrix}$$

Detailed derivations for the constants are included in Appendix C.

CHAPTER 4

ROBUST STATCOM CONTROL

STATCOM control can improve the transmission capacity considerably and can thus enhance the transient stability margin of the power system. Damping enhancement through STATCOM is an active topic of research among power system control engineers in recent times. Many control strategies for STATCOM are reported in the literature. Some of the examples of controllers used are, the simple lead lag controllers, PID controllers etc. Most of these controllers however, are designed through linear models making them operating point dependent. This chapter presents a robust design procedure

which primarily depends on a graphical loop shaping technique. The control design is enhanced by embedding particle swarm optimization (PSO) technique.

4.1 THE ROBUST CONTROLLER DESIGN THROUGH GRAPHICAL LOOP-SHAPING

Robust design of the STATCOM controllers starts by linearizing nonlinear system equations,

$$\dot{x} = f(x, u) \quad (4.1)$$

which correspond to (3.7) for the single machine system and (3.13) for the multimachine power system problem.

The corresponding linearized state models are,

$$\begin{aligned} \dot{x} &= Ax + Bu \\ y &= Hx \end{aligned} \quad (4.2)$$

where x and u represents the perturbations from the nominal states and control variables.

H represents the relation between the state vector x and the chosen output y .

The nominal plant transfer function P between the input u and output y of the linearized system is,

$$P = H[sI - A]^{-1}B \quad (4.3)$$

The changes in operating points of the nonlinear system can be considered as perturbations in the coefficients of the linearized system matrices A , B and H . These perturbations are modeled as multiplicative uncertainties and robust controller design is arrived at for the ranges of perturbation in the design procedure [20, 69, 70]. This section

gives a brief theory of uncertainty modeling, the robust stability criterion and graphical loop-shaping, which is employed to design the robust controller. Finally, the flow chart for robust control design by graphical loop-shaping technique is given.

4.1.1 Uncertainty modeling

Suppose that the nominal plant transfer function of a plant P belongs to a bounded set of transfer functions \mathcal{P} and consider the perturbed transfer function because of the variations of its parameters can be expressed in the form,

$$\hat{P} = [1 + \Delta W_2] P \quad (4.4)$$

where, \hat{P} is a perturbed plant transfer function, Δ is a variable stable transfer function satisfying $\|\Delta\|_\infty \leq 1$ and W_2 is a fixed, stable and proper transfer function (also called the weight)

The infinity norm (∞ -norm) of a function is the least upper bound of its absolute value, also written as $\|\Delta\|_\infty = \sup_\omega |\Delta(j\omega)|$, is the largest value of gain on a Bode magnitude plot.

The uncertainties, which are the variations in system operating conditions, are thus modeled through \hat{P} in (4.4)

In the multiplicative uncertainty model given by (4.4), ΔW_2 is the normalized plant perturbation away from 1. If $\|\Delta\|_\infty < 1$, then

$$\left| \frac{\hat{P}(j\omega)}{P(j\omega)} - 1 \right| \leq |W_2(j\omega)|, \quad \forall \omega \quad (4.5)$$

So, $|W_2(j\omega)|$ provides the uncertainty profile, and in the frequency plane is the upper boundary of all normalized plant transfer functions away from 1.

4.1.2 Robust stability and performance

Consider a multi-input control system given in Fig. 4.1. A controller C provides robust stability if it provides internal stability for every plant in the uncertainty set \mathcal{P} . If L denotes the open-loop transfer function ($L=PC$), then the sensitivity function is written as,

$$S = \frac{1}{1+L} \quad (4.6)$$

The complimentary sensitivity function or the input output-transfer function is given by,

$$T = 1 - S = \frac{PC}{1+PC} \quad (4.7)$$

For a multiplicative perturbation model, robust stability condition is met if and only if $\|W_2T\|_\infty < 1$. This implies that

$$\left| \frac{W_2(j\omega)L(j\omega)}{1+L(j\omega)} \right| < 1, \text{ for all } \omega \quad (4.8)$$

or,

$$|\Delta(j\omega)W_2(j\omega)L(j\omega)| < |1+L(j\omega)| \text{ for all } \omega, \text{ and } \|\Delta\|_\infty < 1 \quad (4.9)$$

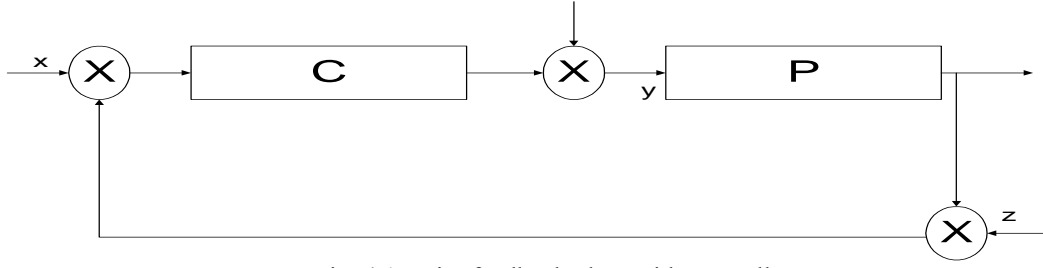


Fig. 4.1 Unity feedback plant with controller

The block diagram of a typical perturbed system, ignoring all inputs, is shown in Fig. 4.2. The transfer function from output of Δ to the input of Δ equals $-W_2T$. The properties of the block diagram can be reduced to those of the configuration given in Fig. 4.3.

The maximum loop gain $-\|W_2T\|_\infty$ is less than 1 for all allowable Δ if and only if the small gain condition $\|W_2T\|_\infty < 1$ holds. The nominal performance condition for an internally stable system is given as $\|W_1S\|_\infty < 1$, where W_1 is a real-rational, stable, minimum phase transfer function, also called a weighting function. If P is perturbed to $\hat{P} = (1 + \Delta W_2)P$, S is perturbed to,

$$\hat{S} = \frac{1}{1 + (1 + \Delta W_2)L} = \frac{S}{1 + \Delta W_2T} \quad (4.10)$$

The robust performance condition can therefore be expressed as,

$$\|W_2T\|_\infty < 1, \text{ and } \left\| \frac{W_1S}{1 + \Delta W_2T} \right\|_\infty < 1, \forall \|\Delta\|_\infty < 1 \quad (4.11)$$

Combining the above equations, it can be shown that a necessary and sufficient condition for robust stability and performance is,

$$\| |W_1S| + |W_2T| \|_\infty < 1 \quad (4.12)$$

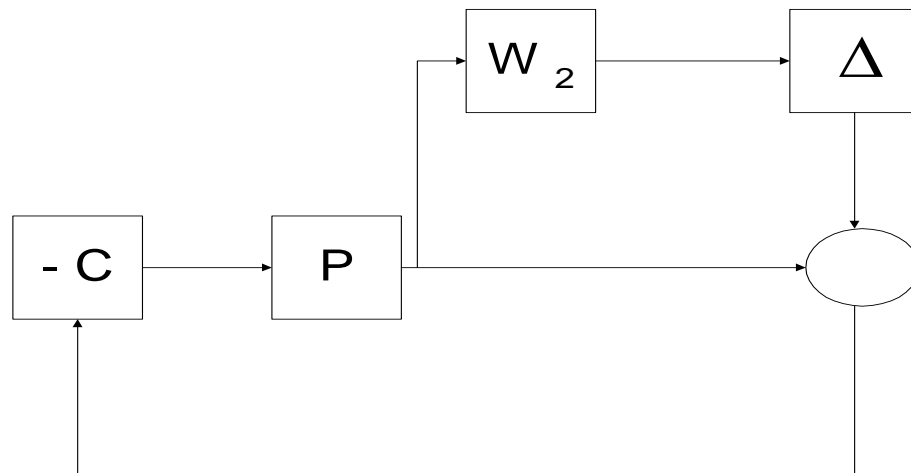


Fig. 4.2 Feed back loop with uncertainty representation.

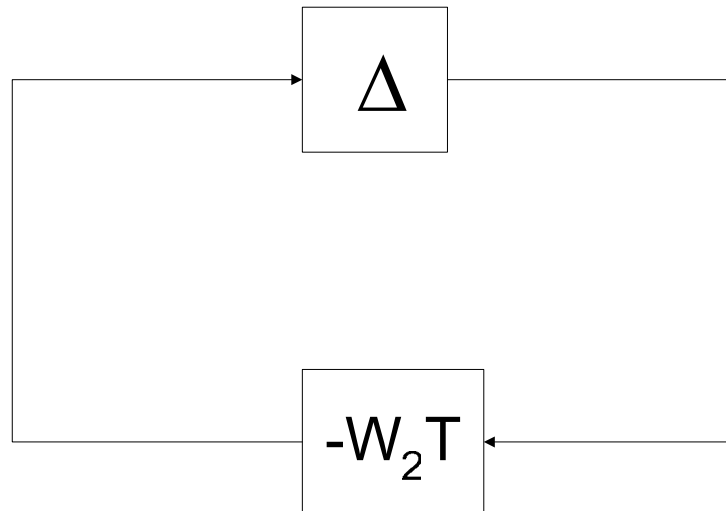


Fig. 4.3 Feed back loop in standard reduced form.

4.1.3 Graphical loop-shaping technique

Loop shaping is a graphical procedure to design a proper controller C satisfying robust stability and performance criteria given in (4.12). The basic idea of the method is to construct the loop transfer function, $L = PC$ to satisfy the robust performance criterion approximately, and then to obtain the controller from the relationship $C = L/P$. Internal stability of the plants and properness of C constitute the constraints of the method. Condition on L is such that PC should not have any pole zero cancellation. A necessary condition for robustness is that either $|W_1|$, $|W_2|$ must be less than 1. For a monotonically decreasing function W_1 , it can be shown that at low frequency the open-loop transfer function L should satisfy

$$|L| > \frac{|W_1|}{1 - |W_2|} \quad (4.13)$$

while, for high frequency,

$$|L| < \frac{1 - |W_1|}{|W_2|} \approx \frac{1}{|W_2|} \quad (4.14)$$

At high frequency $|L|$ should roll off at least as quickly as $|P|$ does. This ensures properness of C . The general features of open loop transfer function are that the gain at low frequency should be large enough, and $|L|$ should not drop-off too quickly near the crossover frequency to avoid internal instability.

Steps in the controller design include: determination of dB-magnitude plots for P and \hat{P} , finding W_2 from (4.5), choosing L subject to (4.13-4.14), check for the robustness criteria, constructing C from L/P and checking internal stability. The process is repeated until satisfactory L and C are obtained.

4.1.4 The Algorithm

The general algorithm for the loop-shaping design procedure can be outlined as,

- Obtain the db-magnitude plot for the nominal as well as perturbed plant transfer functions.
- Construct W_2 satisfying the constraint given in (4.5)

On this plot, fit a graph of the magnitude of the open-loop transfer function L ,

whereby

$$|L| > \frac{|W_1|}{1 - |W_2|} \quad \text{at low frequencies}$$

and

$$|L| < \frac{1 - |W_1|}{|W_2|} \quad \text{at high frequencies.}$$

- Obtain a stable minimum- phase open-loop transfer function L for the gain $|L|$ already constructed, normalizing so that $L(0) > 0$. The latter condition guarantees negative feedback.
- Recover the controller C from the condition $L = PC$
- Verify the nominal and robust stability conditions of (4.12).
- Test for the internal stability by direct simulation of the closed loop transfer function for pre-selected disturbances or inputs.
- Repeat the procedure until satisfactory L and C are obtained. Note that a robust controller may not exist for all nominal conditions, and if it does, it may not be unique.

The flow chart in Fig. 4.4 summarizes the steps outlined.

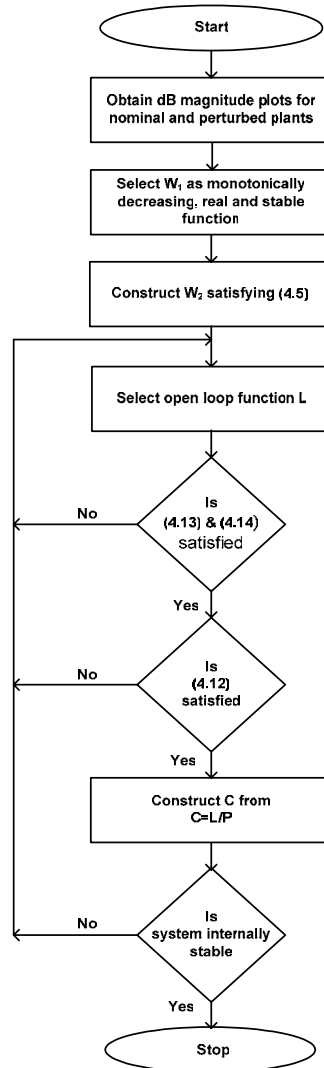


Fig. 4.4 Flow chart for robust control design by graphical method.

4.2 THE PARTICLE SWARM OPTIMIZATION

The robust control design presented in section 4.1 involves an iterative procedure in frequency domain. The procedure starts by assuming an open loop function L subject to satisfying several constraints including (4.13)-(4.14). Once a satisfactory L is constructed, the controller function C is then constructed. Though the method is simple, too many iterations may be needed for a successful design. The method can be enhanced by introducing some optimization algorithm to calculate constraints efficiently thus reducing the amount of iterative calculations. Also, the procedure would be more efficient if it starts with a selection of controller function C , rather than L . In this work, a particle swarm optimization (PSO) algorithm has been employed to replace some of the iterative graphical construction procedure. The theory of the PSO is presented briefly in the following.

The particle swarm optimization is an evolutionary computation technique developed by Eberhart and Kennedy inspired by the social behavior of bird flocking and fish schooling [63]. PSO is a population based optimization tool. Population is formed by a predetermined number of particles; each particle is a candidate solution to the problem. In a PSO system, particles fly around in a multi-dimensional search space until relatively unchanging positions have been encountered or until computational limits are exceeded. During the flight, each particle adjusts its position according to its own experience and experience of its neighboring particles. Compared to other evolutionary algorithms the merit of PSO is that, it has memory i.e., every particle remembers its best solution (local

best, ‘ J_{pbest} ’) as well as the group’s best solution (global best, ‘ J_{gbest} ’). The algorithm is simple, fast and can be programmed in few steps [64, 65, 66].

In PSO each particle adjusts its flight according to its own and its companion’s flying experience. The best position in the course of flight of each particle(s) is called X_{pbest} , and the solution associated with it is denoted by J_{pbest} . Initially J_{gbest} (global best) is set to J_{pbest} and the particle(s) associated with it is denoted by X_{gbest} . Later on as the particle(s) is updated, J_{gbest} represents the best solution attained by the whole population and X_{gbest} denotes the corresponding best position. Every particle(s) updates itself through the above mentioned best positions. The particle(s) updates its own velocity and position according to the following equations [67, 68],

$$V_i = QV_i + K_1 rand_1() (X_{pbest} - X_i) + K_2 rand_2() (X_{gbest} - X_i) \quad (4.15)$$

$$X = X_i + V_i \quad (4.16)$$

where K_1 and K_2 are two positive constants, $rand_1()$ and $rand_2()$ are random numbers in the range $[0, 1]$, and Q is the inertia weight. X_i represents position of the i -th particle and V_i is its velocity. The first term in (4.15) is the former velocity of the particle(s), the second is the cognition modal, which expresses the thought of the particle itself, and the third represents the social model. The three parts together determines the space searching ability. The first part has the ability to search for local minimum. The second part causes the swarm to have a strong ability to search for global minimum and avoid local minimum. The third part reflects the information sharing among the particles. Under the influence of the three parts, the particle can reach the best position.

4.2.1 The Algorithm

The PSO algorithm used in this thesis can be briefly discussed by the following steps.

- 1: Initialize a population of ‘pop’ particles with random positions within the lower and upper bound of the problem space. Similarly initialize randomly ‘pop’ velocities associated with the particles.
- 2: Evaluate the optimization fitness functions J for the initial population.
- 3: Find the minimum fitness value for fitness functions J in step 2 and call it J_{pbest} and let the particle associated with it be X_{pbest} .
- 4: Initially set J_{gbest} equal to J_{pbest} .
- 5: Update the weight Q using the following equation

$$Q = Q_{max} - \left(\frac{Q_{max} - Q_{min}}{iter_{max}} \right) iter \quad (4.17)$$

‘iter’ is the iteration count

- 6: Update the velocity of each particle using (4.15)
- 7: Check V for the range $[V_{max}, V_{min}]$. If not, set it to the limiting values.
- 8: Update the position of each particle using (4.16) which gives the new population.
- 9: Repeat 7 for the new population.
- 10: Evaluate the optimization fitness functions J for new population.
- 11: Obtain J_{pbest} for fitness functions J in step 10.
- 12: Compare the J_{pbest} obtained in step 11 with J_{gbest} . If J_{pbest} is better than J_{gbest} then set J_{gbest} to J_{pbest} .

13: Stop if convergence criteria are met, otherwise go to step 5. The stopping criteria are, good fitness value, reaching maximum number of iterations, or no further improvement in fitness.

4.3 ROBUST CONTROL DESIGN THROUGH PSO BASED LOOP-SHAPING

The graphical loop shaping assumes the open loop function L and calculates the controller function. In the proposed PSO based loop-shaping, the controller structure is pre-selected as,

$$C(s) = \frac{b_m s^m + \dots + b_1 s + b_o}{a_n s^n + \dots + a_1 s + a_o} \quad (4.18)$$

The advantage is that the controller order (n) can be assumed a priori, reducing the computational effort. The open loop function L is then constructed as,

$$L(s) = P(s)C(s) \quad (4.19)$$

The performance index J in steps 2 and 10 of the PSO algorithm is chosen to include the robust performance and stability criterion (4.12), the constraints on L given in (4.13-4.14), etc. The performance index is expressed as,

$$J = \sum_{i=1}^N r_i J_{Bi} + r_o J_S \quad (4.20)$$

where, J_{Bi} are the robust stability indices and J_S is the stability index. r_i and r_o are the penalties associated with the respective indices and N are the number of frequency points in Bode plot of $L(j\omega)$.

In this thesis, robust stability constraints are obtained from graphical method using Bode plots. At each frequency ω_i , the magnitude of open-loop transmission $L(j\omega_i)$ is calculated

and then checked to see whether or not the robust stability constraint is satisfied at that frequency. A robust stability index is included in the performance index and is given by,

$$J_{Bi} = \begin{cases} 0 & \text{if constraint at } \omega_i \text{ is satisfied} \\ 1 & \text{otherwise} \end{cases} \quad (4.21)$$

$i = 1, 2, 3, \dots, N$

The stability of the closed loop nominal system is simply tested by solving the roots of characteristic polynomial and then checking whether all the roots lie in the left side of the complex plane. The stability index J_s is defined as,

$$J_s = \begin{cases} 0 & \text{if stable} \\ 1 & \text{otherwise} \end{cases} \quad (4.22)$$

The coefficients b_m, \dots, b_1 and a_n, \dots, a_1 are searched by the PSO algorithm to satisfy the constraint equations. a_n can be set to 1.

4.3.1 The Algorithm

The PSO algorithm starts by assuming the controller coefficients a 's and b 's in (4.18), calculates $L(j\omega) = P(j\omega)C(j\omega)$ then evaluates the performance index J which includes all the robustness specifications. The PSO algorithm updates the controller parameters using (4.15) and (4.16) until a satisfactory controller is arrived. The algorithm for the search of the desired robust controller using PSO can be stated as,

- 1: Obtain the db-magnitude plot for the nominal as well as perturbed plant transfer functions.
- 2: Construct W_1 and W_2 as explained in sec. 4.1.
- 3: Choose the population size pop , and the number of iterations for PSO.

- 4: Specify the order m of the robust controller
- 5: Specify the lower and upper bounds for optimization variables in Eq. (4.18). In this study the lower and upper bounds chosen are 0 and 10^5 for all the optimization variables.
- 6: Set the iteration counter 'iter' to zero and generate randomly pop particles of optimization variables with in the lower and upper bounds. Also generate randomly initial velocities for all pop particles in the population.
- 7: Construct $C(s)$ and $L(s)$ using Eq. (4.18) and Eq. (4.19) respectively.
- 8: Evaluate the desired performance index J given by Eq. (4.20) for the initial population
- 9: Obtain J_{pbest} and X_{pbest} for the initial population in previous step.
- 10: Initialize J_{gbest} and X_{gbest} to J_{pbest} and X_{pbest} respectively.
- 11: Update the weight Q using Eq. (4.17).
- 12: Update velocity of each particle using Eq. (4.15).
- 13: Check whether the velocities are within the range. If not, adjust the velocities so as to be inside the range.
- 14: Update the position of each particle using Eq. (4.16) which gives the new population and also update X_{gbest} .
- 15: Repeat step 13 for the new population obtained in previous step.
- 16: Obtain J_{pbest} and X_{pbest} for the new population.
- 14: Compare the J_{pbest} obtained in 16 with J_{gbest} . If J_{pbest} is better than J_{gbest} then set J_{gbest} to J_{pbest} .
- 17: Update the iteration counter to $iter+1$.
- 18: Loop to 11, until a stopping a criterion is satisfied.

The flow chart for the proposed PSO based loop-shaping is shown in Fig. 4.5

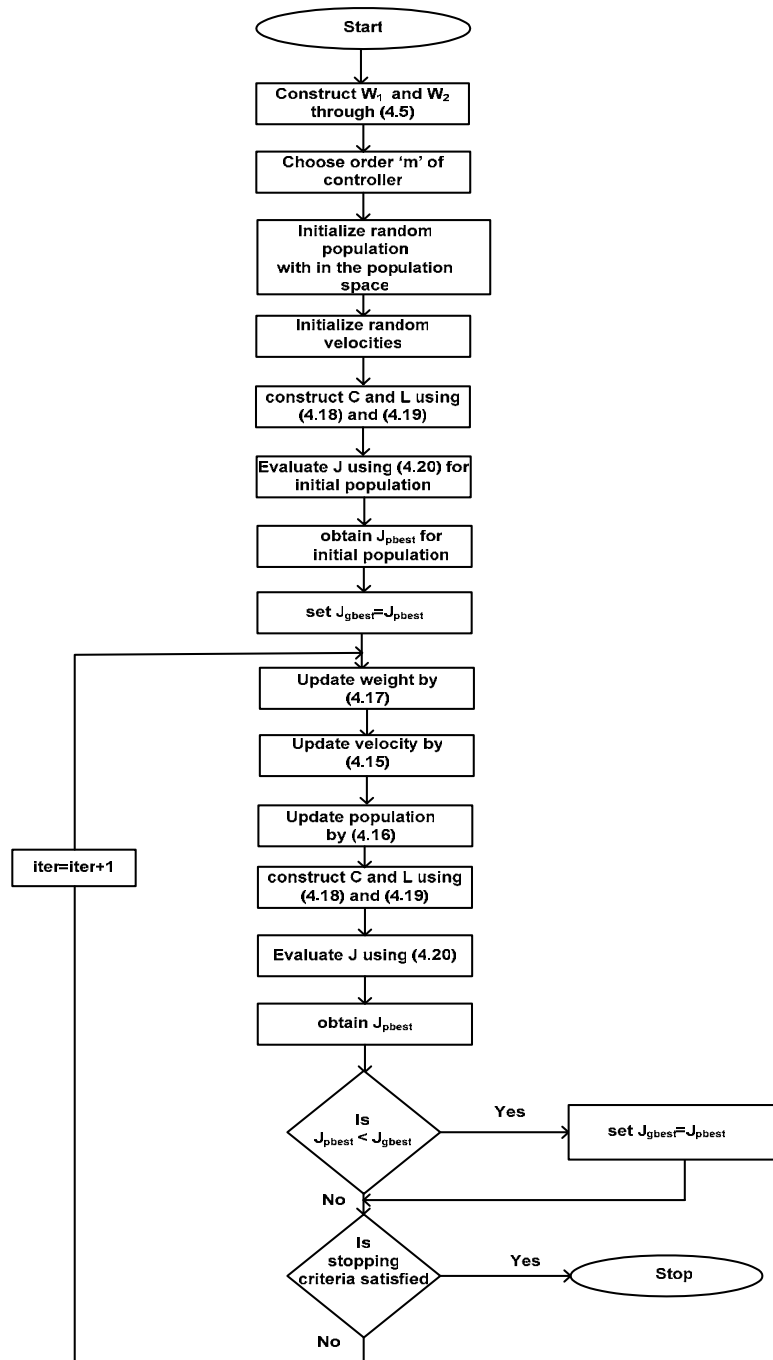


Fig. 4.5 Flow chart for the proposed PSO based loop-shaping.

CHAPTER 5

SIMULATION RESULTS : SINGLE MACHINE CASE

The single machine infinite bus system given in Fig. 5.1 was simulated to test the robust control design. The system data is given in Appendix A. Two STATCOM controls identified for single machine system in (3.13) are Δm and $\Delta \psi$. Earlier studies showed that $\Delta \psi$ control does not provide any extra damping to a power system [20,21,22] and hence has not been included in this study. A manual loop-shaping based robust control design for voltage magnitude has been reported in the literature [20]. This study proposes an enhanced loop-shaping robust controller using PSO, and simulation results with the original loop-shaping method are used for comparison.

Simulation results for robust control design by manual and PSO based loop-shaping are presented in this chapter.

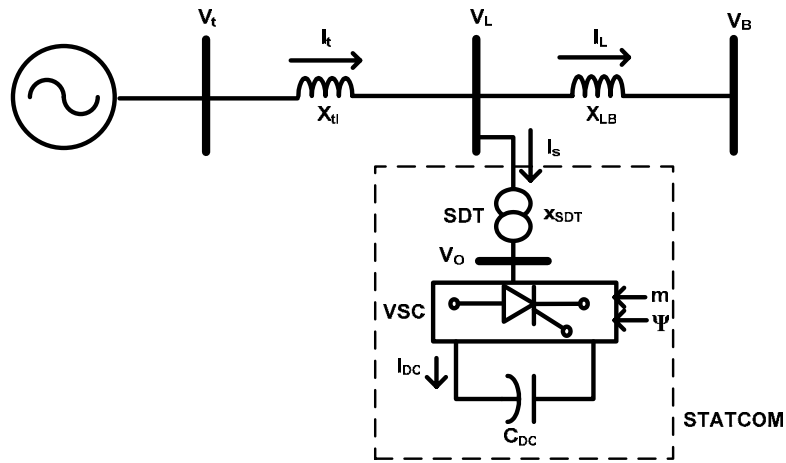


Fig. 5.1 STATCOM installed in SMIB power system

The nominal plant transfer function P is taken for power output of 0.9 at unity power factor load and is obtained as,

$$P = \frac{0.2466s^2(s+100.774)(s-0.214309)}{(s+99.123)(s+1.0901)(s+0.0527)(s^2+0.65484s+21.4956)} \quad (5.1)$$

The collapsed block diagram for magnitude control is shown in Fig. 5.2. The db magnitude vs. frequency plot for the nominal and perturbed plant are shown in Fig. 5.3

from this plot the quantity $|\frac{\hat{P}(j\omega)}{P(j\omega)} - 1|$ is constructed and is shown in Fig. 5.4 off nominal

operating points for output power ranges from 0.8 p.u to 1.4 p.u and the power factor from 0.8 lagging to 0.8 leading were considered. The function W_2 fitting the relationship

$|\frac{\hat{P}(j\omega)}{P(j\omega)} - 1| \leq W_2(j\omega)$ is constructed as,

$$W_2(s) = \frac{0.9(s + 14.6138)(s + 2.0528)}{s^2 + 5s + 31} \quad (5.2)$$

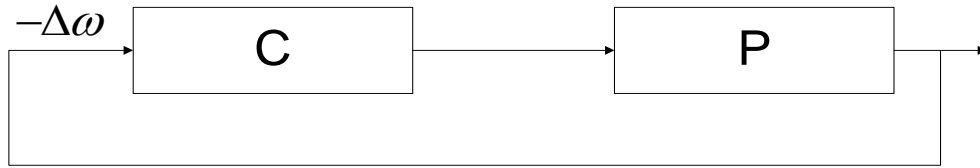


Figure 5.2 Collapsed block diagram for robust C controller

The function W_1 was selected as,

$$W_1(s) = \frac{K_d f_c^2}{s^3 + 2s^2 f_c + 2s f_c^2 + f_c^3} \quad (5.3)$$

K_d and f_c were selected as 0.01 and 1 respectively. The open-loop transfer function $L(s)$ which satisfies the loop-shaping criteria was constructed manually and is given as,

$$L(s) = \frac{5(s + 100.83)(s + 10)(s - 0.2340)(s + 0.01)}{(s + 9.99)(s + 0.10)(s + 0.01)(s^2 + 0.6754s + 21.6344)} \quad (5.4)$$

The db magnitude vs. frequency plot relating L , W_1 and W_2 is shown in Fig. 5.5.

Fig. 5.6 shows the plots for the nominal and robust performance criterion.

From the relation $L(s) = P(s) C(s)$, the controller transfer function was constructed as,

$$C(s) = \frac{23.764(s + 100.84)(s + 0.100)(s + 0.109)(s + 0.047)(s + 0.001)}{s^2(s + 9.28)(s + 0.12)(s + 0.01)} \quad (5.5)$$

The controller designed by graphical loop-shaping technique was tested by simulating the power system model Fig. 5.1 for a disturbance of 50% torque input pulse of 0.1s duration. The simulation results obtained for a number of operating points are given in Fig. 5.7.

The response recorded is the variation in rotor angle. Fig. 5.7 shows the rotor angle variation for the following operating condition:

- a) Power output of 1.2 at 0.98 leading power factor.
- b) Unity power output at 0.95 lagging power factor.
- c) Nominal operating condition and,
- d) Power output of 0.5 at 0.95 lagging power factor.

It was observed that robust controller designed by graphical loop-shaping provides good damping for all operating conditions. Fig. 5.8 shows the variations of the STATCOM DC voltage for a disturbance of 50% torque input pulse of 0.1s.

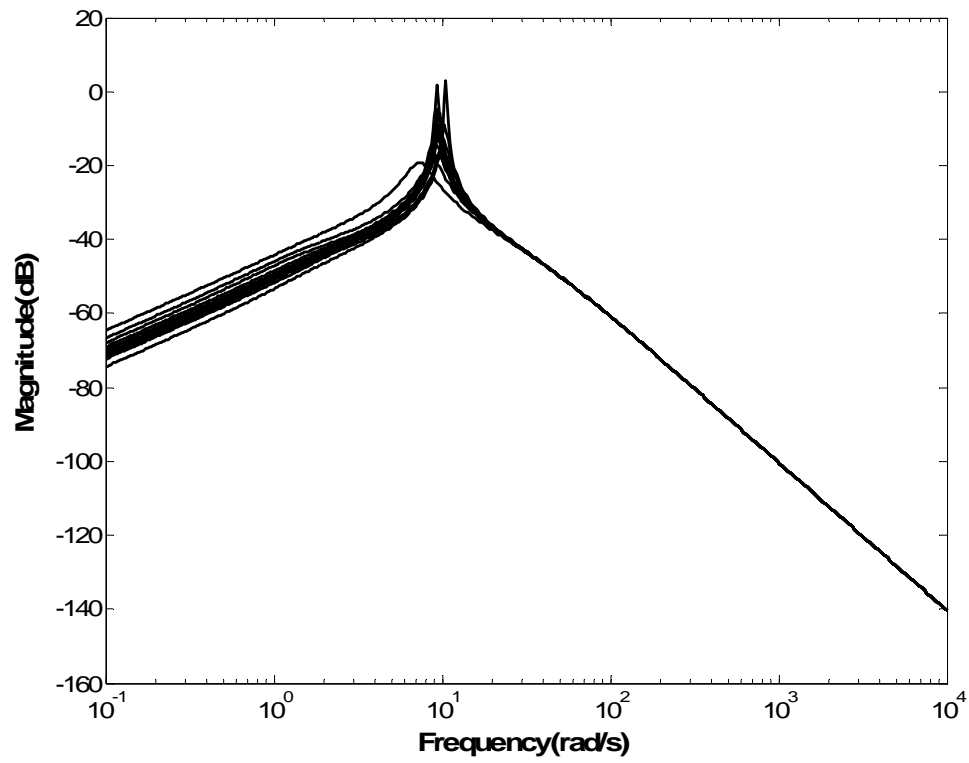


Figure 5.3 nominal and perturbed plant transfer functions for robust speed feedback system.

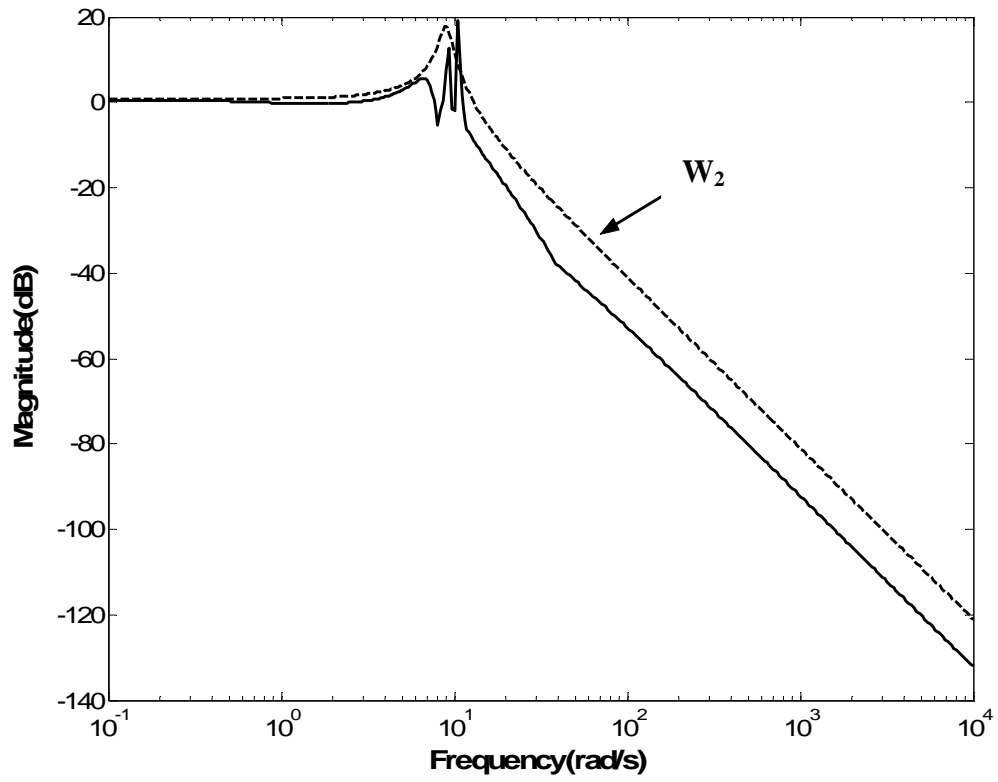


Fig. 5.4 The uncertainty profile and W_2 .

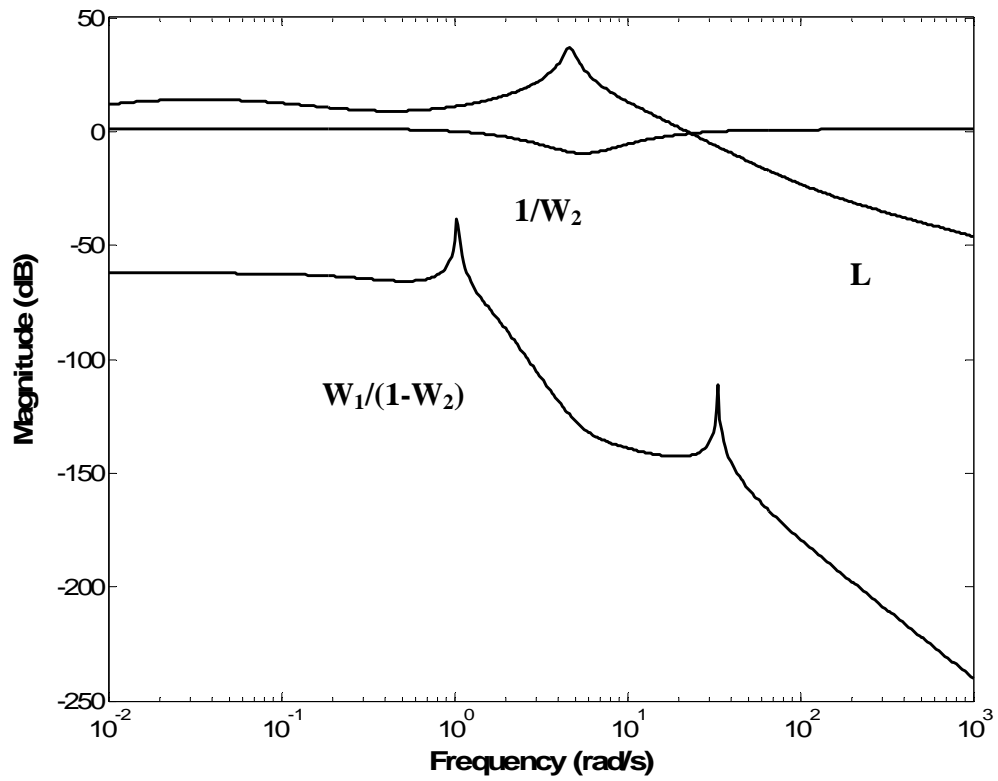


Fig. 5.5 Graphical Loop-Shaping plots relating W_1 , W_2 and L

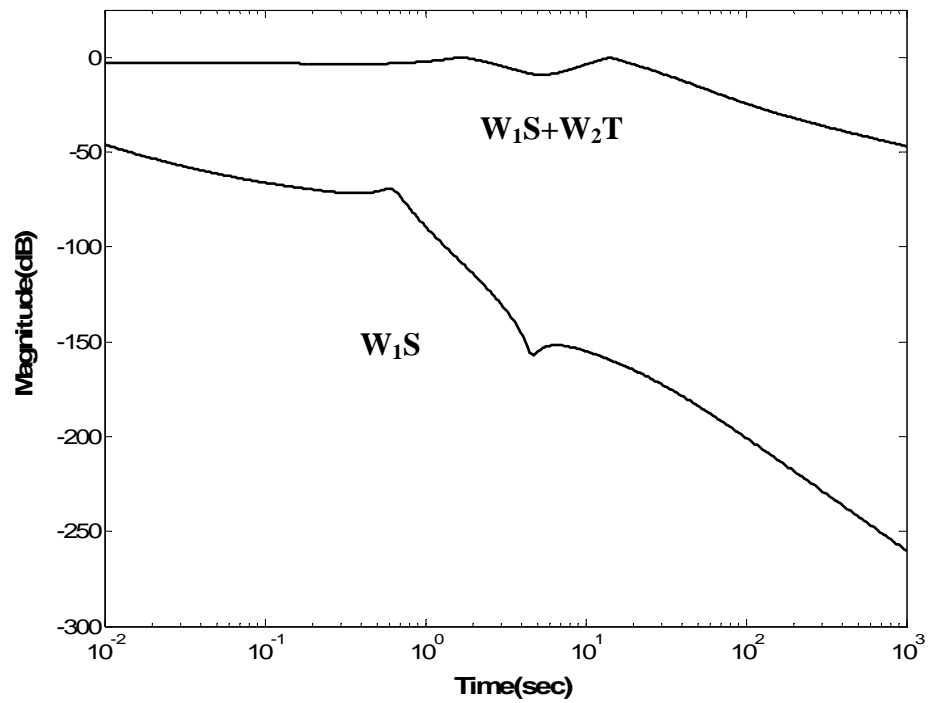


Fig. 5.6 Robust and nominal performance criteria (graphical loop-shaping)

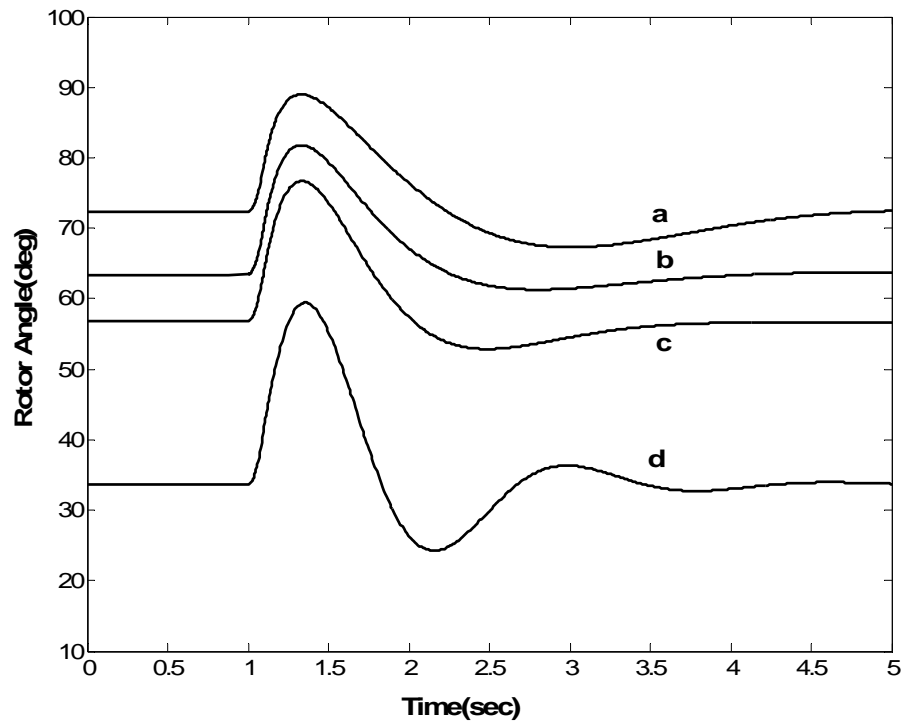


Fig. 5.7 Rotor angle with robust controller for a disturbance of 50% Torque pulse for 0.1s

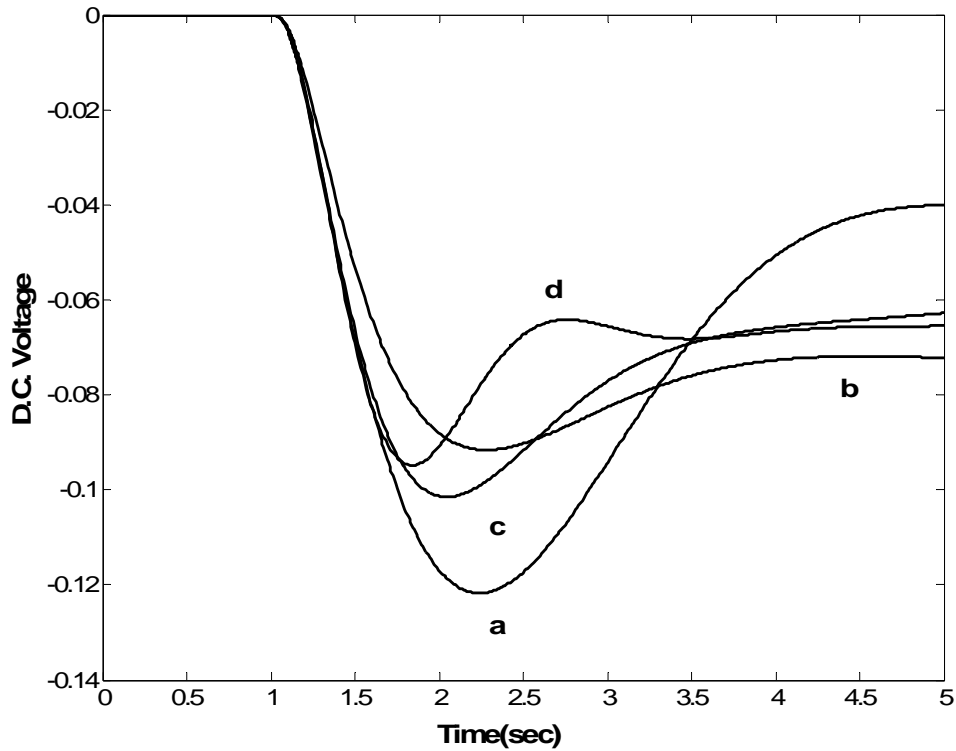


Fig. 5.8 D.C. voltage variations corresponding to Fig. 5.7.

5.1 ROBUST LOOP-SHAPING DESIGN USING PSO

Computation of the robust controller using PSO starts with $W1$ and $W2$ arrived at through the original graphical method given in previous section. A second order controller function was designed by implementing the proposed algorithm. It is given as,

$$C(s) = \frac{b_2 s^2 + b_1 s + b_0}{a_2 s^2 + a_1 s + a_0} \quad (5.6)$$

The coefficients a 's and b 's are determined by the PSO algorithm. The chosen values of the various parameters required by the PSO algorithm are given in Table 5.1.

TABLE 5.1: PSO parameters

Parameters	Values
Maximum iteration	1000
Population size	20
Value of C 1	2.0
Value of C 2	2.0
Maximum Weight	0.90
Minimum Weight	0.40

The PSO algorithm converged to give the following robust controller function,

$$C(s) = \frac{25 \times 10^3 (s + 3.9998)(s + 0.0002)}{s^2 + 0.07454s + 2.797} \quad (5.7)$$

The open loop function $L(s)$ constructed from $L(s) = P(s)C(s)$ is,

$$L(s) = \frac{5.26 \times 10^3 \times s^2 (s + 4)(s + 0.1008)(s - 0.0002)(s + 0.0002)}{(s + 99.18)(s + 1.094)(s + 0.0476)(s^2 + 0.6751s + 21.6318)(s^2 + 0.0745s + 2.7969)} \quad (5.8)$$

The dB magnitude vs. frequency plots relating $L(s)$, $W_1(s)$ and $W_2(s)$ obtained through the PSO based method is shown in Fig. 5.9. It can be observed from the figure that loop-shaping requirements on $L(s)$ are satisfied at all frequencies. The plots for the nominal and robust performance criteria are shown in Fig. 5.10 while the nominal performance measure is well satisfied, the combined robust stability and performance measure has a small peak.

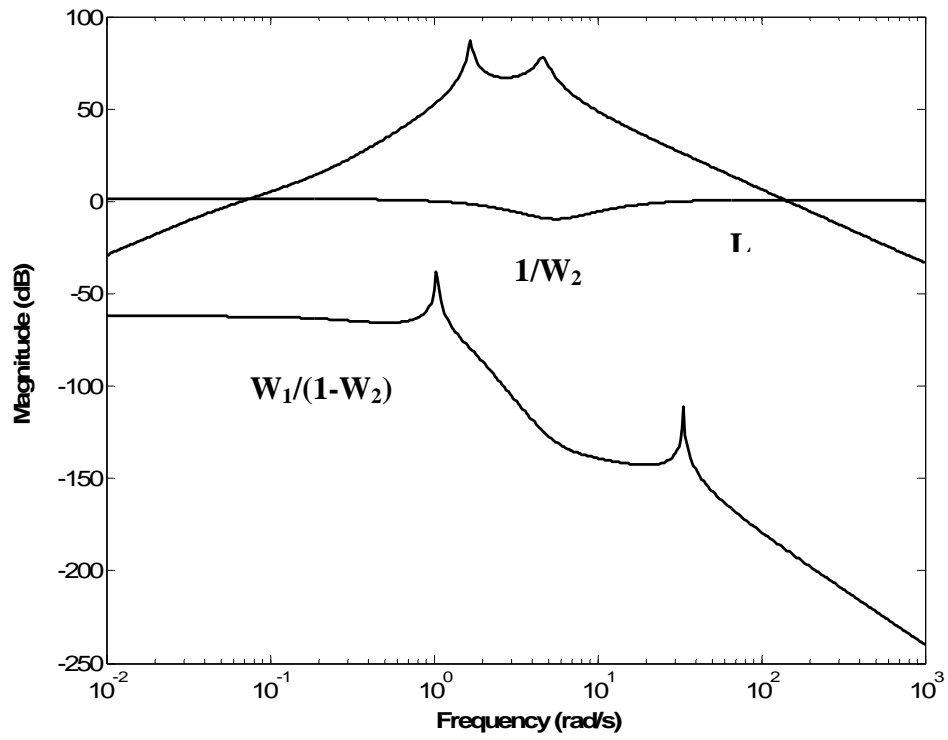


Fig. 5.9 PSO based Loop-Shaping plots relating W_1 , W_2 and L

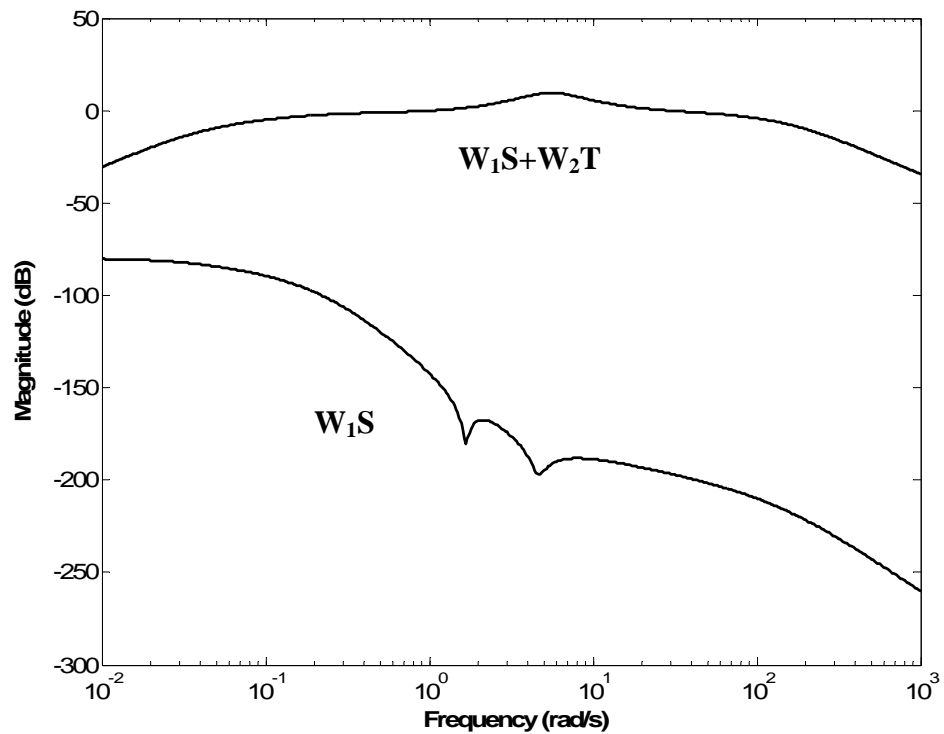


Fig. 5.10 Robust and nominal performance criteria (PSO based loop-shaping)

Once the design criteria are met, the stability and performance of the closed loop system are checked by direct simulation of the system dynamic equations. For a 50% input torque pulse for 0.1s, responses with PSO based controllers are compared with the original manual robust design. The variations in the rotor angle are plotted against time as shown in Fig. 5.11. It can be observed that both graphical and PSO based methods produce controller functions that gives almost identically good transient control. Fig. 5.12 shows the comparison of the dc capacitor voltage variations of the STATCOM.

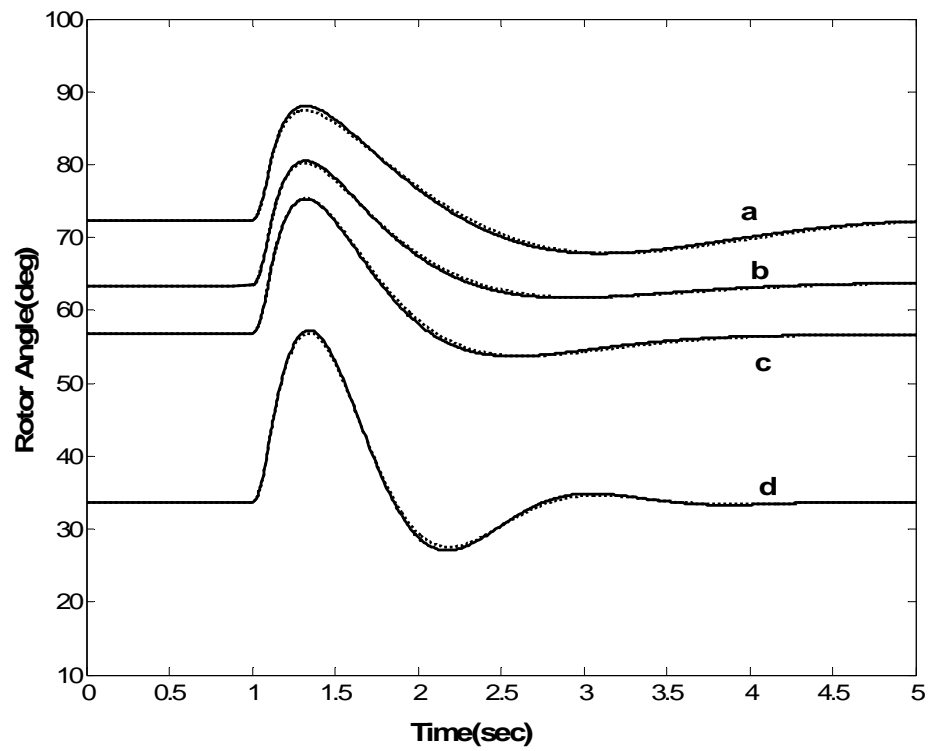


Fig. 5.11 Comparison of generator rotor angle variations following a 50% input torque pulse (solid line is for graphical method and dotted line for automatic loop-shaping).

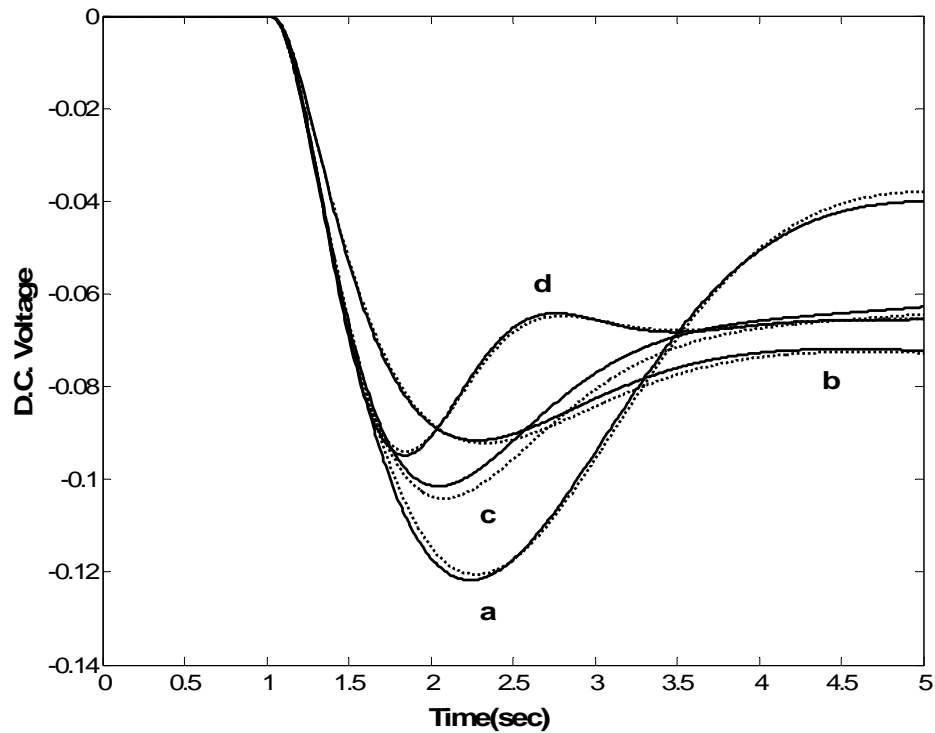


Fig. 5.12 D.C. capacitor voltage variations of the STATCOM corresponding to Fig 5.11.

Comparison of responses with the PSO based robust controller with the original manual one were made for a three phase fault for 0.1 sec at the remote bus. Figs. 5.13 and 5.14 show the generator rotor angle and D.C. voltage variations for various loading conditions. The following cases considered are. a) 1.2 p.u power output at 0.98 leading power factor, b) 1.0 p.u at 0.95 lagging power factor, c) Nominal operating conditions and d) 0.5 p.u at 0.95 lagging power factor.

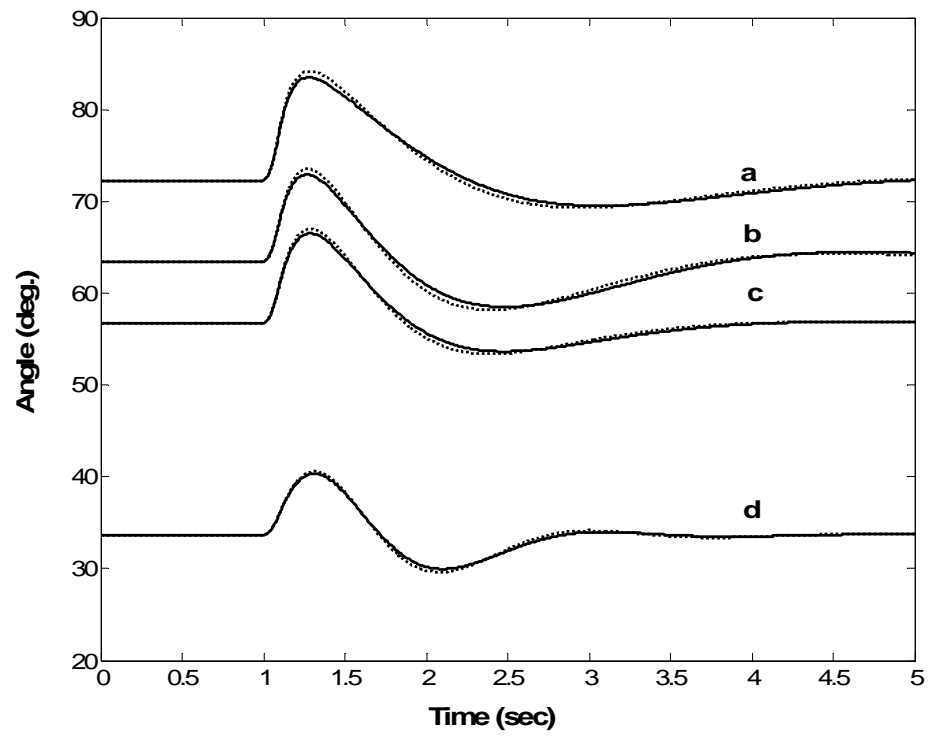


Fig. 5.13 Comparison of generator rotor angle variations following phase fault for 0.1 sec at remote bus.

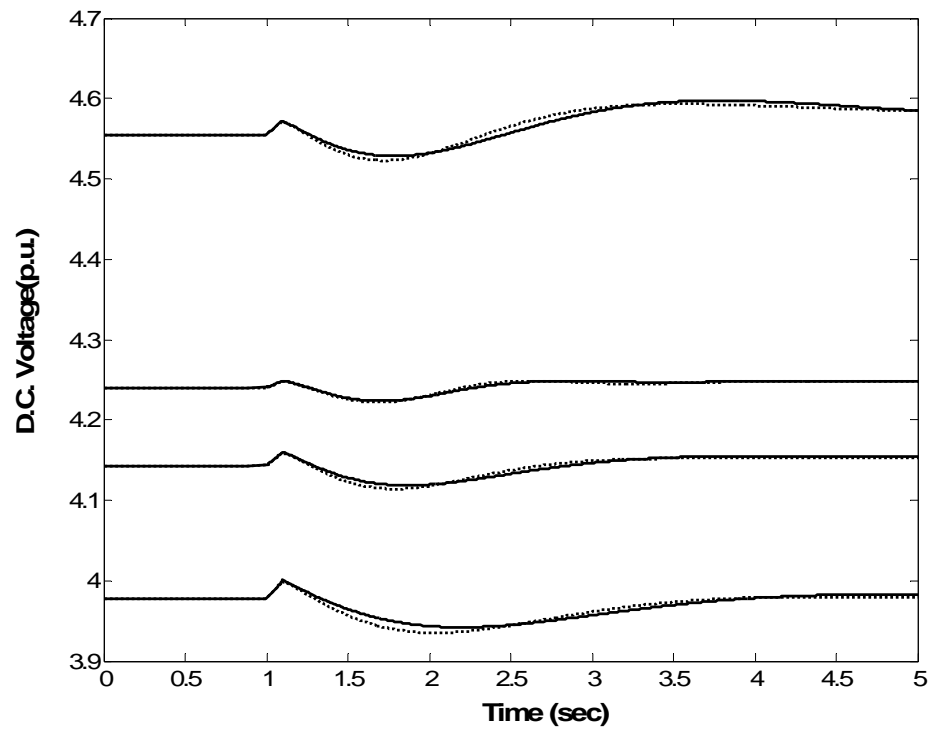


Fig. 5.14 D.C. voltage corresponding to Fig. 5.13.

CHAPTER 6

SIMULATION RESULTS: MULTIMACHINE POWER SYSTEM

The robust STATCOM control designs presented for single machine system in the last chapter are extended to a multimachine power system. Dynamic behavior of multimachine power system with robust STATCOM controller is investigated in this chapter. A four generator 13 - bus and 12 - line multimachine system considered in this study is shown in Fig. 6.1. The system data is provided in Appendix A.

Both the non-linear model and linear model of the system shown in Fig. 6.1 are simulated. The linear model is used for control design while the non-linear is used for time domain simulations following small disturbances like torque pulses and large disturbances like 3 phase fault conditions cleared after a specific time.

This chapter presents simulation results with robust controller design using manual as well as PSO based loop-shaping methods. The following dynamic models are considered for robust design:

- Reduced order multimachine system
- Detailed multimachine system.

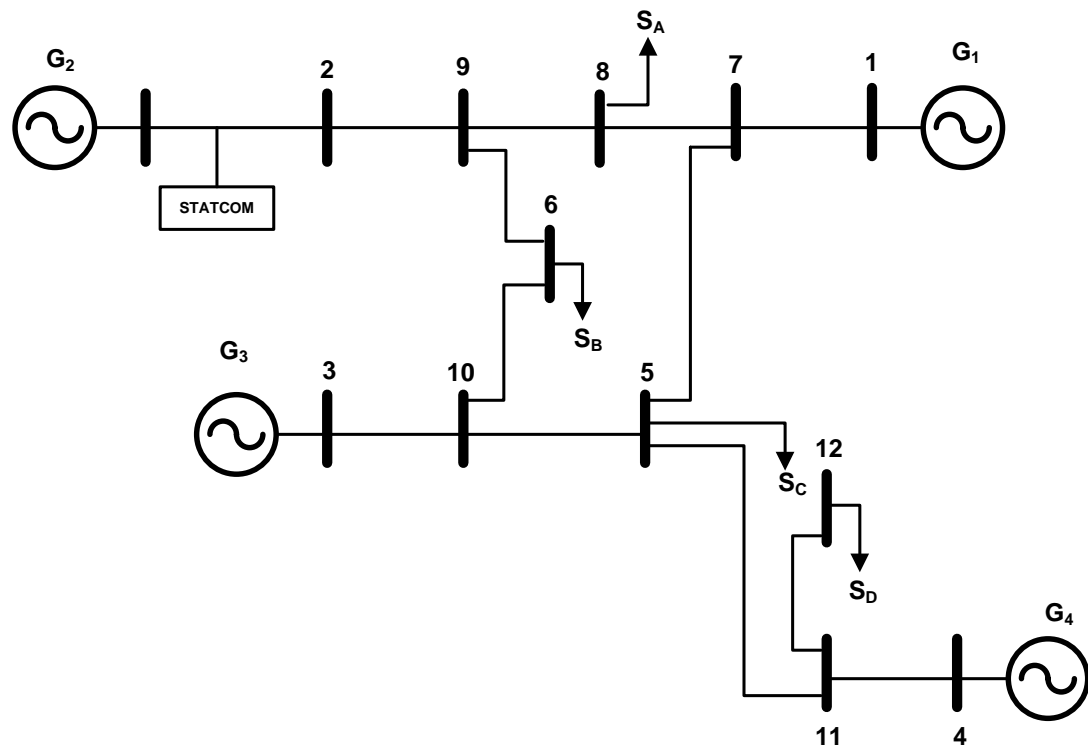


Fig. 6.1 Multimachine power system

6.1 REDUCED ORDER MODEL: MANUAL GRAPHICAL LOOP-SHAPING

The dynamics of the system shown in Fig. 6.1 is obtained in terms of 21 first order differential equations given by (3.13). Designing a robust controller for a system with the plant function having 21 poles through the manual graphical loop-shaping is an involved task. It would be very much desirable to design the controller from a reduced order model if such a model could be obtained without sacrificing accuracy. Model reduction technique based on balanced realization is used to get a reduced order model. The tool box to perform order reduction of large order system is available in MATLAB and is used in this study. The balanced model reduction technique used in this work is included in Appendix D.

The first step in the design is to obtain system matrices for the linearized detailed system. The detailed system is then reduced by using model reduction toolbox in MATLAB. Several reduced order models were examined. Loading considered is given in Tables 6.1 and 6.2. Figs. 6.2 and 6.3 show the comparison of the magnitude and phase plots of the original and the various reduced order models. It can be observed from the figures that the 6th order reduced system has been shown to give the best match with the original system. STATCOM at the middle of transmission line between generator 2 and the network is considered. The plant function is between the STATCOM control input and speed $\Delta\omega$ of generator 2 as the output. The nominal plant function for the 6th order reduced system is,

$$P = \frac{-100s(s - 40.93)(s + 15.27)(s^2 + 0.66s + 17.22)}{s(s + 30)(s + 4.44)(s + 0.33)(s^2 + 0.62s + 31.19)} \quad (6.1)$$

TABLE 6.1 Nominal operating points for generator

Generators	P(MW)	Q(MVAR)
G ₁	231.9	119
G ₂	700	244.5
G ₃	300	193.3
G ₄	450	266.4

TABLE 6.2 Nominal loadings

Loads	P(MW)	Q(MVAR)
S _A	350	195
S _B	350	195
S _C	650	375
S _D	325	155

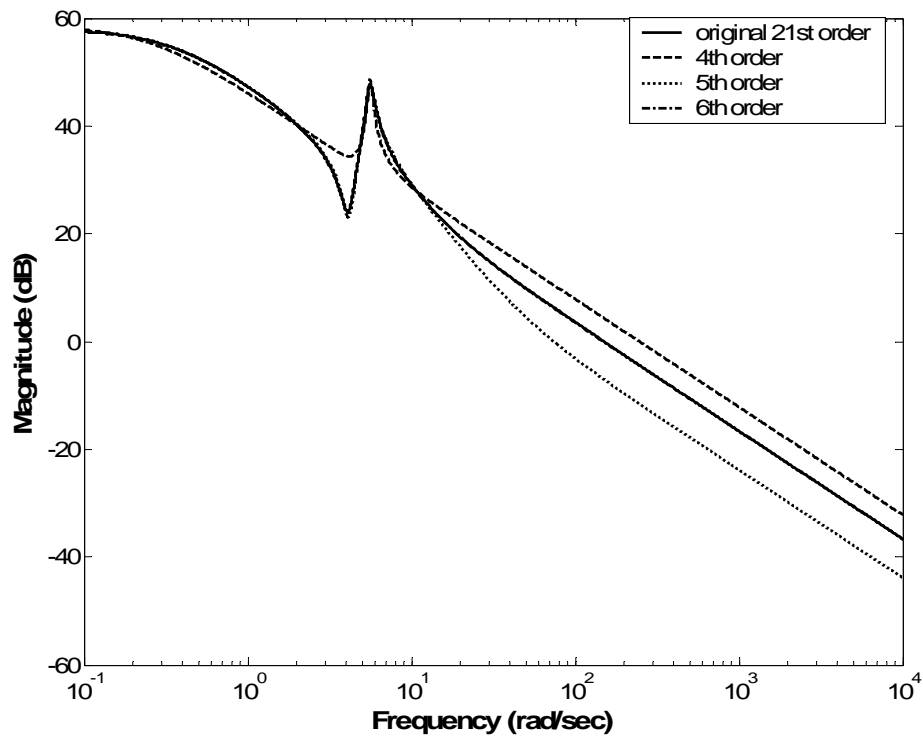


Fig. 6.2 Magnitude plots for original and reduced order systems

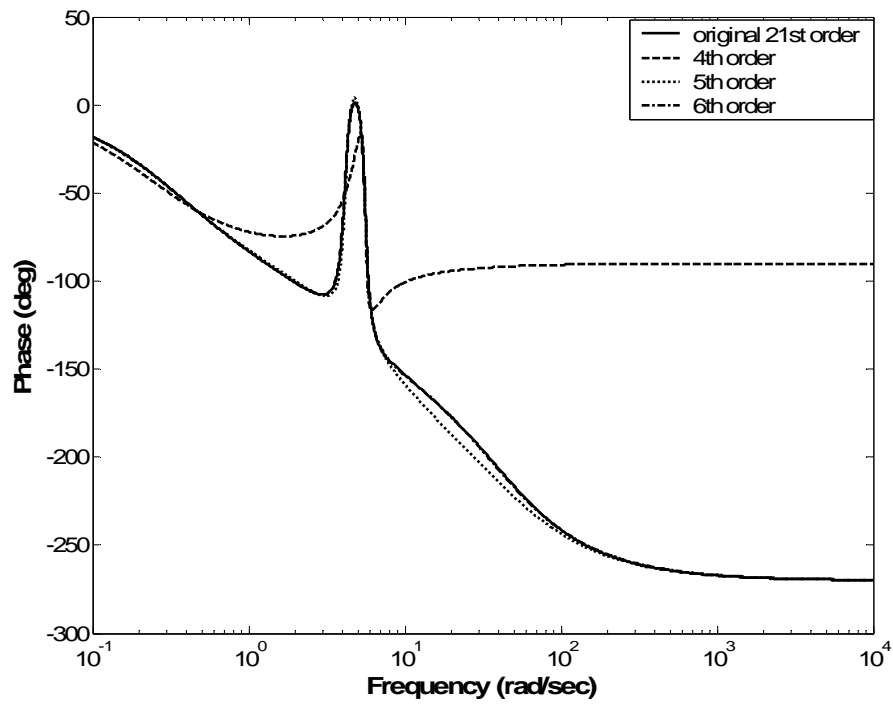


Fig. 6.3 Magnitude plots for original and reduced order systems

For the nominal plant function in (6.1) obtained by model reduction, the dB magnitude vs. frequency plots for the reduced nominal and reduced perturbed plants are plotted. These

are shown in Fig. 6.3. W_2 function constructed from $|\frac{\hat{P}(j\omega)}{P(j\omega)} - 1|$ of the reduced system is,

$$W_2(s) = \frac{0.191(s+20.6)(s+0.86)}{(s^2+10.01s+25.57)} \quad (6.2)$$

The function W_1 is selected as,

$$W_1(s) = \frac{K_d f_c^2}{s^3 + 2s^2 f_c + 2s f_c^2 + f_c^3} \quad (6.3)$$

K_d and f_c were selected as 0.0001 and 1 respectively.

The open loop transfer function $L(s)$ is obtained as,

$$L(s) = \frac{-1.68 \times 10^3 s(s-40.93)(s+15.27)(s^2+0.66s+17.22)}{s(s+30)(s+4.44)(s+0.33)(s^2+0.62s+31.19)} \times \frac{(s+2.63)(s+0.71)(s^2+0.63s+0.39)(s^2+0.46s+0.37)}{(s^2+11.41s+79.21)(s^2+1.68s+1.64)(s^2+0.66s+0.67)} \quad (6.4)$$

The dB magnitude vs. frequency plots relating L , W_1 and W_2 for the reduced system are shown in Fig. 6.6, while the plots for the nominal and robust performance criterion are shown in Fig. 6.7. From the relation, $L(s) = P(s) C(s)$ the controller transfer function is obtained as,

$$C(s) = \frac{16.88(s+2.63)(s+0.71)(s^2+0.63s+0.39)(s^2+0.46s+0.37)}{(s^2+11.41s+79.21)(s^2+1.68s+1.64)(s^2+0.66s+0.67)} \quad (6.5)$$

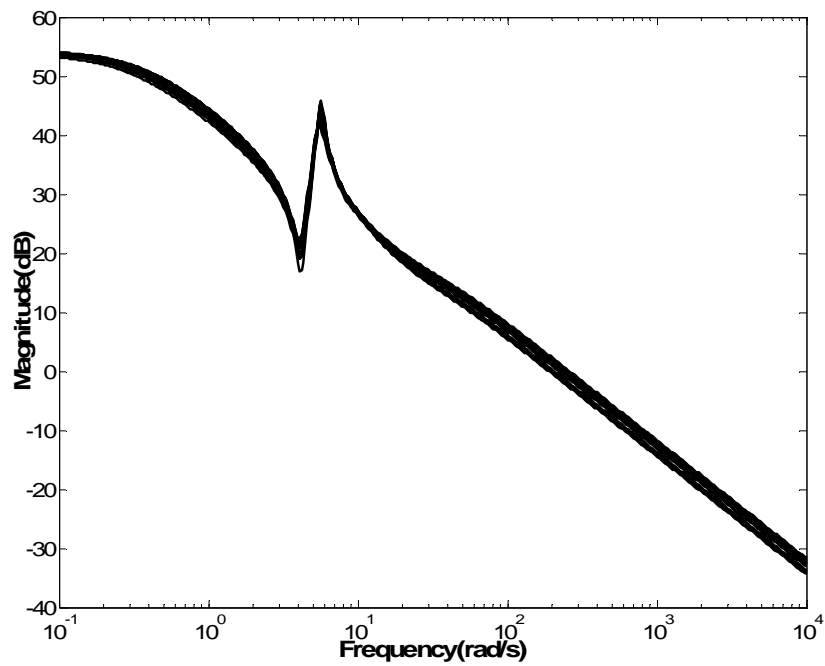


Fig. 6.4 Nominal and perturbed plants

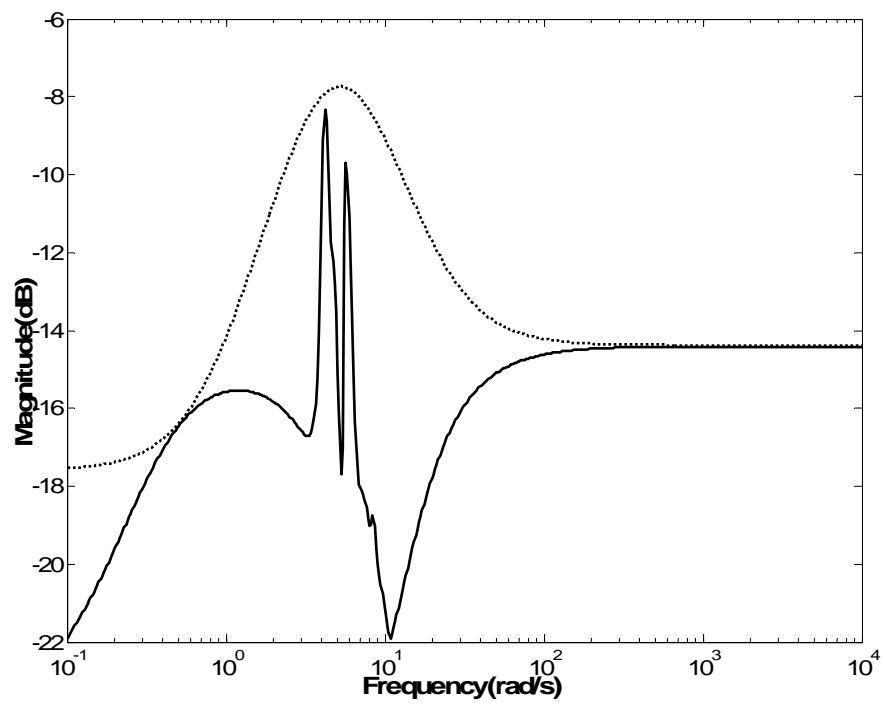


Fig 6.5 Uncertainty profile

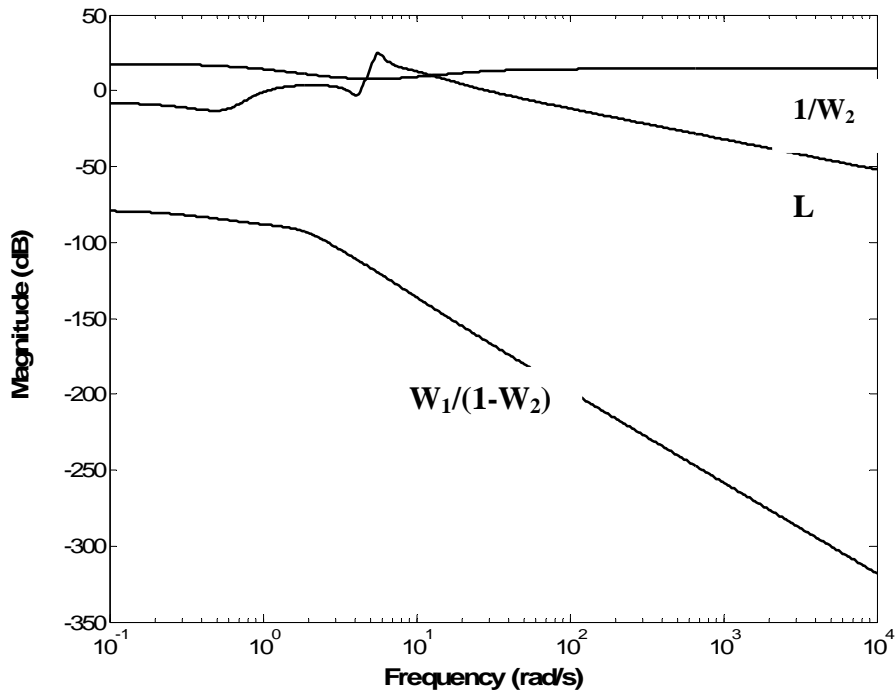


Fig. 6.6 Loop-Shaping plots relating W_1 , W_2 and L (graphical method).

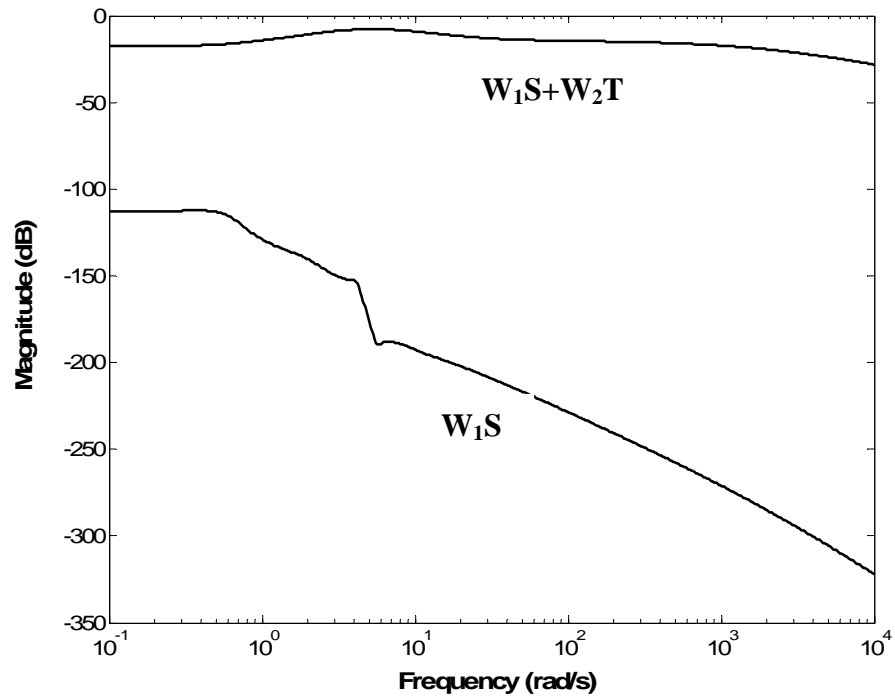


Fig. 6.7 Robust and nominal performance criteria (graphical method).

The controller designed (by manual graphical loop shaping) for the reduced order system is considered in the STATCOM circuit of generator 2 and is tested on the full order system. Fig. 6.8 and Fig. 6.9 show the variations in the relative speeds and relative rotor angles of the various generators considering the robust control and uncontrolled cases. The disturbance considered is 50% torque pulse of 0.1 sec duration on the shaft of generator 2.

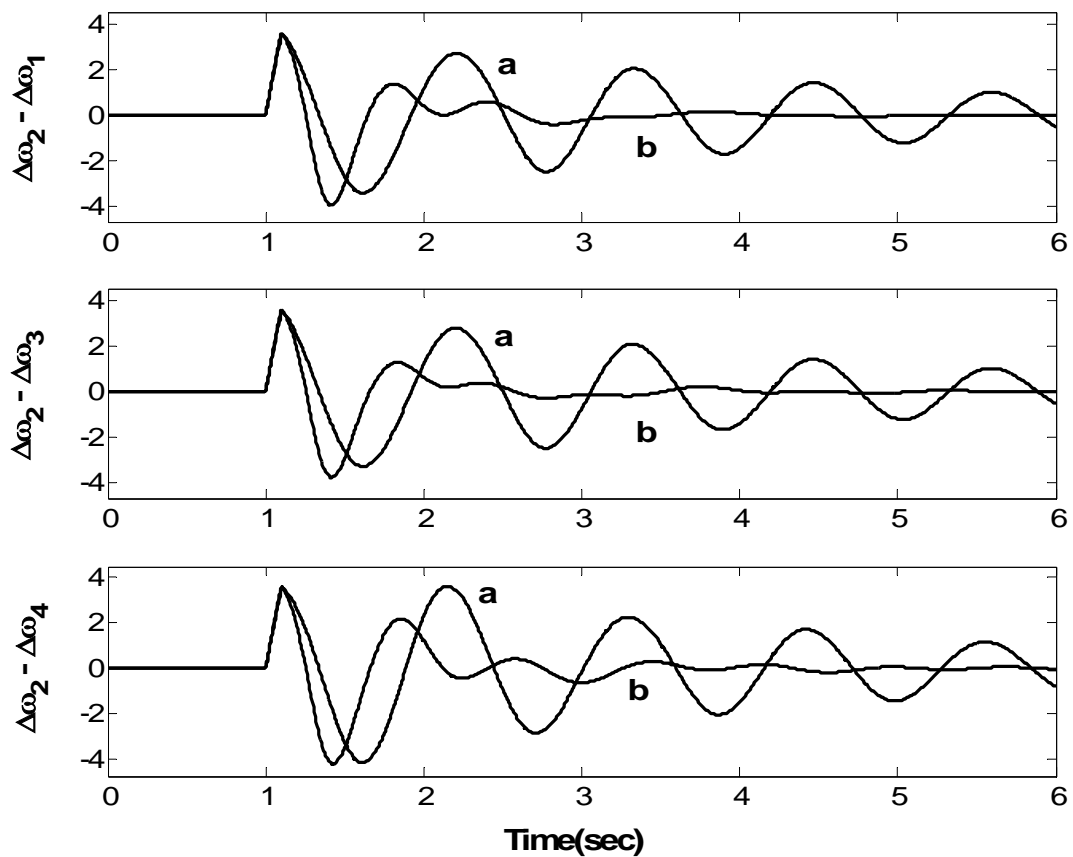


Fig 6.8 Relative speed deviations for 50% torque pulse on generator 2

a) No control

b) With robust controller

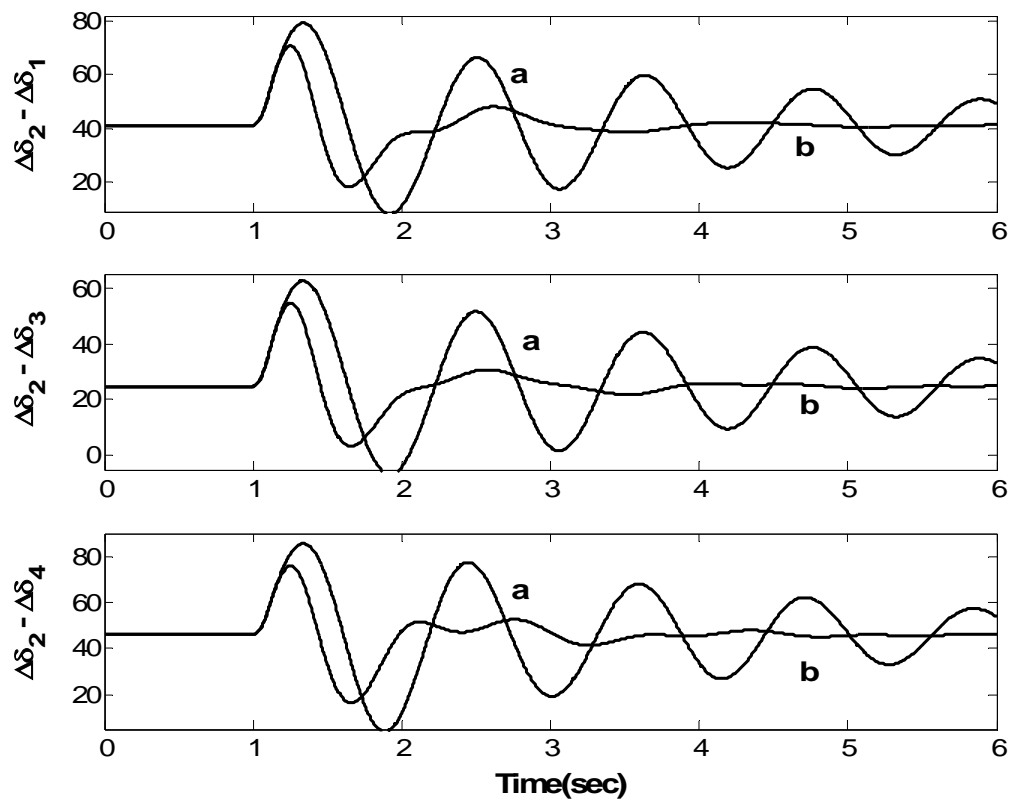


Fig 6.9 Relative angles for 50% torque pulse on generator 2

a) No control

b) With robust controller

6.2 REDUCED ORDER SYSTEM: PSO BASED LOOP SHAPING

PSO based loop-shaping is employed to design robust controller for the reduced order multimachine system. The nominal plant transfer function P , W_1 and W_2 are found as in (6.1), (6.2) and (6.3) respectively.

A second order controller function was pre-selected in the design process. The parameters selected in the PSO algorithm are given in the Table 6.3. The robust controller obtained after the convergence of the algorithm is,

$$C(s) = \frac{12.82(s + 7.33)(s + 0.23)}{s^2 + 3.6768s + 77.455} \quad (6.6)$$

Open loop transfer function is obtained by using relation $L(s) = P(s)C(s)$ is,

$$L(s) = \frac{-1.281 \times 10^3 s(s - 40.93)(s + 15.27)(s + 7.33)(s + 0.22)(s^2 + 0.66s + 17.22)}{s(s + 30)(s + 4.44)(s + 0.33)(s^2 + 3.68s + 77.46)(s^2 + 0.62s + 31.19)} \quad (6.7)$$

TABLE 6.3 PSO parameters

Parameters	Values
Maximum iteration	1500
Population size	20
Value of C 1	2.0
Value of C 2	2.0
Maximum Weight	1.2
Minimum Weight	0.1

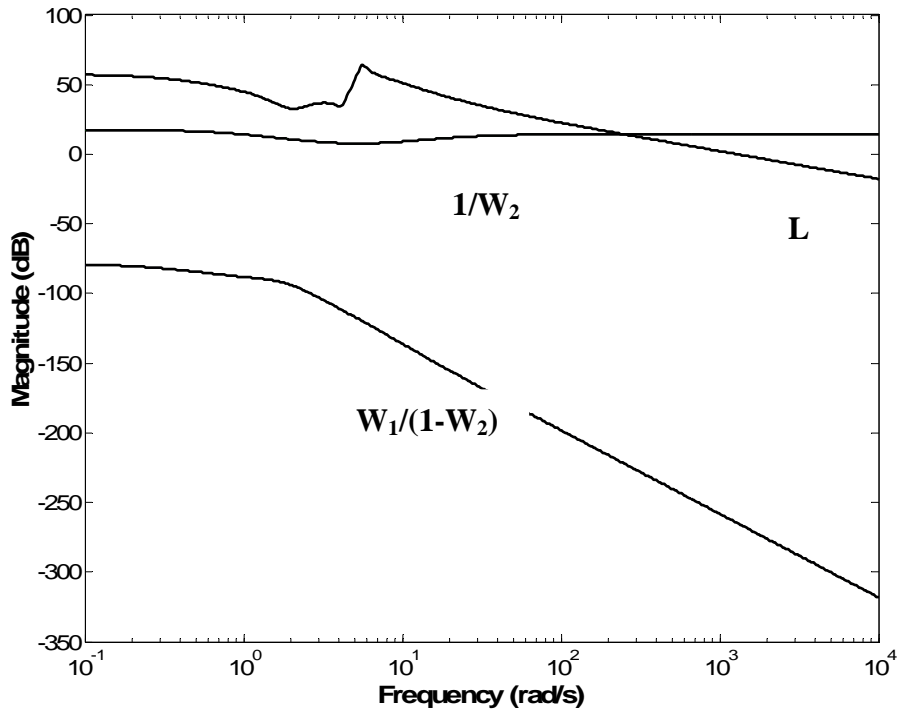


Fig. 6.10 Loop-Shaping plots relating W_1 , W_2 and L (PSO based loop-shaping).

The dB magnitude vs. frequency plots relating $L(s)$, $W_1(s)$ and $W_2(s)$ are shown in Fig. 6.10, while the nominal and robust performance criteria are shown in Fig. 6.11. It can be observed that the various loop-shaping criteria on $L(s)$, nominal performance and robust performance criteria are satisfied at all frequencies.

The second order robust controller obtained using the PSO algorithm for the reduced order multimachine system is tested by simulating through full order system. The nominal operating points are selected to be the same as in the graphical loop-shaping method. Figs. 6.12-6.14 show the variations of relative speeds, relative generator angles and STATCOM DC voltage with and without control. The disturbance considered is 50%

input torque pulse for 6 cycles. It can be observed that though the uncontrolled system is stable it is oscillatory. The designed magnitude controller damps the oscillations in virtually one or two swings.

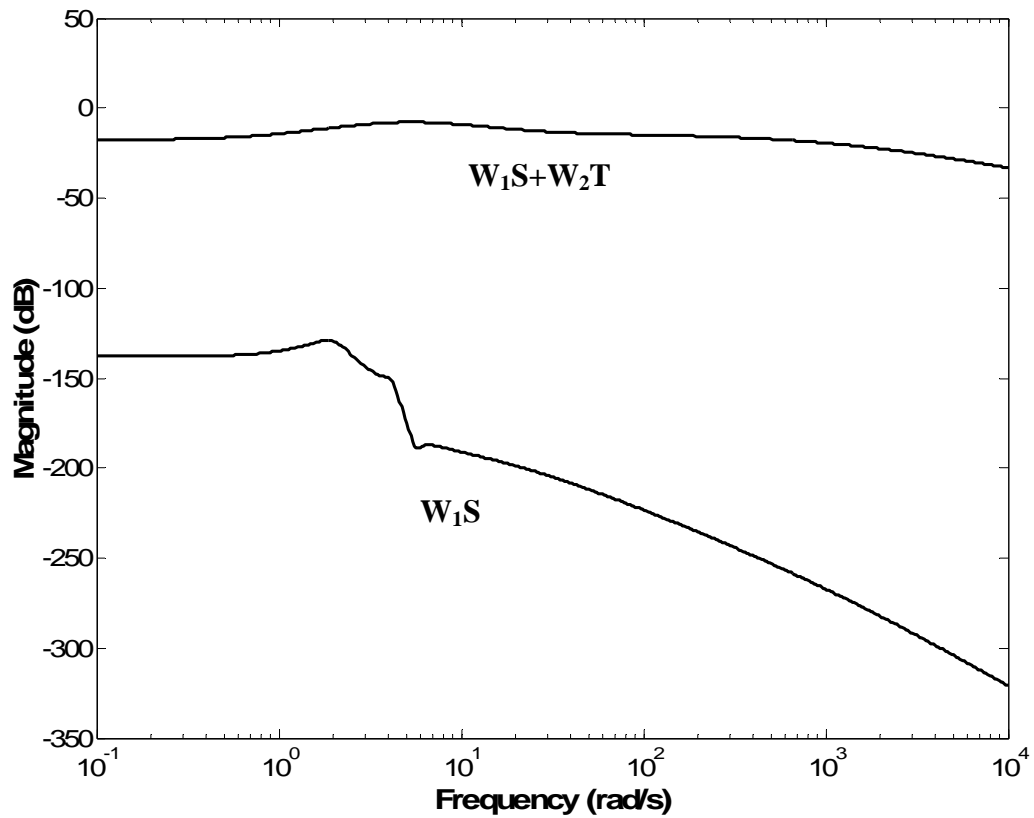


Fig. 6.11 Robust and nominal performance criteria (PSO based loop-shaping)

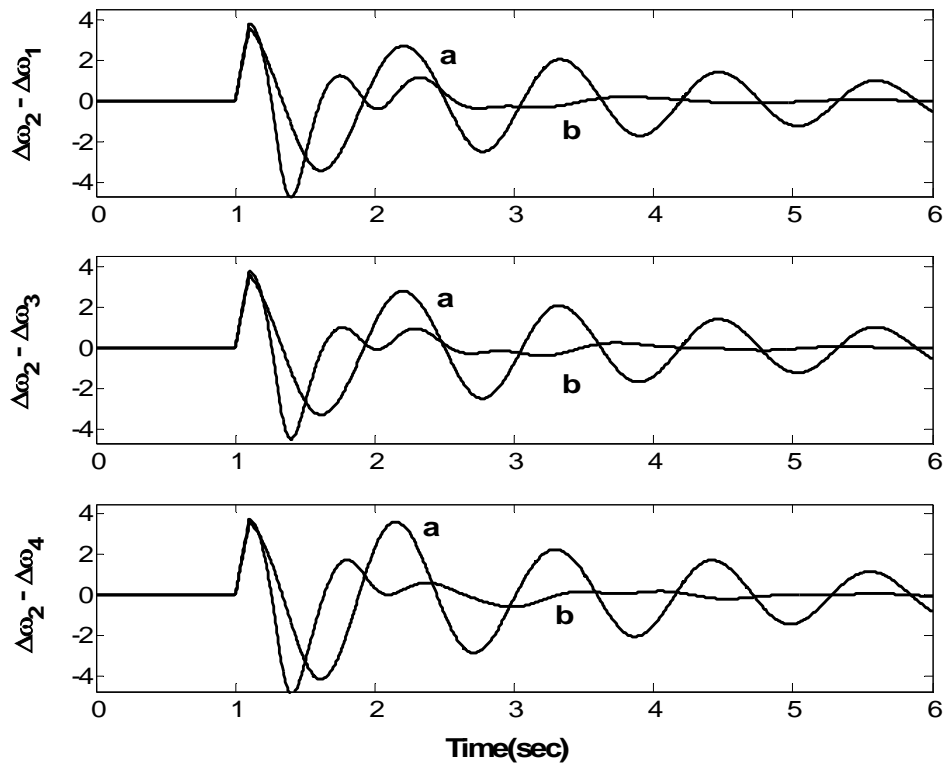


Fig 6.12 Relative speed deviations for 50% torque pulse on generator 2

- a) No control
- b) With robust controller

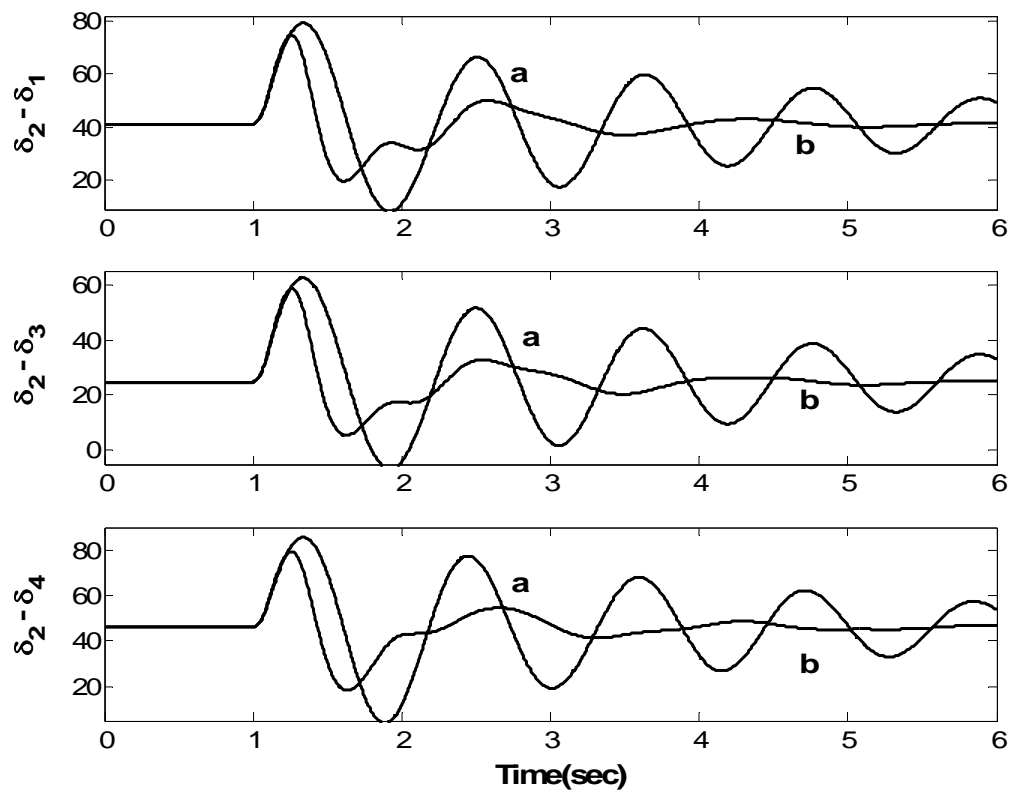


Fig 6.13 Relative angles for 50% torque pulse on generator 2

- a) No control
- b) With robust controller

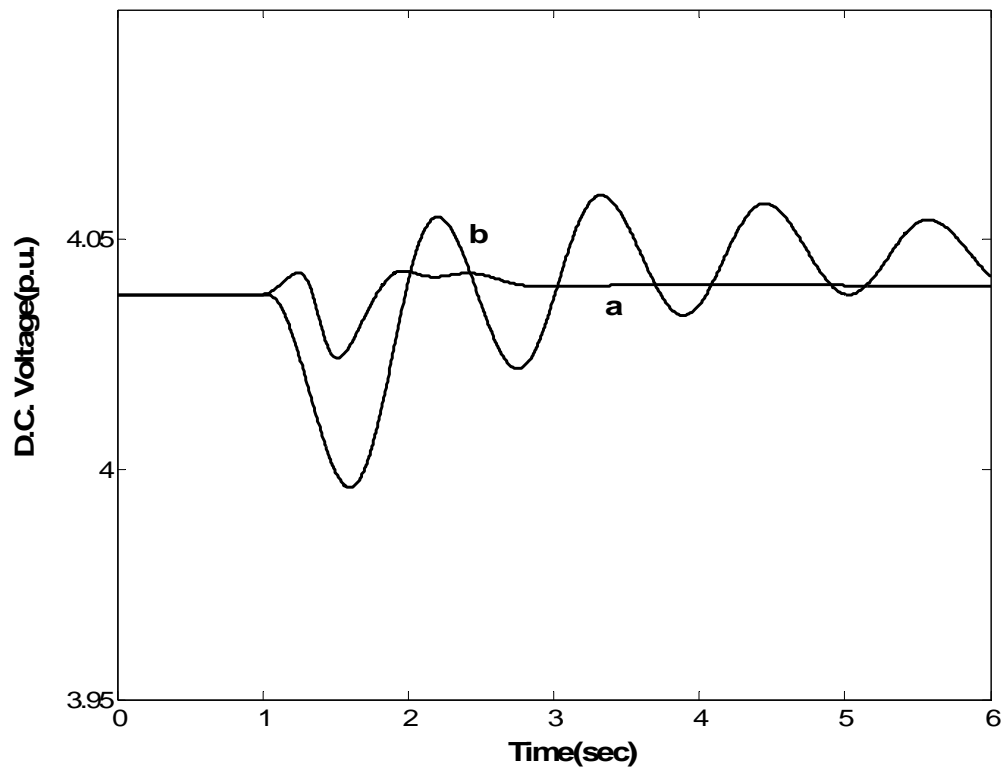


Fig. 6.14 D.C. capacitor voltage corresponding to Fig. 6.12

- a) No control
- b) With robust controller

The effectiveness of robust design was tested for a number of other operating conditions. The various loading conditions tested are given in Table 6.4 and 6.5 respectively. Figs. 6.15 and 6.16 show the variation of relative speeds and relative angles for a disturbance of 50% input torque pulse for 6 cycles on shaft of generator 2. It can be observed from the figures that the oscillations are damped out within one or two swings with the designed robust controller. Results shown in Figs. 6.15-6.16 demonstrate that the robust controller provides good damping for a wide range of operation.

TABLE 6.4 Generator loadings.

Generator	Nominal case		Case 2		Case 3		Case 4	
	P(MW)	Q(MVAR)	P(MW)	Q(MVAR)	P(MW)	Q(MVAR)	P(MW)	Q(MVAR)
G ₁	231.9	119	307.5	225.6	67.7	19.3	123.9	31.3
G ₂	700	244.5	725	366.2	535	77.7	330	49.3
G ₃	300	193.3	575	336.4	165	73.5	165	105.2
G ₄	450	266.4	675	461.2	245	110.7	157	94.9

TABLE 6.5 Loads.

Loads	Nominal case		Case 2		Case 3		Case 4	
	P(MW)	Q(MVAR)	P(MW)	Q(MVAR)	P(MW)	Q(MVAR)	P(MW)	Q(MVAR)
S _A	350	195	460	275	275	135	200	150
S _B	350	195	460	275	175	135	125	175
S _C	650	375	900	475	410	250	350	250
S _D	325	155	450	220	150	100	125	75

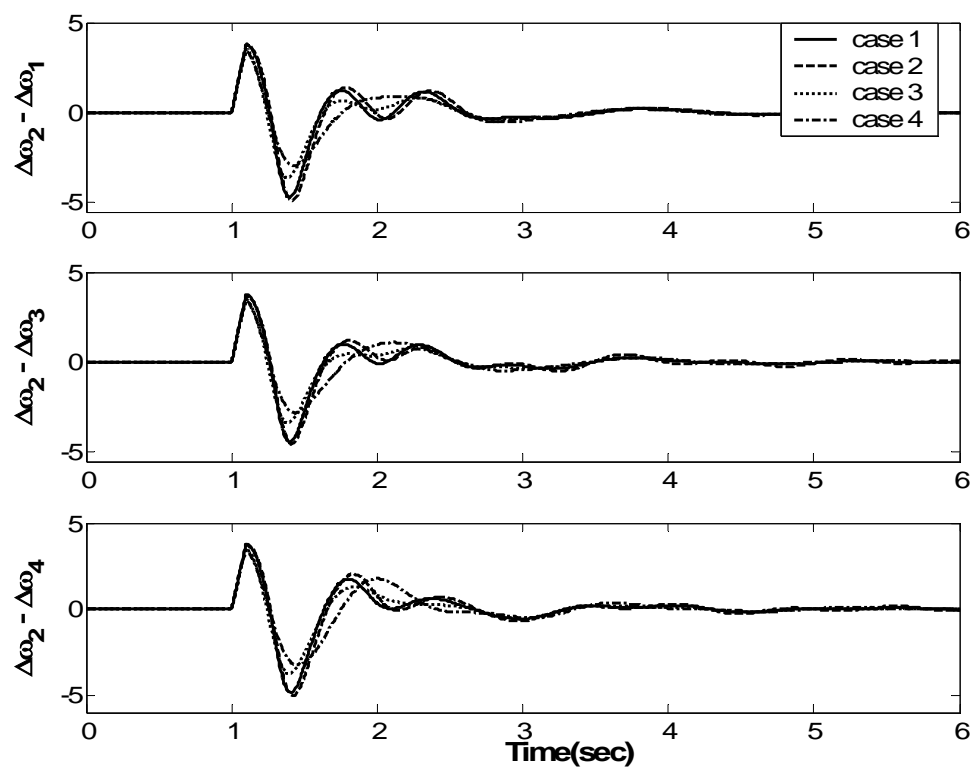


Fig 6.15 Relative speed deviations for 50% torque pulse on generator 2

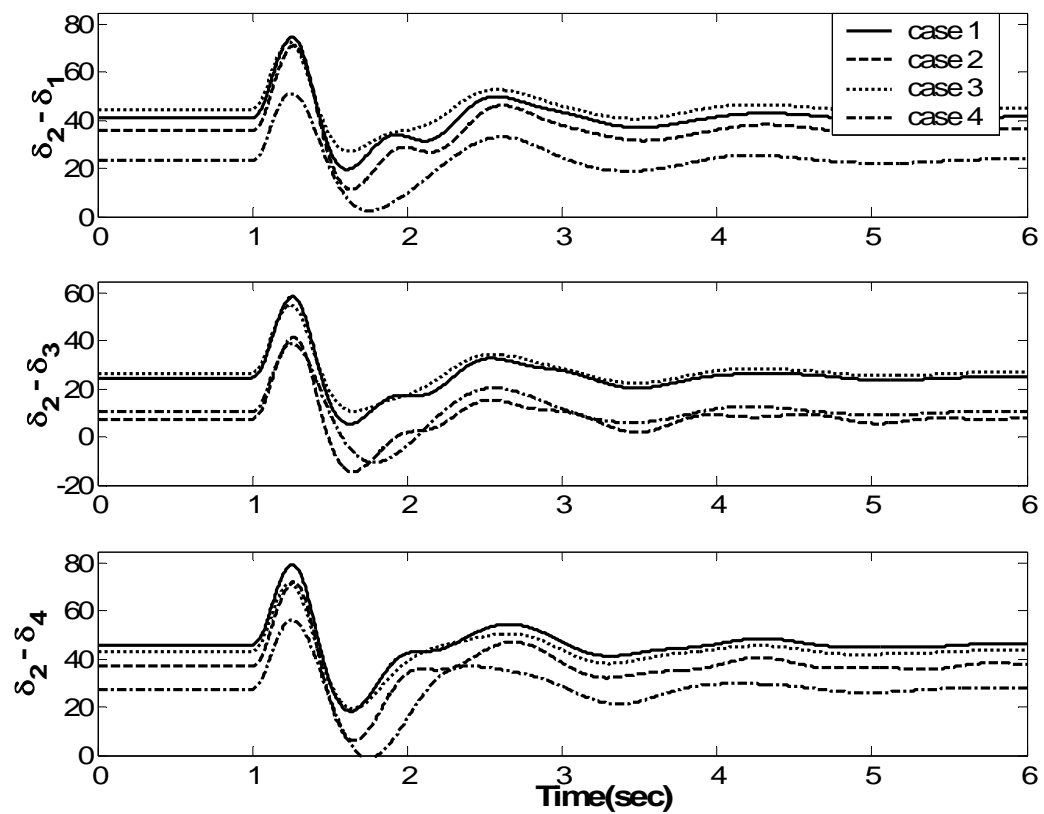


Fig 6.16 Relative angles for 50% torque pulse on generator 2

6.3 DETAILED MODEL: PSO BASED LOOP-SHAPING

Since the robust control design considering the detailed model of the power system is very involved, this section considers only the PSO based design. The nominal plant transfer function obtained for the nominal operating conditions given in Table 6.1 for the 4-machine system is,

$$P(s) = \frac{-149s(s+100.2)(s+95.5)(s+91.3)(s+78)(s-31.2)(s+22.7)(s+16.5)(s+11.9)}{s(s+95.6)(s+95.2)(s+91.3)(s+77.7)(s+35.2)(s+23)(s+11.9)(s+8.9)(s+6.2)} \times \frac{(s+8.9)(s+6.3)(s+2.9)(s+2.54)(s^2+1.5s+69.6)(s^2+2.66s+60)(s^2+0.6s+17.1)}{(s+5.1)(s+2.8)(s+2.5)(s+0.3)(s^2+1.55s+69.6)(s^2+2.67s+60)(s^2+0.63s+31.1)} \quad (6.8)$$

Since the basis of model reduction was similarity between the magnitude plots of original and the reduced system, therefore W_1 and W_2 for the detailed model can be selected as in section 6.1. A second order controller function was pre-selected in the design process. The robust controller obtained after the convergence of the algorithm is,

$$C(s) = \frac{25 \times 10^3 (s + 3.9998)(s + 0.0002)}{s^2 + 0.07454s + 2.797} \quad (6.9)$$

The open loop transfer function is obtained as,

$$L(s) = \frac{-1.89 \times 10^3 s(s+100.2)(s+95.5)(s+91.3)(s+78)(s-31.2)(s+22.7)(s+16.5)(s+11.9)}{s(s+95.6)(s+95.2)(s+91.3)(s+77.7)(s+35.2)(s+23)(s+11.9)(s+8.9)(s+6.2)(s+5.1)} \times \frac{(s+5.39)(s+0.73)(s+8.9)(s+6.3)(s+2.9)(s+2.54)(s^2+1.5s+69.6)(s^2+2.66s+60)(s^2+0.6s+17.1)}{(s+2.8)(s+2.5)(s+0.3)(s^2+1.55s+69.6)(s^2+2.67s+60)(s^2+0.63s+31.1)(s^2+2.55s+2)} \quad (6.10)$$

The db magnitude vs. frequency plot relating L , W_1 and W_2 is shown in Fig. 6.17. The nominal and robust performance criteria are shown in Fig. 6.18. The plots for the detailed and the reduced order system almost overlap each other.

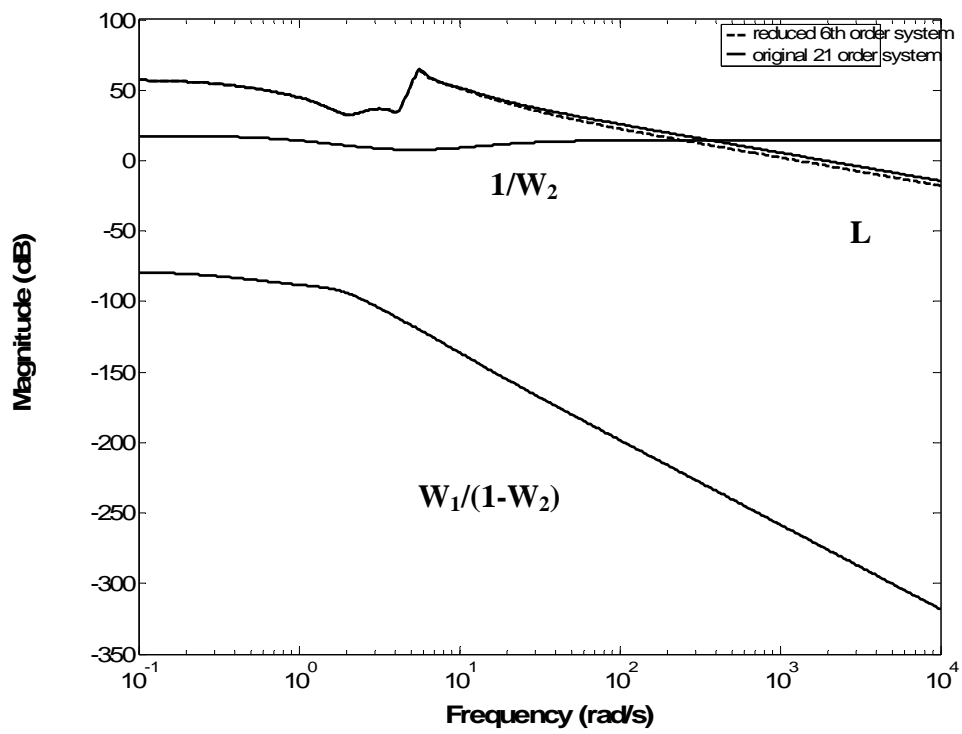


Fig. 6.17 Loop-Shaping plots relating W_1 , W_2 and L (PSO based loop-shaping).

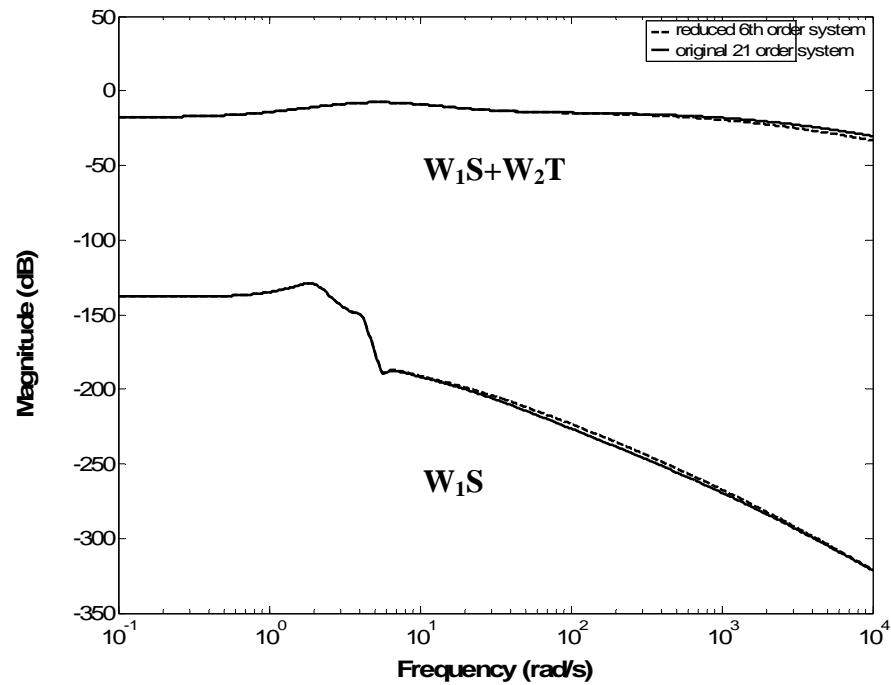


Fig. 6.18 Robust and nominal performance criteria (PSO based loop-shaping)

The controller designed for detailed system is tested for the same operating conditions as for the reduced order system. The simulation results for detailed system are shown in Figs. 6.19 and 6.20. A 50% torque input pulse of duration 10 ms was applied on shaft of generator 2. The results shown are relative speed deviations and relative angles.

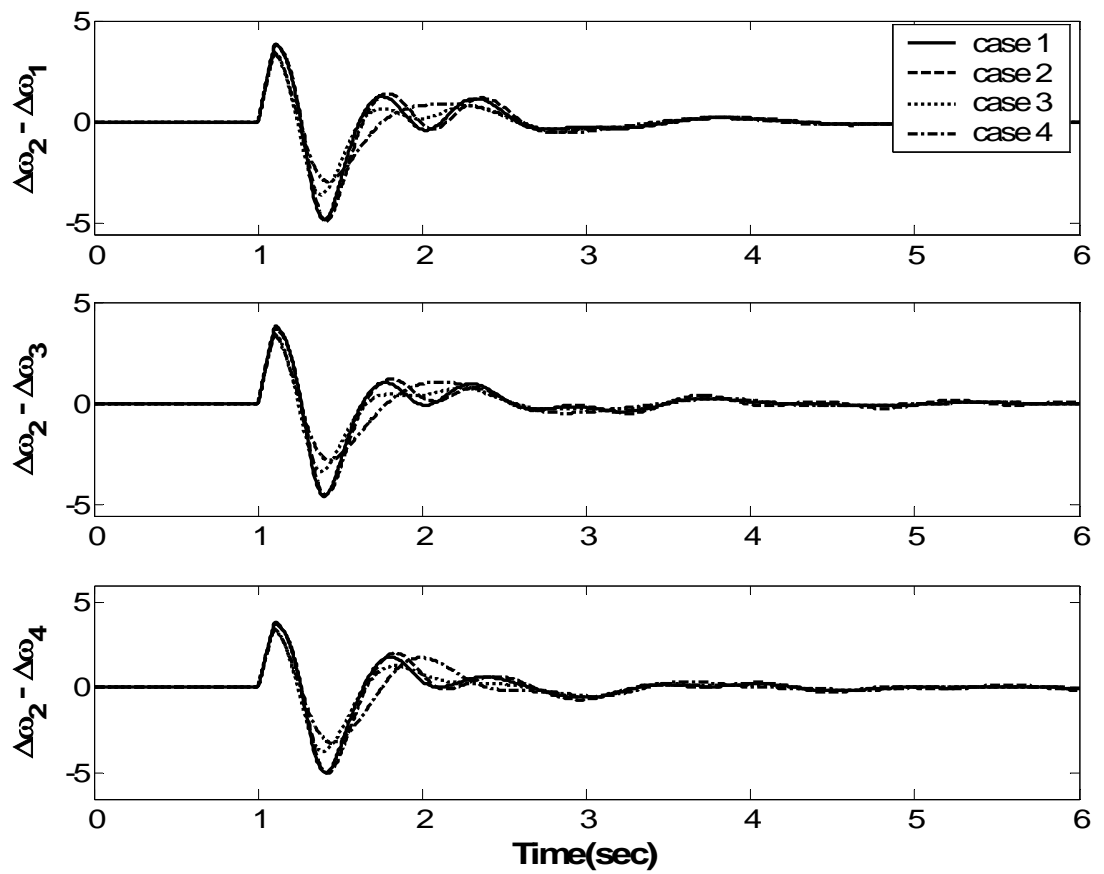


Fig 6.19 Relative speed deviations for 50% torque pulse on generator 2

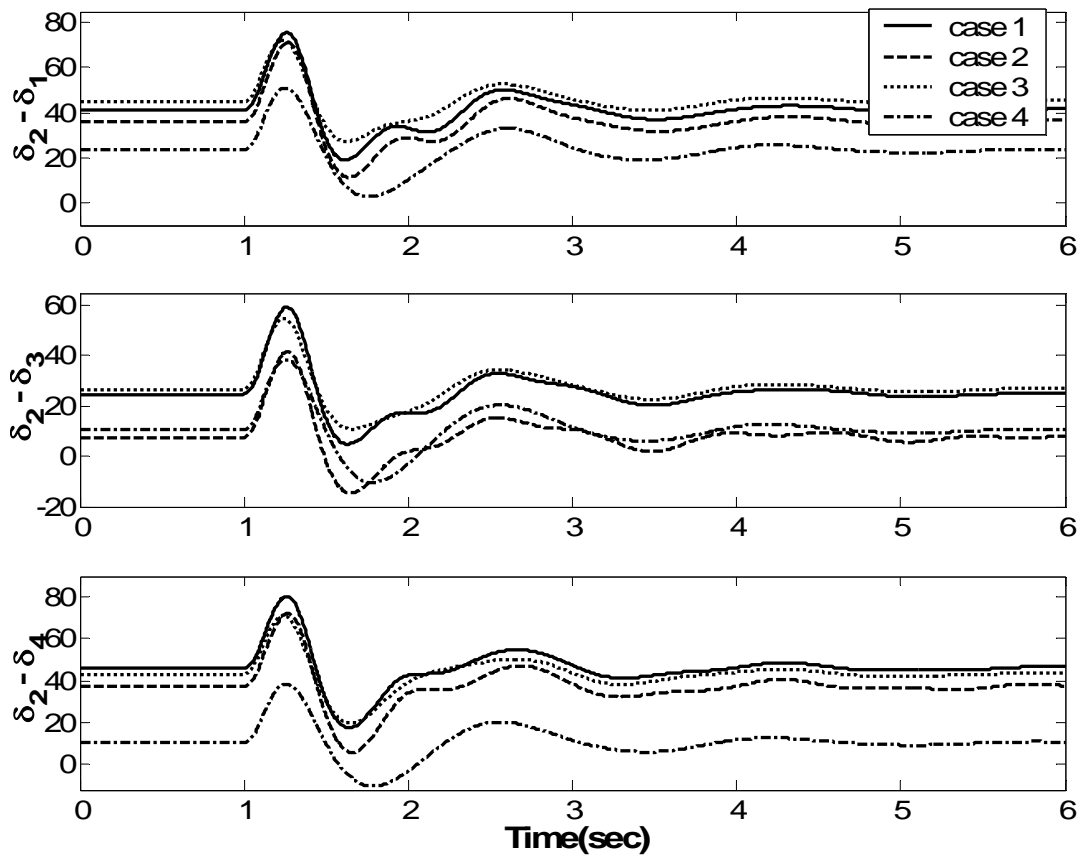


Fig 6.20 Relative rotor angles for 50% torque pulse on generator 2

Robust controller designed for reduced order system by PSO based loop shaping is tested for a 6 cycle three phase fault at the network bus of generator 2. Figs. 6.21-6.23 show the variations of relative speeds, relative generator angles and STATCOM D.C. voltage with and without control under nominal loading conditions. It can be observed that the proposed controller stabilizes the otherwise unstable system.

The proposed robust controller is tested for the set of operating points given in the Tables 6.4 and 6.5 for 6 cycle three phase fault at the network bus of generator 2. The results are given in Figs. 6.24 - 6.25. It can be seen that the controller successfully damps the oscillations for the various operating points considered. It is to be noted that the robust controller is designed to give robust performance near the nominal operating point. For the operating points off the nominal one, the responses may not be as good.

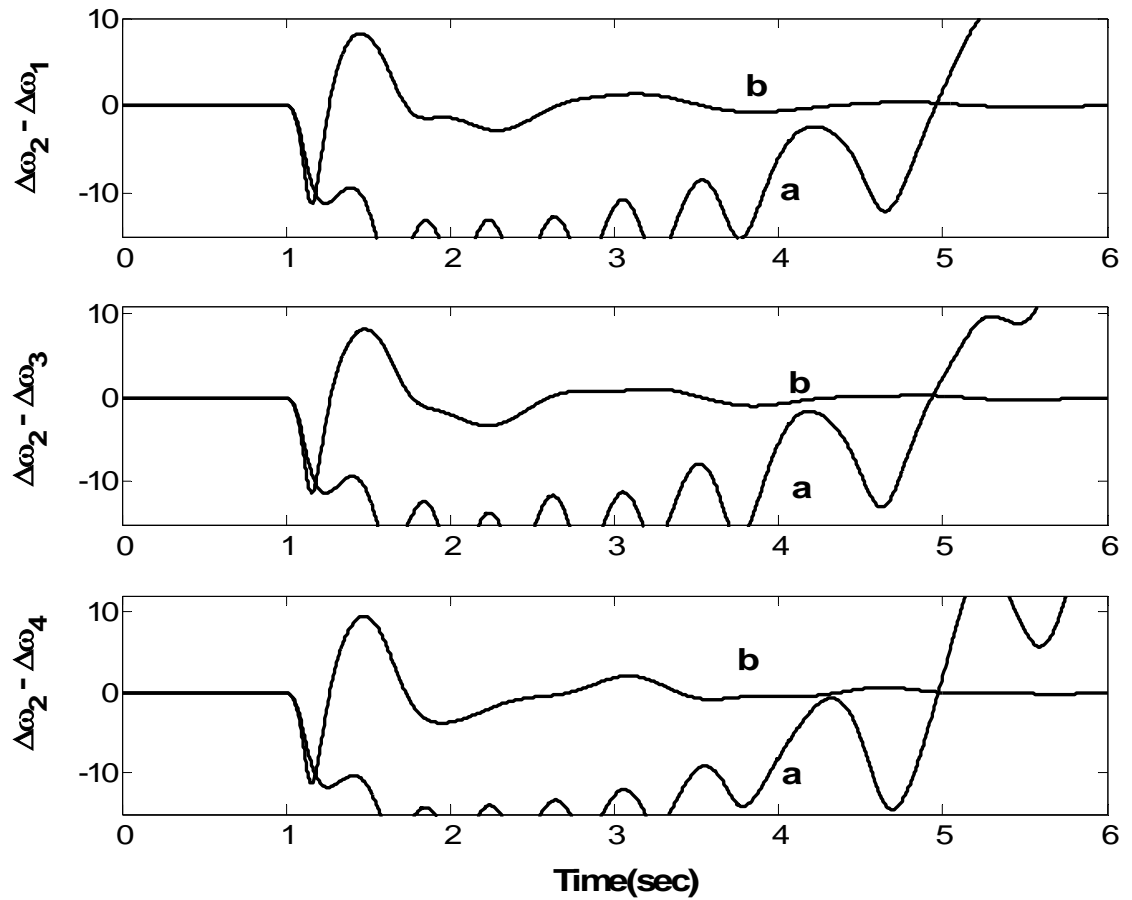


Fig. 6.21 Relative speed deviations for 6 cycle 3 phase fault at network bus of generator 2.

- a) No control
- b) With robust controller

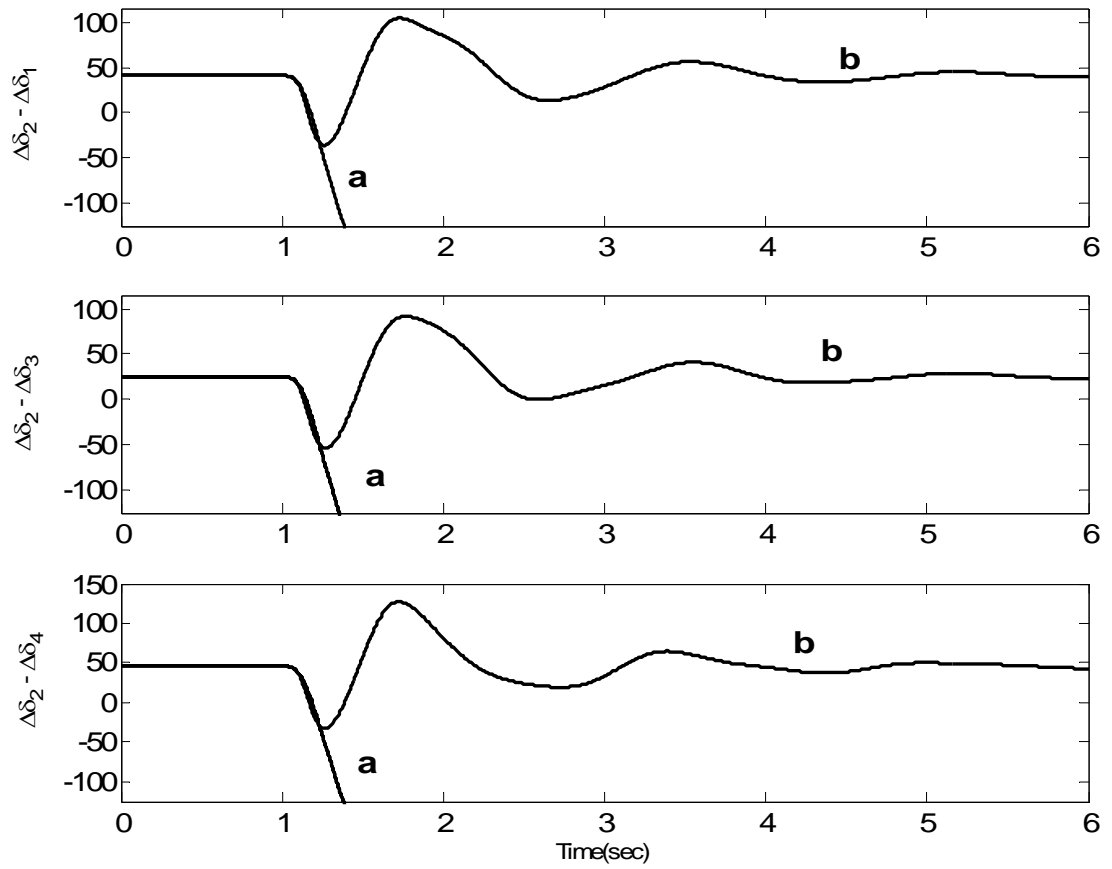


Fig. 6.22 Relative rotor angles for 6 cycle 3 phase fault at network bus of generator 2.

- a) No control
- b) With robust controller

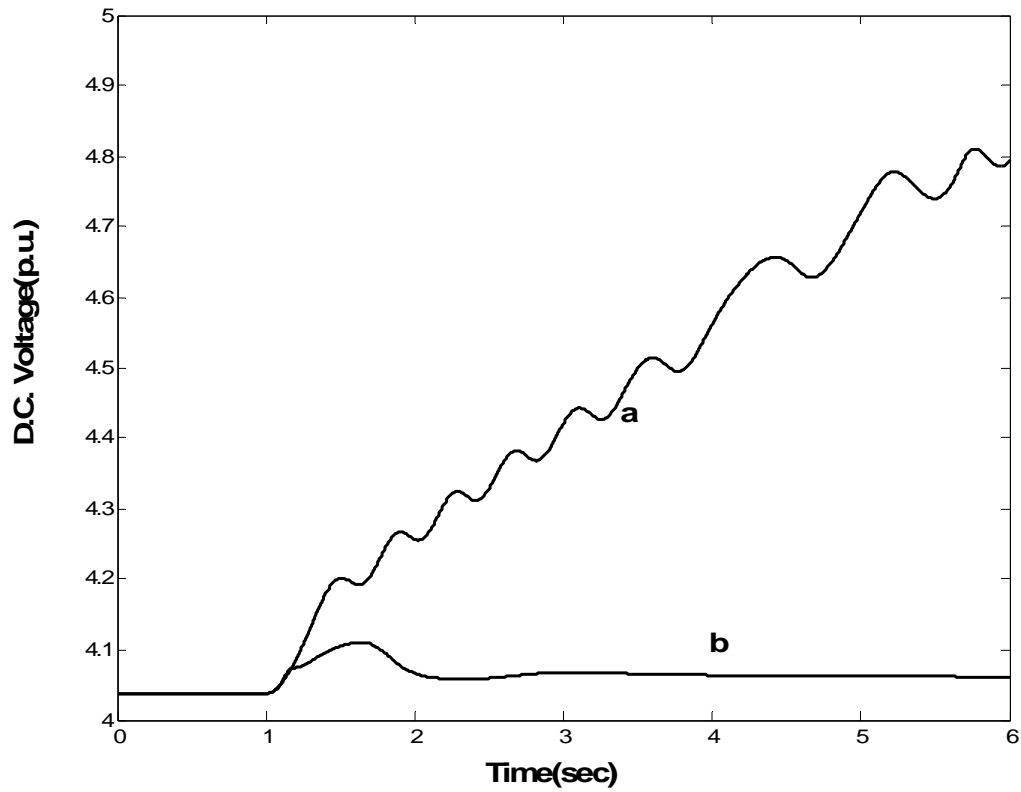


Fig. 6.23 D.C. capacitor voltage for 6 cycle 3 phase fault at network bus of generator 2.

- a) No control
- b) With robust controller

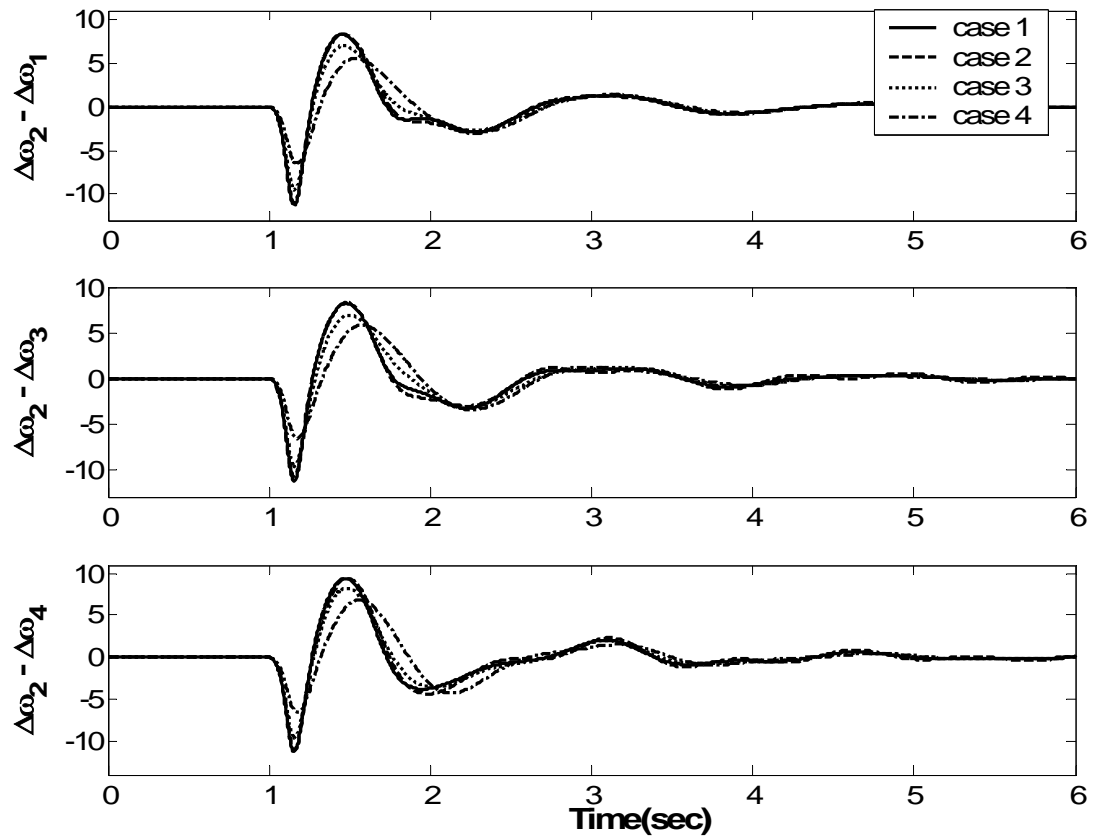


Fig. 6.24 Relative speed deviations for 6 cycle 3 phase fault at network bus of generator 2.

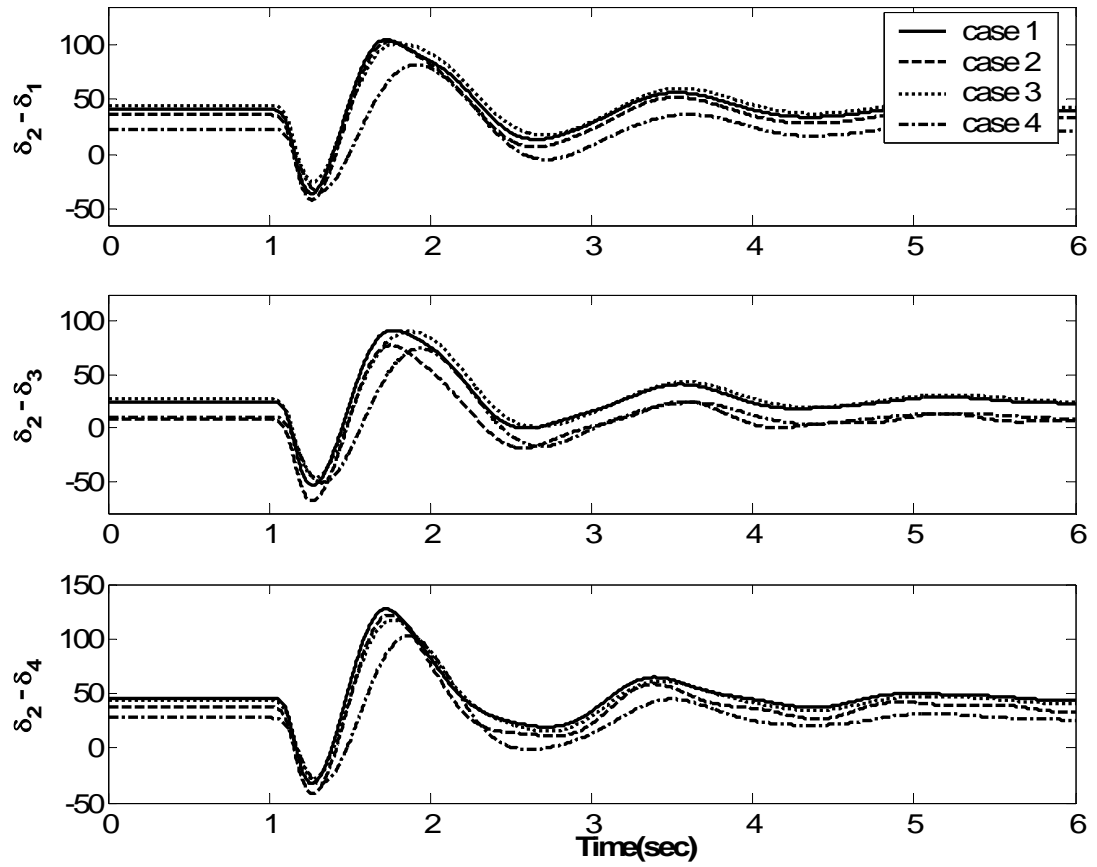


Fig. 6.25 Relative rotor angles for 6 cycle 3 phase fault at network bus of generator 2.

The percentage relative speed variations for above cases are shown in Figs 6.27, 6.28 and 6.29. It is quiet evident from the Figs that the coordinated control is better than the individual ones. The transient performance for the coordinated design shows some peaks, however the subsequent or the steady state performance is improved. The control on generator 3 is not that effective.

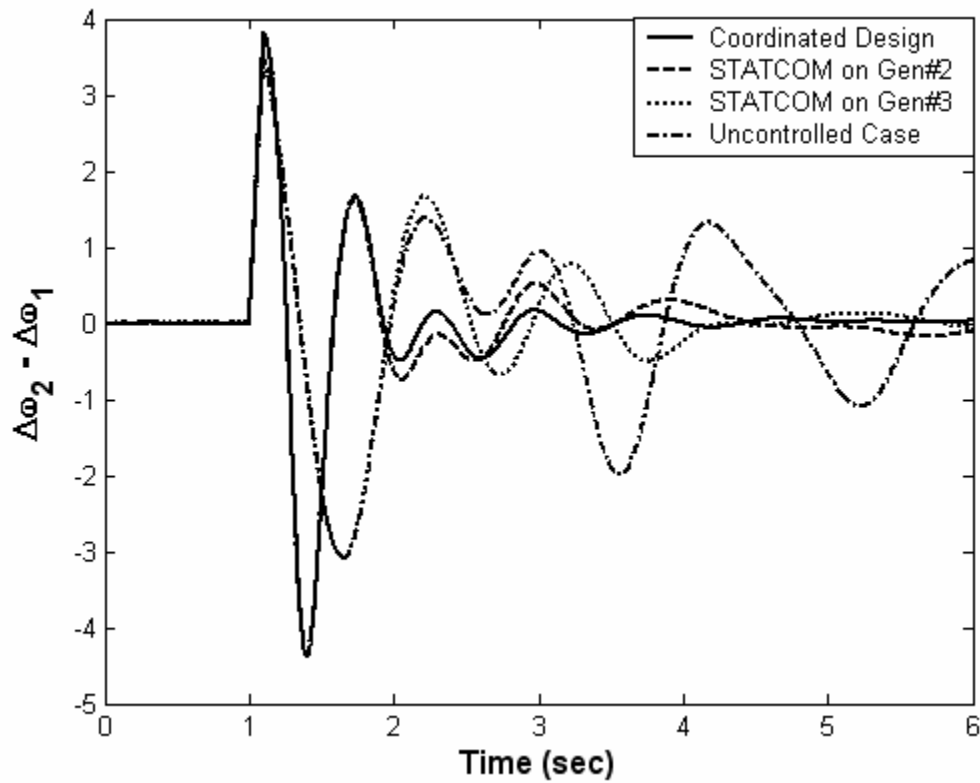


Fig. 6.27 Relative speed variations for generators 1 and 2 for the cases a, b, c and uncontrolled case

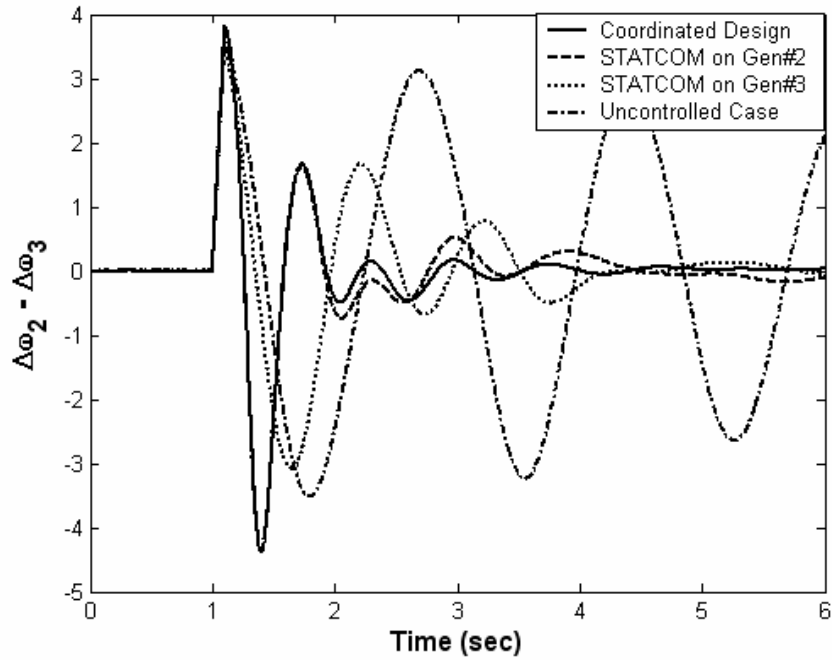


Fig. 6.28 Relative speed variations for generators 2 and 3 for the cases a, b, c and uncontrolled case

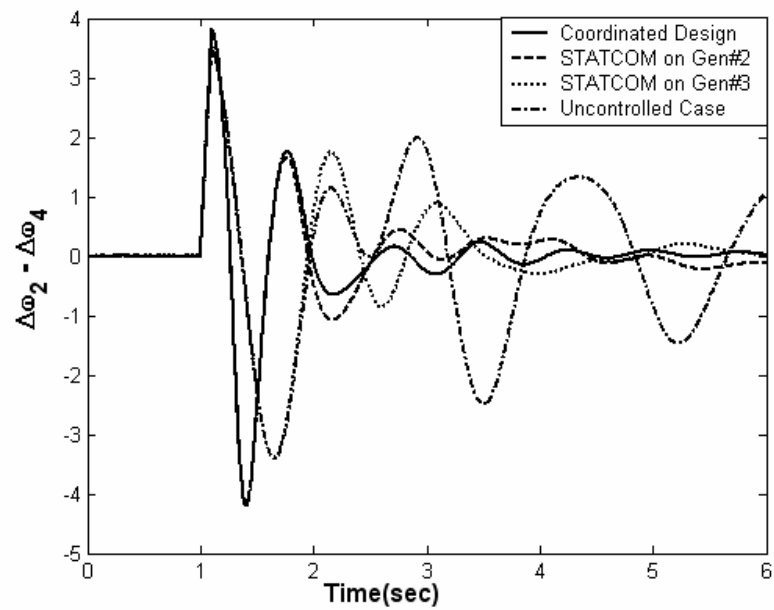


Fig. 6.29 Relative speed variations for generators 2 and 4 for the cases a, b, c and uncontrolled case

CHAPTER 7

CONCLUSIONS AND FUTURE WORK

The dynamic behavior of a single machine infinite bus (SMIB) system and a multimachine power system installed with STATCOM has been investigated. Non-linear and linear models of both single machine as well as multimachine power system have been derived. In multimachine model, network quantities were transformed to generator side instead of commonly used conversion to the network frame. This facilitates the controller design on the generator since the generator variables remain unaltered.

Robust controllers are designed and tested for stabilization of power system when subjected to small as well as large disturbances including symmetrical three phase faults.

The controller design for multimachine system is divided into two parts, reduced order model and detailed model controller design. A method based on balanced realization is used to get a reduced order model. The order of the reduced system is selected based on the comparison between magnitude and phase plots of original and the reduced systems.

Manual as well as PSO based loop-shaping techniques are used to design the robust controllers. Comparison of results obtained for robust controllers designed by graphical and PSO based loop-shaping is made for both single machine and multimachine systems. It has been found that both graphical and PSO based techniques yield controller functions that gives similar transient response. The designed controllers tested for SMIB as well as multimachine systems have been found to be very effective for a range of operation. The operating conditions for which the controller provides good damping performance depend on the spectrum of perturbed plants selected in the design process.

The robust control design through loop-shaping method, as such, chooses an open loop function and constructs the controller subject to satisfying several constraints. The design requires an iterative procedure and each time graphical constraints have to be checked manually. The success of the method depends, to a good extent, on the experience of the designer. The PSO based robust design, though depends on some of the initial constructions of the loop-shaping procedure, eliminates the need for manual checking of the constraints. The PSO based method starts by choosing the controller function, instead of the open loop transfer function, and hence can pre-select the order of the controller function. For control designs of higher order dynamic models like the multimachine system, the PSO embedded loop shaping is computationally very desirable.

7.1 RECOMMENDATIONS FOR FUTURE RESEARCH

The research in this area can be further advanced in the following suggested directions.

- In this research, change in machine speed ($\Delta\omega$) has been used as the feedback signal to design the robust controller. Other signals which are locally available at the STATCOM bus like line flows, driving point reactance seen from STATCOM location etc. need investigation.
- Finding an optimum location(s) of STATCOM(s) in a multimachine system to improve the system damping needs further study.
- This work assumes no other controls in the generators. Coordination of the robust control with other signals like, for example, PSS control will be an interesting area to investigate.
- The robust controller design of STATCOM for damping control with other FACTS devices such as static synchronous series compensator (SSSC), etc. in a multimachine environment also needs careful study and investigation.
- Further research can be extended to evaluate the impact of STATCOM voltage phase angle (ψ) towards the dynamic performance of multimachine power system.

APPENDIX A

SYSTEM DATA

A.1 SINGLE MACHINE INFINITE BUS SYSTEM DATA

- Parameters for the approximate model (in p.u. except indicated)

$$H = 3\text{s}, D = 4.0, K = 1.0, x_1 = 0.3, x'_d = 0.3, x_d = 1.0, T = 0.02, I_{so} = 0.$$

- Parameters for the Detailed model (in p.u. except indicated)

$$H = 3\text{s}, T'_{do} = 6.3, x_d = 1.0, x'_d = 0.3, x_q = 0.6. D = 4.0, X_{tL} = 0.3, X_{LB} = 0.3,$$

$$X_{SDT} = 0.15, K_A = 10.0, T_A = 0.01\text{s}, T_C = 0.05\text{s}, C_{DC} = 1.0, c_o = 0.25, \psi_o = 46.52^\circ$$

- Nominal Plant Operating condition

$$P_{eo} = 0.9, V_{to} = 1.0, \text{p.f.} = 1.0$$

A.2 MULTIMACHINE SYSTEM DATA

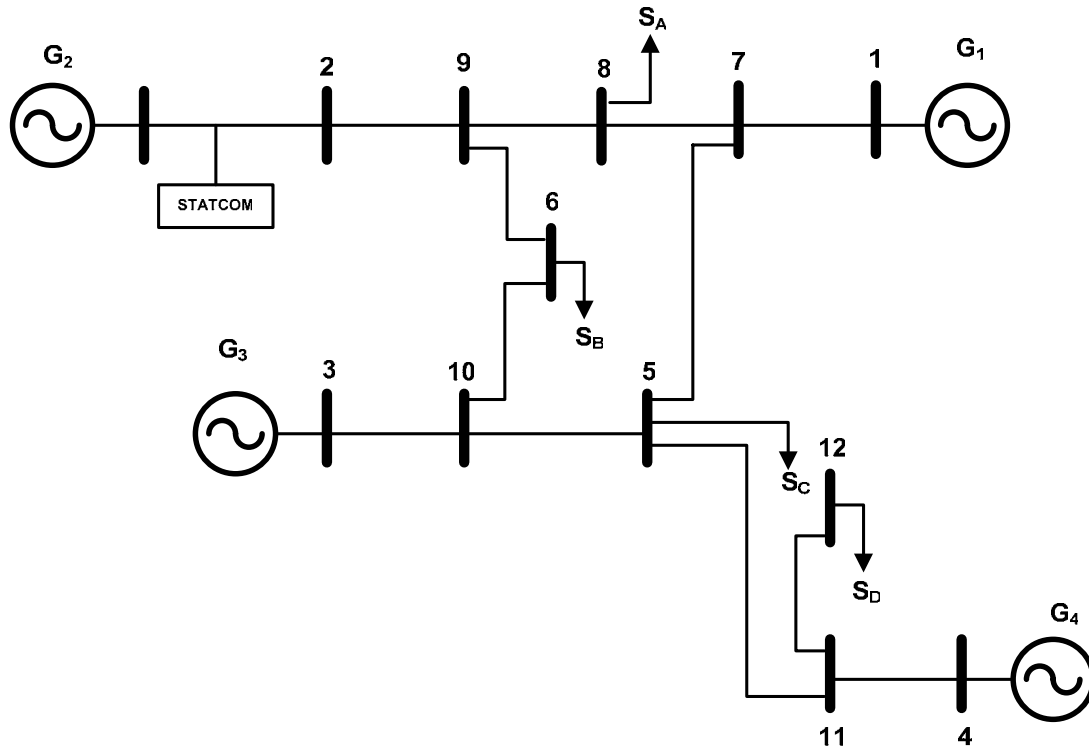


Figure A.1 Multimachine power system

The table A.1 and A.2 show the nominal loadings of Multimachine system

TABLE A.1 Nominal operating points for generator

Generators	P(MW)	Q(MVAR)
G ₁	231.9	119
G ₂	700	244.5
G ₃	300	193.3
G ₄	450	266.4

TABLE A.2 Nominal loadings

Loads	P(MW)	Q(MVAR)
S _A	350	195
S _B	350	195
S _C	650	375
S _D	325	155

The Table A.3 below shows the generator data for multimachine system

TABLE A.3 Generator data for multimachine system

X _d	X _q	X _{d1}	X _{d2}	X _{q2}	H	T _{do1}	T _{qo1}	K _a	T _a	K _D
1.000	0.9550	0.1219	0.026	0.033	6.50	3.48	0.50	75.0	0.01	0
1.244	1.1918	0.1655	0.026	0.033	2.55	8.62	0.10	75.0	0.01	0
2.769	2.6910	0.6017	0.269	0.335	3.28	6.11	0.50	75.0	0.01	0
0.552	0.3972	0.1845	0.029	0.026	3.17	7.39	0.10	75.0	0.01	0

The table A.4 shows the STATCOM data for Multimachine system

TABLE A.4 STATCOM data for multimachine system

X_{LB}	X_{tL}	X_{SDT}	m_o	C_{DC}
0.15	0.15	0.10	0.25	1.00
0.15	0.15	0.10	0.25	1.00
0.15	0.15	0.10	0.25	1.00
0.15	0.15	0.10	0.25	1.00

APPENDIX B

DERIVATION OF THE DETAILED DYNAMIC MODEL OF SMIB INSTALLED WITH STATCOM

The voltage and current relationship for the power system with STATCOM shown in Fig.

B.1 are expressed as

$$I_s = I_{sd} + jI_{sq}$$

$$V_o = mV_{DC} (\cos \psi + j \sin \psi) = mV_{DC} \angle \psi \quad (\text{B.1})$$

$$\frac{dV_{DC}}{dt} = \frac{I_{DC}}{C_{DC}} = \frac{m}{C_{DC}} (I_{sd} \cos \psi + I_{sq} j \sin \psi) \quad (\text{B.2})$$

where

$$m = ek$$

$$k = \frac{\text{AC Voltage}}{\text{DC Voltage}}$$

e = modulation ratio defined by PWM

ψ = phase angle defined by PWM

from Fig. B.1,

$$V_t = jX_{iL} I_t + jX_{LB} I_{LB} + V_B \quad (\text{B.3})$$

Now

$$I_{LB} = I_t - I_s \quad (\text{B.4})$$

$$I_s = \frac{V_L - V_o}{jX_{SDT}} \quad (\text{B.5})$$

$$V_L = V_t - X_{iL} I_t \quad (\text{B.6})$$

Substituting in the expression for I_{LB}

$$I_{LB} = I_t - \frac{V_t - V_o}{jX_{SDT}} = I_t - \left[\frac{(V_t - jX_{iL} I_t) - V_o}{jX_{SDT}} \right] \quad (\text{B.7})$$

$$I_{LB} = \frac{jX_{SDT} I_t - V_t + jX_{iL} I_t + V_o}{jX_{SDT}}$$

Substituting (B.7) in (B.3)

$$V_t = jX_{iL} I_t + jX_{LB} I_{LB} + V_B \quad (\text{B.8})$$

$$V_t = jX_{iL} I_t + jX_{LB} \left[\frac{jX_{SDT} I_t - V_t + jX_{iL} I_t + V_o}{jX_{SDT}} \right] + V_B$$

$$V_t \left[1 + \frac{X_{LB}}{X_{SDT}} \right] = jX_{iL}I_t + jX_{LB}I_t + \frac{jX_{iL}X_{LB}}{X_{SDT}}I_t + V_o \frac{X_{LB}}{X_{SDT}} + V_B \quad (\text{B.9})$$

$$V_t \left[1 + \frac{X_{LB}}{X_{SDT}} \right] = j \left[X_{iL} + X_{LB} + \frac{X_{iL}X_{LB}}{X_{SDT}} \right] I_t + V_o \frac{X_{LB}}{X_{SDT}} + V_B \quad (\text{B.10})$$

Let

$$Z = \left[1 + \frac{X_{LB}}{X_{SDT}} \right] \quad (\text{B.11})$$

$$A = \left[X_{iL} + X_{LB} + \frac{X_{iL}X_{LB}}{X_{SDT}} \right] \quad (\text{B.12})$$

$$ZV_t - \frac{X_{LB}}{X_{SDT}}V_o - V_B = jAI_t \quad (\text{B.13})$$

Now

$$V_t = V_d + jV_q = x_q I_q + j(e'_q - x'_d I_d) \quad (\text{B.14})$$

$$V_o = mV_{DC} \cos \psi + jmV_{DC} \sin \psi \quad (\text{B.15})$$

$$V_B = V_B \sin \delta + jV_B \cos \delta \quad (\text{B.16})$$

$$I_t = I_d + jI_q \quad (\text{B.17})$$

Substituting all in (B.13)

$$\begin{aligned} Z \left[x_q I_q + j(e'_q - x'_d I_d) \right] - \frac{X_{LB}}{X_{SDT}} [mV_{DC} \cos \psi + jmV_{DC} \sin \psi] \\ - V_B \sin \delta - jV_B \cos \delta = jA [I_d + jI_q] \end{aligned}$$

$$\begin{aligned}
 -AI_q + jAI_d = Zx_q I_q - \frac{X_{LB}}{X_{SDT}} mV_{DC} \cos \psi - V_B \sin \delta \\
 + j \left\{ \left[Ze'_q - Zx'_d I_d \right] - \frac{X_{LB}}{X_{SDT}} mV_{DC} \sin \psi - V_B \cos \delta \right\}
 \end{aligned}$$

Comparing the real and imaginary parts,

For real part

$$-AI_q = Zx_q I_q - \frac{X_{LB}}{X_{SDT}} mV_{DC} \cos \psi - V_B \sin \delta \quad (\text{B.18})$$

$$\left[A + Zx_q \right] I_q = \frac{X_{LB}}{X_{SDT}} mV_{DC} \cos \psi + V_B \sin \delta \quad (\text{B.19})$$

$$I_q = \frac{\frac{X_{LB}}{X_{SDT}} mV_{DC} \cos \psi + V_B \sin \delta}{\left[A + Zx_q \right]} \quad (\text{B.20})$$

$$I_q = \frac{\frac{X_{LB}}{X_{SDT}} mV_{DC} \cos \psi + V_B \sin \delta}{\left[X_{iL} + X_{LB} + \frac{X_{iL} X_{LB}}{X_{SDT}} \right] + \left[1 + \frac{X_{LB}}{X_{SDT}} \right] x_q} \quad (\text{B.21})$$

Similarly from imaginary part

$$AI_d = Ze'_q - Zx'_d I_d - \frac{X_{LB}}{X_{SDT}} mV_{DC} \sin \psi - V_B \cos \delta \quad (\text{B.22})$$

$$\left[A + Zx'_d \right] I_d = Ze'_q - \frac{X_{LB}}{X_{SDT}} mV_{DC} \sin \psi - V_B \cos \delta \quad (\text{B.23})$$

$$I_d = \frac{Ze'_q - \frac{X_{LB}}{X_{SDT}} mV_{DC} \sin \psi - V_B \cos \delta}{A + Zx'_d} \quad (\text{B.24})$$

$$\therefore I_d = \frac{\left(1 + \frac{X_{LB}}{X_{SDT}}\right) e'_q - \frac{X_{LB}}{X_{SDT}} mV_{DC} \sin \psi - V_B \cos \delta}{X_{tL} + X_{LB} + \frac{X_{tL}}{X_{SDT}} + \left(1 + \frac{X_{LB}}{X_{SDT}}\right) x'_d} \quad (\text{B.25})$$

Therefore the nonlinear model is given as :

$$\dot{\delta} = \omega_o \omega \quad (\text{B.26})$$

$$\dot{\omega} = \frac{1}{M} \left[P_m - P_e - (x_d - x'_d) I_d \right] \quad (\text{B.27})$$

$$\dot{e}'_q = \left[E_{fd} - e'_q - (x_d - x'_d) I_d \right] \frac{1}{T_{do}'} \quad (\text{B.28})$$

$$\dot{E}_{fd} = -\frac{1}{T_A} (E_{fd} - E_{fd0}) + \frac{K_A}{T_A} (V_{to} - V_t) \quad (\text{B.29})$$

$$\dot{V}_{dc} = \frac{m}{C_{DC}} \left[I_{sd} \cos \psi + I_{sq} \sin \psi \right] \quad (\text{B.30})$$

where

$$P_e = v_d I_d + v_q I_q$$

$$P_e = e'_q I_q + (x_q - x'_d) I_q I_d$$

$$V_t = \sqrt{v_d^2 + v_q^2} = \sqrt{(e'_q - x'_d I_d)^2 + x_q I_q^2}$$

For Linear Model

$$I_d = \frac{\left(1 + \frac{X_{LB}}{X_{SDT}}\right) e'_q - \frac{X_{LB}}{X_{SDT}} m V_{DC} \sin \psi - V_B \cos \delta}{X_{iL} + X_{LB} + \frac{X_{iL}}{X_{SDT}} + \left(1 + \frac{X_{LB}}{X_{SDT}}\right) x'_d} \quad (\text{B.31})$$

$$I_d = \frac{1}{[A]} \left[Z e'_q - \frac{X_{LB}}{X_{SDT}} m_o V_{DC} \sin \psi - V_B \cos \delta \right] \quad (\text{B.32})$$

where

$$[A] = X_{iL} + X_{LB} + \frac{X_{iL}}{X_{SDT}} + \left(1 + \frac{X_{LB}}{X_{SDT}}\right) x'_d \quad (\text{B.33})$$

&

$$Z = 1 + \frac{X_{LB}}{X_{SDT}} \quad (\text{B.34})$$

Linearizing

$$\Delta I_d = \frac{1}{[A]} \left[Z \Delta e'_q - \frac{X_{LB}}{X_{SDT}} m_o V_{DCo} \cos \psi_o \Delta \psi - \frac{X_{LB}}{X_{SDT}} m_o \Delta V_{DC} \sin \psi_o - \frac{X_{LB}}{X_{SDT}} V_{DCo} \sin \psi_o \Delta m + V_B \sin \delta_o \Delta \delta \right] \quad (\text{B.35})$$

$$\Delta I_d = \frac{Z}{[A]} \Delta e'_q + \frac{V_B \sin \delta_o}{[A]} \Delta \delta + \left(-\frac{X_{LB}}{X_{SDT} [A]} V_{DCo} \sin \psi_o \right) \Delta m \times \left(-\frac{X_{LB}}{X_{SDT} [A]} m_o V_{DCo} \cos \psi_o \right) \Delta \psi + \left(-\frac{X_{LB}}{X_{SDT} [A]} m_o \sin \psi_o \right) \Delta V_{DC} \quad (\text{B.36})$$

$$\Delta I_d = C_5 \Delta e'_q + C_6 \Delta \delta + C_7 \Delta \psi + C_8 \Delta m + C_9 \Delta V_{DC} \quad (\text{B.37})$$

Where

$$C_5 = \frac{Z}{[A]}, \quad C_6 = \frac{V_B \sin \delta_o}{[A]}, \quad C_7 = -\frac{X_{LB} m_o V_{DCo} \cos \psi_o}{X_{SDT} [A]}$$

$$C_8 = \frac{X_{LB} V_{DCo} \sin \psi_o}{X_{SDT} [A]}, \quad C_9 = -\frac{X_{LB} m_o \sin \psi_o}{X_{SDT} [A]}$$

Similarly

$$I_q = \frac{\frac{X_{LB}}{X_{SDT}} m V_{DC} \cos \psi + V_B \sin \delta}{\left[X_{iL} + X_{LB} + \frac{X_{iL} X_{LB}}{X_{SDT}} \right] + \left[1 + \frac{X_{LB}}{X_{SDT}} \right] x_q} \quad (\text{B.38})$$

$$I_q = \frac{1}{[B]} \left[\frac{X_{LB}}{X_{SDT}} m V_{DC} \cos \psi + V_B \sin \delta \right] \quad (\text{B.39})$$

Linearizing

$$\Delta I_q = \frac{1}{[B]} \left[V_B \cos \delta_o \Delta \delta - \frac{X_{LB}}{X_{SDT}} m_o V_{DCo} \sin \psi_o \Delta \psi \right. \\ \left. + \frac{X_{LB}}{X_{SDT}} m_o \Delta V_{DC} \sin \psi_o + \frac{X_{LB}}{X_{SDT}} V_{DCo} \sin \psi_o \Delta m_o \right] \quad (\text{B.40})$$

$$\Delta I_q = \frac{V_B \cos \delta_o}{[B]} \Delta \delta + \left(-\frac{X_{LB}}{X_{SDT} [B]} m_o V_{DCo} \sin \psi_o \right) \Delta \psi \\ + \left(\frac{X_{LB}}{X_{SDT} [A]} V_{DCo} \cos \psi_o \right) \Delta m + \left(\frac{X_{LB}}{X_{SDT} [A]} m_o \cos \psi_o \right) \Delta V_{DC} \quad (\text{B.41})$$

$$\Delta I_q = C_1 \Delta \delta + C_2 \Delta \psi + C_3 \Delta m + C_4 \Delta V_{DC} \quad (\text{B.42})$$

where

$$C_1 = \frac{V_B \cos \delta_o}{[B]}, \quad C_2 = -\frac{X_{LB} m_o V_{DCo} \sin \psi_o}{X_{SDT} [B]}$$

$$C_3 = \frac{X_{LB} V_{DCo} \cos \psi_o}{X_{SDT} [A]}, \quad C_4 = \frac{X_{LB} m_o \cos \psi_o}{X_{SDT} [A]}$$

The linearized model of (B.27) to (B.30) is

$$\Delta \dot{\delta} = \omega_o \Delta \omega \quad (\text{B.43})$$

$$\Delta \dot{\omega} = -\frac{1}{M} [\Delta P_e + D \Delta \omega] \quad (\text{B.44})$$

$$\Delta \dot{e}'_q = [\Delta E_{fd} - \Delta e'_q] \frac{1}{T_{do'}} \quad (\text{B.45})$$

$$\Delta \dot{E}_{fd} = -\frac{1}{T_A} \Delta E_{fd} - \frac{K_A}{T_A} \Delta V_t \quad (\text{B.46})$$

$$\Delta \dot{V}_{dc} = \frac{m}{C_{DC}} [I_{sd} \cos \psi + I_{sq} \sin \psi] \quad (\text{B.47})$$

Since

$$e_q = e'_q + (x_d - x'_d) I_d$$

Therefore by linearizing

$$\Delta e_q = \Delta e'_q + (x_d - x'_d) \Delta I_d \quad (\text{B.48})$$

Calculation of ΔP_e

$$P_e = e'_q I_q + (x_q - x'_d) I_d I_q \quad (\text{B.49})$$

linearizing

$$\Delta P_e = e'_{qo} \Delta I_q + I_{qo} \Delta e'_q + (x_q - x'_d) I_{do} \Delta I_q + (x_q - x'_d) I_{qo} \Delta I_d \quad (\text{B.50})$$

$$= \left[e'_{qo} + (x_q - x'_d) I_{do} \right] \Delta I_q + I_{qo} \Delta e'_q + (x_q - x'_d) I_{qo} \Delta I_d \quad (\text{B.51})$$

Substituting the value of ΔI_d & ΔI_q

$$\begin{aligned} \Delta P_e = & \left[e'_{qo} + (x_q - x'_d) I_{do} \right] \{ C_1 \Delta \delta + C_2 \Delta \psi + C_3 \Delta m + C_4 \Delta V_{DC} \} + I_{qo} \Delta e'_q \\ & + (x_q - x'_d) I_{qo} \{ C_5 \Delta e'_q + C_6 \Delta \delta + C_7 \Delta \psi + C_8 \Delta m + C_9 \Delta V_{DC} \} \end{aligned} \quad (\text{B.52})$$

$$\begin{aligned} \Delta P_e = & \left\{ e'_{qo} + (x_q - x'_d) I_{do} C_1 + (x_q - x'_d) I_{do} C_6 \right\} \Delta \delta + \left[I_{qo} \left\{ 1 + (x_q - x'_d) C_5 \right\} \right] \Delta e'_q \\ & + \left[\left\{ e'_{qo} + (x_q - x'_d) I_{do} \right\} C_4 + (x_q - x'_d) I_{qo} C_9 \right] \Delta V_{DC} \\ & + \left[\left\{ e'_{qo} + (x_q - x'_d) I_{do} \right\} C_3 + (x_q - x'_d) I_{qo} C_8 \right] \Delta m \\ & + \left[\left\{ e'_{qo} + (x_q - x'_d) I_{do} \right\} C_2 + (x_q - x'_d) I_{qo} C_7 \right] \Delta \psi \end{aligned} \quad (\text{B.53})$$

Let

$$C_{111} = e'_{qo} + (x_q - x'_d) I_{do}$$

$$C_{112} = (x_q - x'_d) I_{qo}$$

Therefore

$$\begin{aligned}
\Delta P_e = & (C_{111}C_1 + C_{112}C_6)\Delta\delta + \left[I_{qo} \left\{ 1 + (x_q - x'_d)C_5 \right\} \right] \Delta e'_q \\
& + (C_{111}C_4 + C_{112}C_9)\Delta V_{DC} + (C_{111}C_3 + C_{112}C_8)\Delta m \\
& + (C_{111}C_2 + C_{112}C_7)\Delta\psi
\end{aligned} \tag{B.54}$$

$$\Delta P_e = K_1\Delta\delta + K_2\Delta e'_q + K_{pDC}\Delta V_{DC} + K_{pc}\Delta m + K_{p\psi}\Delta\psi \tag{B.55}$$

where

$$\begin{aligned}
K_1 &= C_{111}C_1 + C_{112}C_6, & K_2 &= I_{qo} \left\{ 1 + (x_q - x'_d)C_5 \right\} \\
K_{pDC} &= C_{111}C_4 + C_{112}C_9, & K_{pc} &= C_{111}C_3 + C_{112}C_8 \\
K_{p\psi} &= C_{111}C_2 + C_{112}C_7
\end{aligned}$$

Calculation of Δe_q

$$\begin{aligned}
\Delta e_q &= \Delta e'_q + (x_d - x'_d)\Delta I_d \\
\Delta e_q &= \Delta e'_q + (x_d - x'_d)(C_5\Delta e'_q + C_6\Delta\delta + C_7\Delta\psi + C_8\Delta m + C_9\Delta V_{DC}) \\
&= \left\{ 1 + (x_d - x'_d)C_5 \right\} \Delta e'_q + (x_d - x'_d)C_6\Delta\delta + (x_d - x'_d)C_7\Delta\psi \\
&\quad + (x_d - x'_d)C_8\Delta m + (x_d - x'_d)C_9\Delta V_{DC}
\end{aligned}$$

Let

$$(x_d - x'_d) = J \tag{B.56}$$

$$\begin{aligned}
\Delta e_q &= \{1 + JC_5\} \Delta e'_q + JC_6\Delta\delta + JC_7\Delta\psi + JC_8\Delta m + JC_9\Delta V_{DC} \\
&= K_3\Delta e'_q + K_4\Delta\delta + K_{q\psi}\Delta\psi + K_{qc}\Delta m + K_{qDC}\Delta V_{DC}
\end{aligned}$$

where

$$\begin{aligned}
K_3 &= 1 + JC_5, & K_4 &= JC_6, & K_{q\psi} &= JC_7 \\
K_{qc} &= JC_8, & K_{qDC} &= JC_9
\end{aligned}$$

Calculation of ΔV_t

$$\Delta V_t = \frac{V_{do}}{V_{to}} \Delta V_d + \frac{V_{qo}}{V_{to}} \Delta V_q \quad (\text{B.57})$$

$$= \frac{V_{do}}{V_{to}} (x_q \Delta I_q) + \frac{V_{qo}}{V_{to}} (\Delta e'_q - x'_d \Delta I_d) \quad (\text{B.58})$$

$$= \frac{V_{do}}{V_{to}} (x_q C_5 \Delta e'_q + C_6 \Delta \delta + C_7 \Delta \psi + C_8 \Delta m + C_9 \Delta V_{DC}) + \frac{V_{qo}}{V_{to}} (\Delta e'_q - x'_d \Delta I_d) \quad (\text{B.59})$$

Let

$$L = \frac{1}{V_{to}}$$

therefore

$$\begin{aligned} \Delta V_t = L & (V_{do} x_q C_1 - V_{qo} x'_d C_6) \Delta \delta + L V_{qo} (1 - x'_d C_5) \Delta e'_q + L (V_{do} x_q C_4 - V_{qo} x'_d C_9) \Delta V_{DC} \\ & + L (V_{do} x_q C_3 - V_{qo} x'_d C_8) \Delta m + L (V_{do} x_q C_2 - V_{qo} x'_d C_7) \Delta \psi \end{aligned} \quad (\text{B.60})$$

$$\Delta V_t = K_5 \Delta \delta + K_6 \Delta e'_q + K_{VDC} \Delta V_{DC} + K_{Vm} \Delta m + K_{V\psi} \Delta \psi \quad (\text{B.61})$$

where

$$\begin{aligned} K_5 &= L (V_{do} x_q C_1 - V_{qo} x'_d C_6), & K_6 &= L V_{qo} (1 - x'_d C_5) \\ K_{VDC} &= L (V_{do} x_q C_4 - V_{qo} x'_d C_9), & K_{Vm} &= L (V_{do} x_q C_3 - V_{qo} x'_d C_8) \\ K_{V\psi} &= L (V_{do} x_q C_2 - V_{qo} x'_d C_7) \end{aligned}$$

Substituting all values in the linearized model given by equation (B.44) to (B.48)

$$\Delta \dot{\delta} = \omega_o \Delta \omega \quad (\text{B.62})$$

$$\begin{aligned}
\Delta \dot{\omega} &= -\frac{1}{M} \left[\left\{ K_1 \Delta \delta + K_2 \Delta e'_q + K_{pDC} \Delta V_{DC} + K_{pm} \Delta m + K_{p\psi} \Delta \psi \right\} + D \Delta \omega \right] \\
&= -\frac{K_1}{M} \Delta \delta - \frac{K_2}{M} \Delta e'_q - \frac{K_{pDC}}{M} \Delta V_{DC} - \frac{K_{pm}}{M} \Delta m - \frac{K_{p\psi}}{M} \Delta \psi - \frac{D}{M} \Delta \omega \\
&= -\frac{K_1}{M} \Delta \delta - \frac{D}{M} \Delta \omega - \frac{K_2}{M} \Delta e'_q - \frac{K_{pDC}}{M} \Delta V_{DC} - \frac{K_{pm}}{M} \Delta m - \frac{K_{p\psi}}{M} \Delta \psi
\end{aligned} \tag{B.63}$$

$$\Delta \dot{e}'_q = \left[\Delta E_{fd} - \Delta e'_q \right] \frac{1}{T_{do}'} \tag{B.64}$$

$$\begin{aligned}
\Delta \dot{e}'_q &= \frac{1}{T_{do}'} \left[- \left(K_3 \Delta e'_q + K_4 \Delta \delta + K_{q\psi} \Delta \psi + K_{qm} \Delta m + K_{qDC} \Delta V_{DC} \right) + \Delta E_{fd} \right] \\
&= -\frac{K_3}{T_{do}'} \Delta e'_q - \frac{K_4}{T_{do}'} \Delta \delta - \frac{K_{q\psi}}{T_{do}'} \Delta \psi - \frac{K_{qm}}{T_{do}'} \Delta m - \frac{K_{qDC}}{T_{do}'} \Delta V_{DC} + \frac{1}{T_{do}'} \Delta E_{fd}
\end{aligned} \tag{B.65}$$

$$\Delta \dot{E}_{fd} = -\frac{1}{T_A} \Delta E_{fd} - \frac{K_A}{T_A} \Delta V_t \tag{B.66}$$

$$\begin{aligned}
\Delta \dot{E}_{fd} &= -\frac{1}{T_A} \Delta E_{fd} - \frac{K_A}{T_A} \\
&\quad \left[K_5 \Delta \delta + K_6 \Delta e'_q + K_{VDC} \Delta V_{DC} + K_{Vm} \Delta m + K_{V\psi} \Delta \psi \right]
\end{aligned} \tag{B.67}$$

$$\begin{aligned}
&= -\frac{K_A K_5}{T_A} \Delta \delta - \frac{K_A K_6}{T_A} \Delta e'_q - \frac{1}{T_A} \Delta E_{fd} - \frac{K_A K_{VDC}}{T_A} \Delta V_{DC} \\
&\quad - \frac{K_A K_{Vm}}{T_A} \Delta m - \frac{K_A K_{V\psi}}{T_A} \Delta \psi
\end{aligned} \tag{B.68}$$

In matrix form

$$\begin{aligned}
 \begin{bmatrix} \Delta \dot{\delta} \\ \Delta \dot{\omega} \\ \Delta \dot{e}'_q \\ \Delta \dot{E}_{fd} \end{bmatrix} &= \begin{pmatrix} 0 & \omega_o & 0 & 0 \\ -\frac{K_1}{M} & -\frac{D}{M} & -\frac{K_2}{M} & 0 \\ -\frac{K_4}{T_{do'}} & 0 & -\frac{K_3}{T_{do'}} & \frac{1}{T_{do'}} \\ -\frac{K_A K_5}{T_A} & 0 & -\frac{K_A K_6}{T_A} & -\frac{1}{T_A} \end{pmatrix} \begin{bmatrix} \Delta \delta \\ \Delta \omega \\ \Delta e'_q \\ \Delta E_{fd} \end{bmatrix} + \\
 &\begin{bmatrix} 0 \\ -\frac{K_{pDC}}{M} \\ -\frac{K_{qDC}}{T_{do'}} \\ -\frac{K_A K_{VDC}}{T_A} \end{bmatrix} \Delta V_{DC} + \begin{pmatrix} 0 & 0 \\ -\frac{K_{pm}}{M} & -\frac{K_{p\psi}}{M} \\ -\frac{K_{qm}}{T_{do'}} & -\frac{K_{q\psi}}{T_{do'}} \\ -\frac{K_A K_{Vm}}{T_A} & -\frac{K_A K_{V\psi}}{T_A} \end{pmatrix} \begin{bmatrix} \Delta m \\ \Delta \psi \end{bmatrix}
 \end{aligned} \tag{B.69}$$

Now,

$$I_s = \frac{V_L - V_o}{jX_{SDT}} \tag{B.70}$$

$$I_s = \frac{(V_t - jX_{tL}I_t) - V_o}{jX_{SDT}} \tag{B.71}$$

Substituting values of I_s , V_t , I_t , V_o

$$\begin{aligned}
 I_{sd} + jI_{sq} &= \frac{1}{jX_{SDT}} \left[x_q I_q + j(e'_q - x'_d I_d) - jX_{tL} (I_d + jI_q) \right. \\
 &\quad \left. - mV_{DC} (\cos \psi + j \sin \psi) \right]
 \end{aligned} \tag{B.72}$$

$$I_{sd} + jI_{sq} = \frac{1}{jX_{SDT}} \left[x_q I_q + j(e'_q - x'_d I_d) - jX_{tL} I_d + X_{tL} I_q - mV_{DC} \cos \psi - jmV_{DC} \sin \psi \right] \quad (\text{B.73})$$

$$I_{sd} + jI_{sq} = \frac{1}{jX_{SDT}} \left[\left\{ (x_q + X_{tL}) I_q - mV_{DC} \cos \psi \right\} + j \left\{ e'_q - (x'_d + X_{tL}) I_q - mV_{DC} \sin \psi \right\} \right] \quad (\text{B.74})$$

$$I_{sd} + jI_{sq} = \frac{e'_q - (x'_d + X_{tL}) I_q - mV_{DC} \sin \psi}{X_{SDT}} + j \frac{\left\{ mV_{DC} \cos \psi - (x_q + X_{tL}) I_q \right\}}{X_{SDT}} \quad (\text{B.75})$$

Comparing real and imaginary parts

$$I_{sd} = \frac{e'_q}{X_{SDT}} - \frac{(x'_d + X_{tL}) I_q}{X_{SDT}} - \frac{mV_{DC} \sin \psi}{X_{SDT}} \quad (\text{B.76})$$

$$I_{sq} = \frac{mV_{DC} \cos \psi}{X_{SDT}} - \frac{(x_q + X_{tL}) I_q}{X_{SDT}} \quad (\text{B.77})$$

Linearizing equation (B.76) and (B.77)

$$I_{sd} = \frac{1}{X_{SDT}} \Delta e'_q - \frac{(x'_d + X_{tL})}{X_{SDT}} \Delta I_d - \frac{m_o \sin \psi_o}{X_{SDT}} \Delta V_{DC} - \frac{m_o V_{DCo} \cos \psi_o}{X_{SDT}} \Delta \psi - \frac{V_{DCo} \sin \psi_o}{X_{SDT}} \Delta m \quad (\text{B.78})$$

$$I_{sd} = \frac{1}{X_{SDT}} \Delta e'_q - \frac{(x'_d + X_{tL})}{X_{SDT}} \left\{ C_5 \Delta e'_q + C_6 \Delta \delta + C_7 \Delta \psi + C_8 \Delta m + C_9 \Delta V_{DC} \right\} - \frac{m_o \sin \psi_o}{X_{SDT}} \Delta V_{DC} - \frac{m_o V_{DCo} \cos \psi_o}{X_{SDT}} \Delta \psi - \frac{V_{DCo} \sin \psi_o}{X_{SDT}} \Delta m \quad (\text{B.79})$$

$$\begin{aligned}
I_{sd} = & \frac{1}{X_{SDT}} \left\{ 1 - (x'_d + X_{iL}) C_5 \right\} \Delta e'_q - \frac{(x'_d + X_{iL})}{X_{SDT}} C_6 \Delta \delta - \frac{(x'_d + X_{iL})}{X_{SDT}} C_7 \Delta \psi \\
& - \frac{(x'_d + X_{iL})}{X_{SDT}} C_8 \Delta m - \frac{(x'_d + X_{iL})}{X_{SDT}} C_9 \Delta V_{DC} - \frac{m_o \sin \psi_o}{X_{SDT}} \Delta V_{DC} \\
& - \frac{m_o V_{DCo} \cos \psi_o}{X_{SDT}} \Delta \psi - \frac{V_{DCo} \sin \psi_o}{X_{SDT}} \Delta m
\end{aligned} \tag{B.80}$$

Let

$$\frac{(x'_d + X_{iL})}{X_{SDT}} = E \quad \text{and} \quad \frac{\sin \psi_o}{X_{SDT}} = G$$

$$\begin{aligned}
I_{sd} = & \frac{1}{X_{SDT}} \left\{ 1 - (x'_d + X_{iL}) C_5 \right\} \Delta e'_q - EC_6 \Delta \delta - EC_7 \Delta \psi - EC_8 \Delta m - EC_9 \Delta V_{DC} \\
& - \frac{m_o V_{DCo} \cos \psi_o}{X_{SDT}} \Delta \psi - Gm_o \Delta V_{DC} - GV_{DCo} \Delta m
\end{aligned} \tag{B.81}$$

$$I_{sd} = C_{10} \Delta e'_q + C_{11} \Delta \delta + C_{12} \Delta \psi + C_{13} \Delta m + C_{14} \Delta V_{DC} \tag{B.82}$$

where

$$\begin{aligned}
C_{10} &= \frac{1}{X_{SDT}} \left\{ 1 - (x'_d + X_{iL}) C_5 \right\}, & C_{11} &= -EC_6 \\
C_{12} &= - \left\{ EC_7 + \frac{m_o V_{DCo} \cos \psi_o}{X_{SDT}} \right\}, & C_{13} &= - \{ EC_8 + GV_{DCo} \} \\
C_{14} &= - \{ EC_9 + Gm_o \}
\end{aligned}$$

Similarly

$$\Delta I_{sq} = -\frac{m_o V_{DCo} \sin \psi_o}{X_{SDT}} \Delta \psi + \frac{m_o \cos \psi_o}{X_{SDT}} \Delta V_{DC} + \frac{V_{DCo} \cos \psi}{X_{SDT}} \Delta m - \frac{(x_q + X_{iL})}{X_{SDT}} \Delta I_q \quad (\text{B.83})$$

$$\Delta I_{sq} = -\frac{m_o V_{DCo} \sin \psi_o}{X_{SDT}} \Delta \psi + \frac{m_o \cos \psi_o}{X_{SDT}} \Delta V_{DC} + \frac{V_{DCo} \cos \psi}{X_{SDT}} \Delta m - \frac{(x_q + X_{iL})}{X_{SDT}} \{C_1 \Delta \delta + C_2 \Delta \psi + C_3 \Delta m + C_4 \Delta V_{DC}\} \quad (\text{B.84})$$

$$\Delta I_{sq} = -\frac{(x_q + X_{iL})}{X_{SDT}} C_1 \Delta \delta - \left\{ m_o V_{DCo} G + \frac{(x_q + X_{iL})}{X_{SDT}} C_2 \right\} \Delta \psi + \left\{ \frac{m_o \cos \psi_o}{X_{SDT}} - \frac{(x_q + X_{iL})}{X_{SDT}} C_4 \right\} \Delta V_{DC} + \left\{ \frac{V_{DCo} \cos \psi_o}{X_{SDT}} + \frac{(x_q + X_{iL})}{X_{SDT}} C_3 \right\} \Delta m \quad (\text{B.85})$$

Let

$$\frac{(x_q + X_{iL})}{X_{SDT}} = W$$

$$\Delta I_{sq} = -WC_1 \Delta \delta - \left\{ m_o V_{DCo} G + W C_2 \right\} \Delta \psi + \left\{ \frac{m_o \cos \psi_o}{X_{SDT}} - WC_4 \right\} \Delta V_{DC} + \left\{ \frac{V_{DCo} \cos \psi_o}{X_{SDT}} - WC_3 \right\} \Delta m \quad (\text{B.86})$$

$$\Delta I_{sq} = C_{15} \Delta \delta + C_{16} \Delta \psi + C_{17} \Delta V_{DC} + C_{18} \Delta m \quad (\text{B.87})$$

where

$$C_{15} = -WC_1, \quad C_{16} = -\left\{ m_o V_{DCo} G + W C_2 \right\}$$

$$C_{17} = \left\{ \frac{m_o \cos \psi_o}{X_{SDT}} - WC_4 \right\}, \quad C_{18} = \left\{ \frac{V_{DCo} \cos \psi_o}{X_{SDT}} - WC_3 \right\}$$

Now since the expression for \dot{V}_{DC} is given as

$$\dot{V}_{DC} = \frac{m}{C_{DC}} (I_{sd} \cos \psi + j I_{sq} \sin \psi) \quad (\text{B.88})$$

Linearizing with $\frac{1}{C_{DC}} = N$

$$\Delta \dot{V}_{DC} = N [(I_{sd_o} \cos \psi_o + I_{sq_o} \sin \psi_o) \Delta m + m_o (-I_{sd_o} \sin \psi_o + I_{sq_o} \cos \psi_o) \Delta \psi + m_o (\cos \psi_o \Delta I_{sd} + \sin \psi_o \Delta I_{sq})] \quad (\text{B.89})$$

Substituting the value of ΔI_{sd} and ΔI_{sq}

$$\Delta \dot{V}_{DC} = N [(I_{sd_o} \cos \psi_o + I_{sq_o} \sin \psi_o) \Delta m + m_o (-I_{sd_o} \sin \psi_o + I_{sq_o} \cos \psi_o) \Delta \psi + m_o \cos \psi_o (C_{10} \Delta e'_q + C_{11} \Delta \delta + C_{12} \Delta \psi + C_{13} \Delta m + C_{14} \Delta V_{DC}) + m_o \sin \psi_o (C_{15} \Delta \delta + C_{16} \Delta \psi + C_{17} \Delta V_{DC} + C_{18} \Delta m)] \quad (\text{B.90})$$

$$\Delta \dot{V}_{DC} = N m_o (\cos \psi_o C_{11} + \sin \psi_o C_{15}) \Delta \delta + (N m_o \cos \psi_o C_{10}) \Delta e'_q + N m_o (\cos \psi_o C_{14} + \sin \psi_o C_{17}) \Delta V_{DC} + N (I_{sd_o} \cos \psi_o + I_{sq_o} \sin \psi_o + m_o \cos \psi_o C_{13} + m_o \sin \psi_o C_{18}) \Delta m + N m_o (-I_{sd_o} \sin \psi_o + I_{sq_o} \cos \psi_o + \cos \psi_o C_{12} + \sin \psi_o C_{16}) \Delta \psi \quad (\text{B.91})$$

$$\Delta \dot{V}_{DC} = K_7 \Delta \delta + K_8 \Delta e'_q + K_9 \Delta V_{DC} + K_{DC} \Delta m + K_{d\psi} \Delta \psi \quad (\text{B.92})$$

Where

$$\begin{aligned}
K_7 &= Nm_o (\cos \psi_o C_{11} + \sin \psi_o C_{15}) \\
K_8 &= (Nm_o \cos \psi_o C_{10}) \\
K_9 &= Nm_o (\cos \psi_o C_{14} + \sin \psi_o C_{17}) \\
K_{DC} &= N(I_{sd_o} \cos \psi_o + I_{sq_o} \sin \psi_o + m_o \cos \psi_o C_{13} + m_o \sin \psi_o C_{18}) \\
K_{d\psi} &= Nm_o (-I_{sd_o} \sin \psi_o + I_{sq_o} \cos \psi_o + \cos \psi_o C_{12} + \sin \psi_o C_{16})
\end{aligned}$$

In matrix form

$$\begin{aligned}
\begin{bmatrix} \Delta \dot{\delta} \\ \Delta \dot{\omega} \\ \Delta \dot{e}'_q \\ \Delta \dot{E}_{fd} \\ \Delta \dot{V}_{DC} \end{bmatrix} &= \begin{pmatrix} 0 & \omega_o & 0 & 0 & 0 \\ -\frac{K_1}{M} & -\frac{D}{M} & -\frac{K_2}{M} & 0 & -\frac{K_{pDC}}{M} \\ -\frac{K_4}{T_{do'}} & 0 & -\frac{K_3}{T_{do'}} & \frac{1}{T_{do'}} & -\frac{K_{qDC}}{T_{do'}} \\ -\frac{K_A K_5}{T_A} & 0 & -\frac{K_A K_6}{T_A} & -\frac{1}{T_A} & -\frac{K_A K_{VDC}}{T_A} \\ K_7 & 0 & K_8 & K_9 & 0 \end{pmatrix} \begin{bmatrix} \Delta \delta \\ \Delta \omega \\ \Delta e'_q \\ \Delta E_{fd} \\ \Delta V_{DC} \end{bmatrix} + \\
&+ \begin{pmatrix} 0 & 0 \\ -\frac{K_{pm}}{M} & -\frac{K_{p\psi}}{M} \\ -\frac{K_{qm}}{T_{do'}} & -\frac{K_{q\psi}}{T_{do'}} \\ -\frac{K_A K_{Vm}}{T_A} & -\frac{K_A K_{V\psi}}{T_A} \\ K_{DC} & K_{d\psi} \end{pmatrix} \begin{bmatrix} \Delta m \\ \Delta \psi \end{bmatrix}
\end{aligned} \tag{B.93}$$

APPENDIX C

DERIVATION OF DETAILED MODEL OF MULTIMACHINE POWER SYSTEM INSTALLED WITH STATCOM

It is assumed that STATCOM is installed on all generators of multimachine power system as shown in Fig. C.1

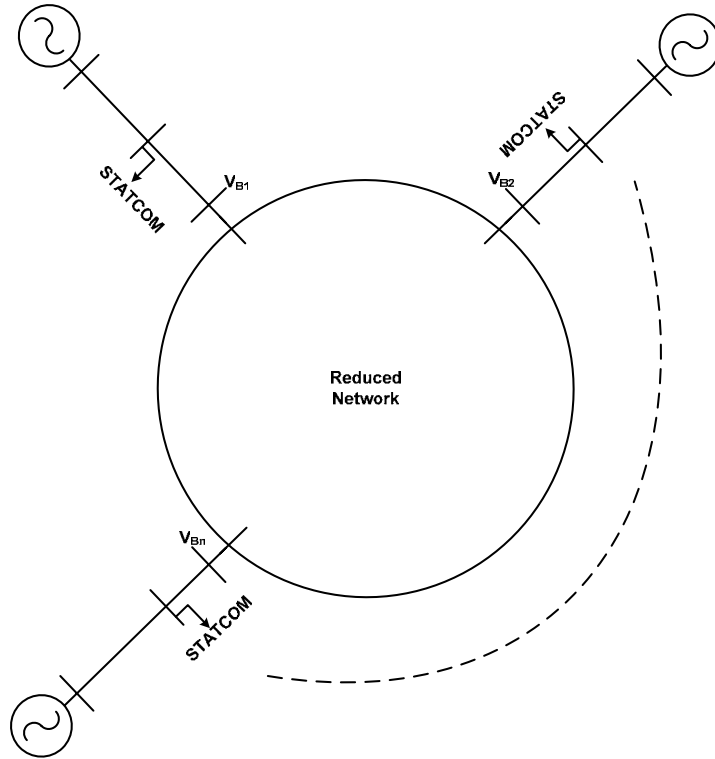


Fig. C.1 Reduced multimachine system configuration showing the generators and STATCOMS

The network equations are written as,

$$I_L = Y_b V_B \quad (\text{C.1})$$

where, $Y_m = (T_r^{-1} Y_b T_r)$ is the reduced admittance matrix referred to generator side, I_L and

V_B are network currents and voltages referred to generator side.

Breaking (C.1) in d – q components yields,

$$I_{Ld} + jI_{Lq} = (G_m + jB_m)(V_{Bd} + jV_{Bq}) \quad (\text{C.2})$$

To obtain the expressions for I_{Ld} and I_{Lq} in (C.2), consider the configuration of the i -th machine injecting current into the network as shown in Fig. C.2

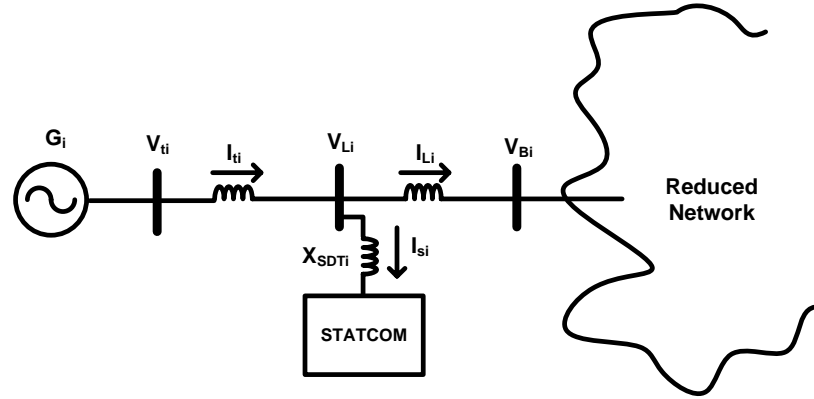


Fig. C.2 Configuration of the i -th generator in n – machine system

It is clear from Fig. C.2 that the problem is similar to single machine case.

The vector of generator currents of multimachine system installed with STATCOM can be expressed as,

$$I_{Ld} = \frac{\left(I + \frac{X_{LB}}{X_{SDT}} \right) e'_q - \frac{X_{LB}}{X_{SDT}} mV_{DC} \sin \psi - V_{Bq}}{X_{tL} + X_{LB} + \frac{X_{tL} X_{LB}}{X_{SDT}} + \left(I + \frac{X_{LB}}{X_{SDT}} \right) x'_d} \quad (C.3)$$

$$I_{Lq} = \frac{-\left[\frac{X_{LB}}{X_{SDT}} \right] e'_d + \frac{X_{LB}}{X_{SDT}} mV_{DC} \cos \psi + V_{Bd}}{\left[X_{tL} + X_{LB} + \frac{X_{tL} X_{LB}}{X_{SDT}} \right] + \left[I + \frac{X_{LB}}{X_{SDT}} \right] x'_d} \quad (C.4)$$

Here, it is to remembered that from now onwards currents, voltages, ψ and m are expressed as vectors and reactances are expressed as diagonal matrices unless mentioned otherwise.

Let

$$\begin{aligned}
 N_1 &= \frac{X_{LB}}{X_{SDT}} \\
 A &= X_{iL} + X_{LB} + \frac{X_{iL}X_{LB}}{X_{SDT}} \\
 Z &= \left(I + \frac{X_{LB}}{X_{SDT}} \right) \\
 D_1 &= D_2 = A + ZX'_d
 \end{aligned} \tag{C.5}$$

Substituting (C.5) in (C.3) and (C.4), solving for V_{Bd} and V_{Bq} yields,

$$V_{Bd} = Ze'_d - N_1 m V_{DC} \cos \psi + D_1 I_q \tag{C.6}$$

$$V_{Bq} = Ze'_q - N_1 m V_{DC} \sin \psi - D_2 I_d \tag{C.7}$$

From Fig. C.2 I_L can also be written as

$$I_L = Z_1 I_t + j \frac{V_t}{X_{SDT}} - j \frac{V_o}{X_{SDT}} \tag{C.8}$$

where,

$$Z_1 = \left(I + \frac{X_{LB}}{X_{SDT}} \right)$$

Breaking (C.8) in d – q components gives,

$$I_{Ld} + jI_{Lq} = Z_1 [I_d + I_q] + j \frac{[V_d + jV_q]}{X_{SDT}} - j \frac{[mV_{DC} \cos \psi + jmV_{DC} \sin \psi]}{X_{SDT}} \quad (C.9)$$

Solving (C.9) for I_{Ld} and I_{Lq} gives,

$$I_{Ld} = Z_2 I_d - \frac{e'_d}{X_{SDT}} + \frac{mV_{DC} \sin \psi}{X_{SDT}} \quad (C.10)$$

$$I_{Lq} = Z_3 I_q + \frac{e'_d}{X_{SDT}} - \frac{mV_{DC} \cos \psi}{X_{SDT}} \quad (C.11)$$

where,

$$Z_2 = \left[Z_1 + \frac{x'_d}{X_{SDT}} \right]$$

$$Z_3 = \left[Z_1 + \frac{x'_d}{X_{SDT}} \right]$$

substituting (C.10) and (C.11) in (C.6) and (C.7), and solving for V_{Bd} and V_{Bq} results in,

$$V_{Bd} = A_{1d} e'_d + A_3 V_{DC} \cos \psi + N_3 I_{Lq} \quad (C.12)$$

$$V_{Bq} = A_1 e'_q + A_2 V_{DC} \sin \psi - N_2 I_{Ld} \quad (C.13)$$

where,

$$\begin{aligned} N_2 &= D_2 Z_2^{-1}, & A_1 &= \left[Z - \frac{N_2}{X_{SDT}} \right], & A_2 &= \left[\frac{N_2}{X_{SDT}} - N_1 \right], \\ N_3 &= D_1 Z_3^{-1}, & A_{1d} &= \left[Z - \frac{N_3}{X_{SDT}} \right], & A_3 &= \left[\frac{N_3}{X_{SDT}} - N_1 \right] \end{aligned} \quad (C.14)$$

Substituting (C.12) and (C.13) in (C.2) gives,

$$I_{Ld} + jI_{Lq} = (G_m + jB_m) \left[(A_{1d}e'_d + A_3mV_{DC} \cos \psi + N_3I_{Lq}) + A_1e'_q + A_2mV_{DC} \sin \psi - N_2I_{Ld} \right] \quad (C.15)$$

Breaking (C.15) in d – q components yields,

$$I_{Ld} = G_m [N_3I_{Lq} + A_3mV_{DC} \cos \psi + A_{1d}e'_d] - B_m [A_1e'_q + A_2mV_{DC} \sin \psi - N_2I_{Ld}] \quad (C.16)$$

$$I_{Lq} = G_m [A_1e'_q + A_2mV_{DC} \sin \psi - N_2I_{Ld}] + B_m [N_3I_{Lq} + A_3mV_{DC} \cos \psi + A_{1d}e'_d] \quad (C.17)$$

Solving (C.16) and (C.17) for I_{Ld} and I_{Lq} respectively,

$$I_{Ld} = K_1^{-1} \{ G_m N_3 I_{Lq} + G_m m A_3 V_{DC} \cos \psi + G_m A_{1d} e'_d - B_m A_1 e'_q - B_m m A_2 V_{DC} \sin \psi \} \quad (C.18)$$

$$I_{Lq} = K_2^{-1} \{ G_m A_1 e'_q + G_m m A_2 V_{DC} \sin \psi - G_m N_2 I_{Ld} + B_m m A_3 V_{DC} \cos \psi + B_m A_{1d} e'_d \} \quad (C.19)$$

where,

$$K_1 = [I - B_m N_2]$$

$$K_2 = [I - B_m N_3]$$

Solving (C.18) and (C.19) simultaneously gives,

$$I_{Ld} = K_4^{-1} K_1^{-1} \{ [K_3 B_m A_{1d} + G_{m1} A_{1d}] e'_d + [K_3 G_m A_1 - B_m A_1] e'_q + [K_3 B_m A_3 + G_m A_3] m V_{DC} \cos \psi + [K_3 G_m A_2 - B_m A_2] m V_{DC} \sin \psi \} \quad (C.20)$$

$$I_{Lq} = K_2^{-1} \{ B_m A_{1d} e'_d + B_m m A_3 V_{DC} \cos \psi + G_m A_1 e'_q + G_m m A_2 V_{DC} \sin \psi - G_m N_2 I_{Ld} \} \quad (C.21)$$

where,

$$K_3 = G_m N_3 K_2^{-1}$$

$$K_4 = [1 + K_1 K_3 G_m N_2]$$

The STATCOM current vector is given by

$$I_s = \frac{V_L - V_o}{jX_{SDT}} \quad (C.22)$$

where, $V_L = V_B + jX_{tL} I_L$ (C.23)

Hence, generator current vector I_t is given by

$$I_t = I_L + I_s \quad (C.24)$$

The vector of state equations is given by

$$\dot{e}'_q = [E_{fd} - e'_q - (x_d - x'_d) I_d] \frac{1}{T'_{do}}$$

$$\dot{e}'_d = [E_{fd} - e'_q - (x_d - x'_d) I_d] \frac{1}{T'_{qo}}$$

$$\dot{\omega} = -\frac{1}{2H} [P_m - P_e + K_D \omega] \quad (C.25)$$

$$\dot{\delta} = \omega_o \omega$$

$$\dot{E}_{fd} = -\frac{1}{T_A} E_{fd} + \frac{K_A}{T_A} [V_{to} - V_t]$$

$$\dot{V}_{dc} = \frac{m}{C_{DC}} [I_{sd} \cos \psi + I_{sq} \sin \psi]$$

It is to be noted here that all the states, $[e'_d, e'_q, \omega, \delta, E_{fd}, V_{DC}]$ are expressed as vector of n variables each.

where,

$$\begin{aligned} P_e &= V_d I_d + V_q I_q \\ V_d &= e'_d + x'_d I_d \\ V_q &= e'_q - x'_q I_q \\ V_t &= \sqrt{V_d^2 + V_q^2} \end{aligned}$$

Linear Model

Linearizing the network current (C.1) gives,

$$\Delta I_L = Y_{mo} \Delta V_B + \Delta Y_m V_{Bo} \quad (C.26)$$

also,

$$\Delta Y_m = -j[\Delta \delta Y_{mo} - Y_{mo} \Delta \delta] \quad (C.27)$$

Linearising (C.12) and (C.13) gives,

$$\begin{aligned} \Delta V_{Bd} &= A_{1d} \Delta e'_d + A_3 [\Delta C V_{DC0} + C_o \Delta V_{DC}] + N_3 \Delta I_{Lq} \\ \Delta V_{Bq} &= A_1 \Delta e'_q + A_2 [\Delta C V_{DC0} + C_o \Delta V_{DC}] - N_2 \Delta I_{Ld} \end{aligned} \quad (C.28)$$

Now let us define M as

$$Y_m = T_r^{-1} Y_b T_r \quad (C.29)$$

Also linearising (C.29) we have

$$\Delta Y_m = -j(\Delta \delta Y_{mo} - Y_{mo} \Delta \delta) \quad (C.30)$$

Now, the network currents are given by

$$I_L = Y_m V_B \quad (C.31)$$

Linearising (C.31) we have

$$\Delta I_L = Y_{mo} \Delta V_B + \Delta Y_m V_{Bo} \quad (C.32)$$

Splitting (7) in real and imaginary terms we have

$$\Delta I_d + j\Delta I_q = (G_{mo} + jB_{mo}) (\Delta V_{Bd} + j\Delta V_{Bq}) + \left\{ -j(\Delta\delta Y_{mo} - Y_{mo}\Delta\delta) (V_{Bdo} + jV_{Bqo}) \right\} \quad (C.33)$$

Substituting (C.28) in (C.33) we have

$$\begin{aligned} \Delta I_d + j\Delta I_q &= (G_{mo} + jB_{mo}) \left\{ \left[A_{1d}\Delta e'_d + A_3 [\Delta m V_{DC0} + m_o \Delta V_{DC}] + N_3 \Delta I_{Lq} \right] + \right. \\ &\quad \left. j \left[A_{1q}\Delta e'_q + A_2 [\Delta m V_{DC0} + m_o \Delta V_{DC}] - N_2 \Delta I_{Ld} \right] \right\} + \left\{ -j(\Delta\delta Y_{mo} - Y_{mo}\Delta\delta) (V_{Bdo} + jV_{Bqo}) \right\} \\ &= G_{mo} A_{1d} \Delta e'_d + G_{mo} A_3 m_o \Delta V_{DC} + G_{mo} A_3 \Delta m V_{DC0} + G_{mo} N_3 \Delta I_{Lq} - B_{mo} A_{1q} \Delta e'_q - B_{mo} A_2 m_o \Delta V_{DC} \\ &\quad - B_{mo} A_2 \Delta m V_{DC0} + B_{mo} N_2 \Delta I_{Ld} + j \left\{ G_{mo} A_{1q} \Delta e'_q + G_{mo} A_2 m_o \Delta V_{DC} + G_{mo} A_2 \Delta m V_{DC0} - G_{mo} N_2 \Delta I_{Ld} \right. \\ &\quad \left. + B_{mo} A_{1d} \Delta e'_d + B_{mo} A_3 m_o \Delta V_{DC} + B_{mo} A_3 \Delta m V_{DC0} + B_{mo} N_3 \Delta I_{Lq} \right\} + \left\{ -j \Delta\delta G_1 + \Delta\delta B_1 + jG_{mo} \Delta\delta V_{Bdo} \right. \\ &\quad \left. - jB_{mo} \Delta\delta V_{Bqo} - B_{mo} \Delta\delta V_{Bdo} - G_{mo} \Delta\delta V - G_{mo} \Delta\delta V_{Bqo} \right\} \end{aligned} \quad (C.34)$$

where

$$G_1 = G_{mo} V_{Bdo} - B_{mo} V_{Bqo}$$

$$B_1 = B_{mo} V_{Bdo} + G_{mo} V_{Bqo}$$

Separating real and imaginary terms in (C.34) we have

$$\begin{aligned} \Delta I_d &= G_{mo} A_{1d} \Delta e'_d + G_{mo} A_3 m_o \Delta V_{DC} + G_{mo} A_3 \Delta m V_{DC0} + G_{mo} N_3 \Delta I_{Lq} - B_{mo} A_{1q} \Delta e'_q \\ &\quad - B_{mo} A_2 m_o \Delta V_{DC} - B_{mo} A_2 \Delta m V_{DC0} + B_{mo} N_2 \Delta I_{Ld} + \Delta\delta B_1 - B_{mo} \Delta\delta V_{Bdo} - G_{mo} \Delta\delta V_{Bqo} \end{aligned} \quad (C.35)$$

$$\begin{aligned} \Delta I_q &= G_{mo} A_1 \Delta e'_q + G_{mo} A_2 m_o \Delta V_{DC} + G_{mo} A_2 \Delta m V_{DC0} - G_{mo} N_2 \Delta I_{Ld} + B_{mo} A_{1d} \Delta e'_d \\ &+ B_{mo} A_3 m_o \Delta V_{DC} + B_{mo} A_3 \Delta m V_{DC0} + B_{mo} N_3 \Delta I_{Lq} + G_{mo} \Delta \delta V_{Bdo} - \Delta \delta G_1 - B_{mo} \Delta \delta V_{Bqo} \end{aligned} \quad (C.36)$$

From (C.35) we have

$$\Delta I_{Ld} = K_1^{-1} \left\{ G_{mo} A_{1d} \Delta e'_d - B_{mo} A_{1d} \Delta e'_q + G_{V1} \Delta V_{DC} + G_{C1} \Delta m + G_{nv} N_3 \Delta I_{Lq} + \Delta \delta B_1 - B_{nv} \Delta \delta V_{Bdo} - G_{mo} \Delta \delta V_{Bqo} \right\} \quad (C.37)$$

$$\Delta I_{Lq} = K_2^{-1} \left\{ G_{mo} A_{1d} \Delta e'_q + B_{mo} A_{1d} \Delta e'_d + G_{V2} \Delta V_{DC} + G_{C2} \Delta m - G_{mo} N_2 \Delta I_{Ld} + G_{nv} \Delta \delta V_{Bdo} - \Delta \delta G_1 - B_{mo} \Delta \delta V_{Bqo} \right\} \quad (C.38)$$

Substituting (C.38) in (C.37)

$$\begin{aligned} \therefore \Delta I_{Ld} &= K_4^{-1} K_1^{-1} (G_{mo} A_{1d} + K_3 B_{mo} A_{1d}) \Delta e'_d + K_4^{-1} K_1^{-1} (K_3 G_{mo} A_1 - B_{mo} A_1) \Delta e'_q \\ &+ K_4^{-1} K_1^{-1} (G_{V1} + K_3 G_{V2}) \Delta V_{DC} + K_4^{-1} K_1^{-1} (G_{C1} + K_3 G_{C2}) \Delta m + K_4^{-1} K_1^{-1} \Delta \delta B_1 - K_4^{-1} K_1^{-1} B_{mo} \Delta \delta V_{Bdo} \\ &- K_4^{-1} K_1^{-1} G_{mo} \Delta \delta V_{Bqo} + K_4^{-1} K_1^{-1} K_3 G_{mo} \Delta \delta V_{Bdo} - K_4^{-1} K_1^{-1} K_3 \Delta \delta G_1 - K_4^{-1} K_1^{-1} K_3 B_{mo} \Delta \delta V_{Bqo} \\ &\therefore \Delta I_{Ld} = Y_{L1} \Delta e'_d + Y_{L2} \Delta e'_q + Y_{L3} \Delta V_{DC} + Y_{L4} \Delta m + w_1 \Delta \delta B_1 - w_2 \Delta \delta V_{Bdo} \\ &- w_3 \Delta \delta V_{Bqo} + w_5 \Delta \delta V_{Bdo} - w_4 \Delta \delta G_1 - w_6 \Delta \delta V_{Bqo} \end{aligned} \quad (C.39)$$

where

$$Y_{L1} = K_4^{-1} K_1^{-1} (G_{mo} A_{1d} + K_3 B_{mo} A_{1d})$$

$$Y_{L2} = K_4^{-1} K_1^{-1} (K_3 G_{mo} A_1 - B_{mo} A_1)$$

$$Y_{L3} = K_4^{-1} K_1^{-1} (G_{V1} + K_3 G_{V2})$$

$$Y_{L4} = K_4^{-1} K_1^{-1} (G_{C1} + K_3 G_{C2})$$

$$w_1 = K_4^{-1} K_1^{-1}$$

$$w_2 = K_4^{-1} K_1^{-1} B_{mo}$$

$$w_3 = K_4^{-1} K_1^{-1} G_{mo}$$

$$w_5 = K_4^{-1} K_1^{-1} K_3 G_{mo}$$

$$w_4 = K_4^{-1} K_1^{-1} K_3$$

$$w_6 = K_4^{-1} K_1^{-1} K_3 B_{mo}$$

By proper matrix manipulations equation (C.39) can be written as

$$\begin{aligned}\Delta I_{Ld} &= Y_{L1}\Delta e'_d + Y_{L2}\Delta e'_q + Y_{L3}\Delta V_{DC} + Y_{L4}\Delta m + (D_1 - D_2 - D_3 - D_4 + D_5 - D_6)\Delta\delta \\ \Delta I_{Ld} &= \{Y_{L1}\Delta e'_d + Y_{L2}\Delta e'_q + Y_{L3}\Delta V_{DC} + Y_{L4}\Delta m + Y_{L5}\Delta\delta\}\end{aligned}\quad (C.40)$$

where

$$Y_{L5} = (D_1 - D_2 - D_3 - D_4 + D_5 - D_6)$$

Substituting (C.40) in (C.38) we have

$$\begin{aligned}\Delta I_{Lq} &= K_2^{-1} \{G_{mo}A_1\Delta e'_q + B_{mo}A_{1d}\Delta e'_d + GV_2\Delta V_{DC} + G_{C2}\Delta m + G_{mo}\Delta\delta V_{Bdo} - \Delta\delta G_1 \\ &\quad - B_{mo}\Delta\delta V_{Bqo}\} - K_2^{-1}G_{mo}N_2 \{Y_{L1}\Delta e'_d + Y_{L2}\Delta e'_q + Y_{L3}\Delta V_{DC} + Y_{L4}\Delta m + Y_{L5}\Delta\delta\}\end{aligned}$$

$$\Delta I_{Lq} = Y_{L6}\Delta e'_d + Y_{L7}\Delta e'_q + Y_{L8}\Delta V_{DC} + Y_{L9}\Delta m + w_8\Delta\delta V_{Bdo} - w_7\Delta\delta G_1 - w_9\Delta\delta V_{Bqo} - K_2^{-1}K_5Y_{L5}\Delta\delta \quad (C.41)$$

By proper matrix manipulations equation (C.41) can be written as

$$\begin{aligned}\Delta I_{Lq} &= Y_{L6}\Delta e'_d + Y_{L7}\Delta e'_q + Y_{L8}\Delta V_{DC} + Y_{L9}\Delta m + (-D_7 + D_8 - D_9 - K_2^{-1}K_5Y_{L5})\Delta\delta \\ \therefore \Delta I_{Lq} &= Y_{L6}\Delta e'_d + Y_{L7}\Delta e'_q + Y_{L8}\Delta V_{DC} + Y_{L9}\Delta m + Y_{L10}\Delta\delta\end{aligned}\quad (C.42)$$

where

$$Y_{L6} = K_2^{-1} (B_{mo} A_{1d} - K_5 Y_{L1})$$

$$Y_{L7} = K_2^{-1} (G_{mo} A_1 - K_5 Y_{L2})$$

$$Y_{L8} = K_2^{-1} (G V_2 - K_5 Y_{L3})$$

$$Y_{L9} = K_2^{-1} (G_{C2} - K_5 Y_{L4})$$

$$w_8 = K_2^{-1} G_{mo}$$

$$w_7 = K_2^{-1}$$

$$w_9 = K_2^{-1} B_{mo}$$

$$Y_{L10} = (-D_7 + D_8 - D_9 - K_2^{-1} K_5 Y_{L5})$$

The currents entering the STATCOM are given by

$$I_s = \frac{V_L - V_o}{jX_{SDT}} \quad (C.43)$$

$$I_s = -jX_{SDT}^{-1} (V_L - V_o)$$

$$I_s = -j \text{inv}X_{SDT} (V_L - V_o) \quad (C.44)$$

where

$$\text{inv}X_{SDT} = X_{SDT}^{-1}$$

Linearising (C.44) we have

$$\Delta I_s = -j \text{inv}X_{SDT} (\Delta V_L - \Delta V_o) \quad (C.45)$$

but

$$V_L = jX_{LB} I_L + V_B \quad (C.46)$$

$$\begin{aligned}
\Delta V_L &= jX_{LB}\Delta I_L + \Delta V_B \\
\Delta V_L &= jX_{LB}(\Delta I_{Ld} + j\Delta I_{Lq}) + (\Delta V_{Bd} + j\Delta V_{Bq}) \\
\Delta V_L &= jX_{LB}\Delta I_{Ld} - X_{LB}\Delta I_{Lq} + \Delta V_{Bd} + j\Delta V_{Bq}
\end{aligned} \tag{C.47}$$

Substituting (C.28) in (C.47)

$$\begin{aligned}
\Delta V_L &= jX_{LB}\Delta I_{Ld} - X_{LB}\Delta I_{Lq} + [A_{1d}\Delta e'_d + A_3[\Delta mV_{DC0} + m_o\Delta V_{DC}] + N_3\Delta I_{Lq}] \\
&+ j[A_1\Delta e'_q + A_2[\Delta mV_{DC0} + m_o\Delta V_{DC}] - N_2\Delta I_{Ld}] \\
\therefore \Delta V_L &= [A_{1d}\Delta e'_d + A_3C_o\Delta V_{DC} + A_3\Delta CV_{DC0} + L_1\Delta I_{Lq}] \\
&+ j[A_1\Delta e'_q + A_2C_o\Delta V_{DC} + A_2\Delta CV_{DC0} + L_2\Delta I_{Ld}]
\end{aligned} \tag{C.48}$$

where

$$\begin{aligned}
L_1 &= (N_3 - X_{LB}) \\
L_2 &= (X_{LB} - N_2)
\end{aligned}$$

Substituting (C.40) and (C.42) in (C.48), we have

$$\begin{aligned}
\Delta V_L &= \{(A_{1d} + L_1Y_{L6})\Delta e'_d + (L_1Y_{L7})\Delta e'_q + (A_3m_o + L_1Y_{LB})\Delta V_{DC} + (A_3V_{DCo} + L_1Y_{L9})\Delta m + (L_1Y_{L10})\Delta \delta\} + \\
&j\{(L_2Y_{L1})\Delta e'_d + (A_1 + L_2Y_{L2})\Delta e'_q + (A_2m_o + L_2Y_{L3})\Delta V_{DC} + (A_2V_{DCo} + L_2Y_{L4})\Delta m + (L_2Y_{L5})\Delta \delta\} \\
\therefore \Delta V_L &= \{V_{L1}\Delta e'_d + V_{L2}\Delta e'_q + V_{L3}\Delta V_{DC} + V_{L4}\Delta m + V_{L5}\Delta \delta\} + j\{V_{L6}\Delta e'_d + V_{L7}\Delta e'_q + V_{L8}\Delta V_{DC} + V_{L9}\Delta m + V_{L10}\Delta \delta\} \tag{C.49}
\end{aligned}$$

where

$$\begin{aligned}
V_{L1} &= (A_{1d} + L_1 Y_{L6}) \\
V_{L2} &= (L_1 Y_{L7}) \\
V_{L3} &= (A_3 m_o + L_1 Y_{LB}) \\
V_{L4} &= (A_3 V_{DCo} + L_1 Y_{L9}) \\
V_{L5} &= (L_1 Y_{L10}) \\
V_{L6} &= (L_2 Y_{L1}) \\
V_{L7} &= (A_1 + L_2 Y_{L2}) \\
V_{L8} &= (A_2 m_o + L_2 Y_{L3}) \\
V_{L9} &= (A_2 V_{DCo} + L_2 Y_{L4}) \\
V_{L10} &= (L_2 Y_{L5})
\end{aligned}$$

Now V_o is given by

$$V_o = mV_{DC} \cos\psi + jmV_{DC} \sin\psi$$

$$V_o = mV_{DC} F_d + jmV_{DC} F_q \quad (C.50)$$

Linearising (C.50), we have

$$\Delta V_o = \{F_d C_o \Delta V_{DC} + F_d V_{DCo} \Delta C\} + j \{F_q C_o \Delta V_{DC} + F_q V_{DCo} \Delta C\} \quad (C.51)$$

Substituting (C.49) and (C.51) in (C.45)

$$\begin{aligned}
\Delta I_s = -j \text{inv} X_{SDT} \left\{ \left[V_{L1} \Delta e'_d + V_{L2} \Delta e'_q + V_{L3} \Delta V_{DC} + V_{L4} \Delta m + V_{L5} \Delta \delta - F_d m_o \Delta V_{DC} - F_d V_{DCo} \Delta m \right] + \right. \\
\left. j \left[V_{L6} \Delta e'_d + V_{L7} \Delta e'_q + V_{L8} \Delta V_{DC} + V_{L9} \Delta m + V_{L10} \Delta \delta - F_q m_o \Delta V_{DC} - F_q V_{DCo} \Delta m \right] \right\} \quad (C.52)
\end{aligned}$$

Separating real and imaginary terms in (C.52)

$$\therefore \Delta I_{sd} = Y_{L01} \Delta e'_d + Y_{L02} \Delta e'_q + Y_{L03} \Delta V_{DC} + Y_{L04} \Delta m + Y_{L05} \Delta \delta \quad (C.53)$$

$$\therefore \Delta I_{sq} = Y_{L06} \Delta e'_d + Y_{L07} \Delta e'_q + Y_{L08} \Delta V_{DC} + Y_{L09} \Delta m + Y_{L010} \Delta \delta \quad (C.54)$$

where

$$\begin{aligned}
Y_{L01} &= \text{inv}X_{SDT} V_{L6} \\
Y_{L02} &= \text{inv}X_{SDT} V_{L7} \\
Y_{L03} &= \text{inv}X_{SDT} (V_{L8} - F_q m_o) \\
Y_{L04} &= \text{inv}X_{SDT} (V_{L9} - F_q V_{DC0}) \\
Y_{L05} &= \text{inv}X_{SDT} V_{L10} \\
Y_{L06} &= (-\text{inv}X_{SDT} V_{L1}) \\
Y_{L07} &= (-\text{inv}X_{SDT} V_{L2}) \\
Y_{L08} &= \text{inv}X_{SDT} (-V_{L3} + F_{dco}) \\
Y_{L09} &= \text{inv}X_{SDT} (-V_{L4} + F_d V_{DC0}) \\
Y_{L010} &= (-\text{inv}X_{SDT} V_{L5})
\end{aligned}$$

(C.53) and (C.54) can be written as

$$\begin{aligned}
\begin{bmatrix} \Delta I_{sd1} \\ \Delta I_{sq1} \\ \Delta I_{sd2} \\ \Delta I_{sq2} \\ \vdots \\ \Delta I_{sqn} \end{bmatrix} &= [Y_{L0N}] \Delta e'_N + [Y_{L0V}] \Delta V_{DC} + [Y_{L0C}] \Delta m + [Y_{L0D}] \Delta \delta \\
\therefore \Delta I_s &= [Y_{L0N}] \Delta e'_N + [Y_{L0V}] \Delta V_{DC} + [Y_{L0C}] \Delta m + [Y_{L0D}] \Delta \delta
\end{aligned} \tag{C.55}$$

where

$$\Delta e'_N = [\Delta e'_{d1} \Delta e'_{q1} \Delta e'_{d2} \Delta e'_{q2} \dots \Delta e'_{qn}]^T$$

The linearized generator currents are given by

$$\begin{aligned}
\Delta I_t &= \Delta I_L + \Delta I_s \\
\Delta I_t &= [Y_{L1} + Y_{L01}] \Delta e'_d + [Y_{L2} + Y_{L02}] \Delta e'_q + [Y_{L3} + Y_{L03}] \Delta V_{DC} + [Y_{L4} + Y_{L04}] \Delta m + [Y_{L5} + Y_{L05}] \Delta \delta \\
&+ j \{ [Y_{L6} + Y_{L06}] \Delta e'_d + [Y_{L7} + Y_{L07}] \Delta e'_q + [Y_{L8} + Y_{L08}] \Delta V_{DC} + [Y_{L9} + Y_{L09}] \Delta m + [Y_{L10} + Y_{L010}] \Delta \delta \}
\end{aligned}$$

$$\Delta I_t = \{Y_1 \Delta e'_d + Y_2 \Delta e'_q + Y_3 \Delta V_{DC} + Y_4 \Delta m + Y_5 \Delta \delta\} + j \{Y_6 \Delta e'_d + Y_7 \Delta e'_q + Y_8 \Delta V_{DC} + Y_9 \Delta m + Y_{10} \Delta \delta\} \quad (\text{C.56})$$

Separating real and imaginary terms in (C.56)

$$\begin{aligned} \therefore \Delta I_{td} &= \{Y_1 \Delta e'_d + Y_2 \Delta e'_q + Y_3 \Delta V_{DC} + Y_4 \Delta C + Y_5 \Delta \delta\} \\ \Delta I_{tq} &= j \{Y_6 \Delta e'_d + Y_7 \Delta e'_q + Y_8 \Delta V_{DC} + Y_9 \Delta C + Y_{10} \Delta \delta\} \end{aligned} \quad (\text{C.57})$$

where

$$\begin{aligned} Y_1 &= [Y_{L1} + Y_{L01}] \\ Y_2 &= [Y_{L2} + Y_{L02}] \\ Y_3 &= [Y_{L3} + Y_{L03}] \\ Y_4 &= [Y_{L4} + Y_{L04}] \\ Y_5 &= [Y_{L5} + Y_{L05}] \\ Y_6 &= [Y_{L6} + Y_{L06}] \\ Y_7 &= [Y_{L7} + Y_{L07}] \\ Y_8 &= [Y_{L8} + Y_{L08}] \\ Y_9 &= [Y_{L9} + Y_{L09}] \\ Y_{10} &= [Y_{L10} + Y_{L010}] \end{aligned}$$

(C.57) can be written as

$$\begin{bmatrix} \Delta I_{td1} \\ \Delta I_{tq1} \\ \Delta I_{td2} \\ \Delta I_{tq2} \\ \vdots \\ \Delta I_{tqn} \end{bmatrix} = [Y_N] \Delta e'_N + [Y_{NV}] \Delta V_{DC} + [Y_{NC}] \Delta m + [Y_{ND}] \Delta \delta$$

$$\Delta I_t = \{[Y_N] \Delta e'_N + [Y_{NV}] \Delta V_{DC} + [Y_{NC}] \Delta m + [Y_{ND}] \Delta \delta\} \quad (\text{C.58})$$

Then

$$\begin{aligned}\Delta \dot{X}_g &= [H_t] \Delta I_t + [D] \Delta X_g + [B_e] \Delta E_{fd} \\ \Delta \dot{X}_g &= [H_t] \left\{ [Y_N] \Delta e'_N + [Y_{NV}] \Delta V_{DC} + [Y_{NC}] \Delta m + [Y_{ND}] \Delta \delta \right\} + [D] \Delta X_g + [B_e] \Delta E_{fd} \\ \therefore \Delta \dot{X}_g &= \left\{ [R_1] \Delta e'_N + [A_V] \Delta V_{DC} + [B_{C1}] \Delta m + [Q_1] \Delta \delta \right\} + [D] \Delta X_g + [B_e] \Delta E_{fd} \quad (\text{C.59})\end{aligned}$$

where

$$\begin{aligned}R_1 &= [H_t] [Y_N] \\ A_V &= [H_t] [Y_{NV}] \\ B_{C1} &= [H_t] [Y_{NC}] \\ Q_1 &= [H_t] [Y_{ND}]\end{aligned}$$

Since $\Delta e'_N$ and $\Delta \delta$ are subsets of ΔX_m , by proper matrix manipulations (C.59) can be written as

$$\Delta \dot{X}_g = [A_m] \Delta X_g + [A_V] \Delta V_{DC} + B_e [\Delta E_{fd}] + [B_{C1}] \Delta m \quad (\text{C.60})$$

Once we add equations for exciter and STATCOM, ΔE_{fd} and ΔV_{DC} in (C.60) forms a part of state vector.

Exciter system

The state equation for the exciter is given by

$$\Delta X_e = [A_e] \Delta X_e + [E] \Delta V_N \quad (\text{C.61})$$

but

$$\Delta V_N = [Z_a] \Delta I_t + \Delta e'_N \quad (\text{C.62})$$

Substituting (C.58) in (C.59)

$$\Delta V_N = \left[\{ [Z_a][Y_N] + 1 \} \Delta e'_N + [Z_a][Y_{NV}] \Delta V_{DC} + [Z_a][Y_{NC}] \Delta m + [Z_a][Y_{ND}] \Delta \delta \right] \quad (\text{C.63})$$

Substituting (C.63) in (C.61) we have

$$\begin{aligned} \Delta X_e &= [A_e] \Delta X_e + [E] \{ [Z_a][Y_N] + 1 \} \Delta e'_N + [E][Z_a][Y_{NV}] \Delta V_{DC} \\ &\quad + [E][Z_a][Y_{NC}] \Delta m + [E][Z_a][Y_{ND}] \Delta \delta \\ \therefore \Delta X_e &= [A_e] \Delta X_e + [R_2] \Delta e'_N + [A_{Ve}] \Delta V_{DC} + [B_{C2}] \Delta m + [Q_2] \Delta \delta \end{aligned} \quad (\text{C.64})$$

where

$$\begin{aligned} R_2 &= [E] \{ [Z_a][Y_N] + 1 \} \\ A_{Ve} &= [E][Z_a][Y_{NV}] \\ B_{C2} &= [E][Z_a][Y_{NC}] \\ Q_2 &= [E][Z_a][Y_{ND}] \end{aligned}$$

Since $\Delta e'_N$ and $\Delta \delta$ are subsets of ΔX_g , therefore by proper matrix manipulations (C.64)

can be written as,

$$\Delta X_e = [A_{me}] \Delta X_m + [A_e] \Delta X_e + [A_{Ve}] \Delta V_{DC} + [B_{C2}] \Delta m \quad (\text{C.65})$$

STATCOM equation

$$\dot{V}_{dc} = \frac{m}{C_{DC}} \left[\cos \psi I_{lod} + \sin \psi I_{loq} \right]$$

$$\dot{V}_{dc} = \frac{m}{C_{DC}} \left[F_d I_{lod} + F_q I_{loq} \right] \quad (\text{C.66})$$

Linearising (C.66) we have,

$$\Delta \dot{V}_{DC} = \begin{bmatrix} \frac{F_d m_o}{C_{DC}} & \frac{F_d m_0}{C_{DC}} \end{bmatrix} \begin{bmatrix} \Delta I_{sd} \\ \Delta I_{sq} \end{bmatrix}$$

$$\Delta \dot{V}_{DC} = [Y_{Lo}] \Delta I_s \quad (C.67)$$

Substituting (C.55) in (C.67)

$$\Delta \dot{V}_{DC} = [Y_{Lo}] \{ [Y_{LON}] \Delta e'_N + [Y_{LOV}] \Delta V_{DC} + [Y_{LOC}] \Delta m + [Y_{LOD}] \Delta \delta \}$$

$$\Delta \dot{V}_{DC} = \{ [Y_{Lo}] [Y_{LON}] \Delta e'_N + [Y_{Lo}] [Y_{LOV}] \Delta V_{DC} + [Y_{Lo}] [Y_{LOC}] \Delta m + [Y_{Lo}] [Y_{LOD}] \Delta \delta \}$$

$$\Delta \dot{V}_{DC} = \{ [R_3] \Delta e'_N + [A_{LOV}] \Delta V_{DC} + [B_{C3}] \Delta m + [Q_3] \Delta \delta \} \quad (C.68)$$

Since $\Delta e'_N$ and $\Delta \delta$ are subsets of ΔX_m , therefore by proper matrix manipulations (C.68)

can be written as,

$$\Delta \dot{V}_{DC} = \{ [A_{L0m}] \Delta X_g + [A_{LOV}] \Delta V_{DC} + [B_{C3}] \Delta m \} \quad (C.69)$$

where,

$$R_3 = [Y_{Lo}] [Y_{LON}]$$

$$A_{LOV} = [Y_{Lo}] [Y_{LOV}]$$

$$B_{C3} = [Y_{Lo}] [Y_{LOC}]$$

$$Q_3 = [Y_{Lo}] [Y_{LOD}]$$

The final state space model of multimachine system with STATCOM can be written as

$$\Delta \dot{X} = [A_{matrix}] \Delta X + [B_{matrix}] \Delta m \quad (C.70)$$

where,

$$[A_{matrix}] = \begin{pmatrix} A_m & B_e & A_v \\ A_{me} & A_e & A_{ve} \\ A_{tom} & 0 & A_{tov} \end{pmatrix}$$

$$[B] = \begin{bmatrix} B_{c1} \\ B_{c2} \\ B_{c3} \end{bmatrix}$$

$$\Delta X = [\Delta e'_{d1} \Delta e'_{q1} \Delta \omega_1 \Delta \delta_1 \cdots \Delta \delta_n \Delta E_{fd1} \Delta E_{fd2} \cdots \Delta E_{fdn} \Delta V_{DC1} \Delta V_{DC2} \cdots \Delta V_{DCn}]'$$

APPENDIX D

MODEL REDUCTION

The theory of model reduction based on balanced realization is briefly outlined in this appendix. Further details on model reduction can be found in [71].

Consider a stable linear time-invariant model (A, B, C) of the standard form

$$\dot{x}(t) = Ax(t) + Bu(t), \quad y(t) = Cx(t) \tag{D.1}$$

Where $x(t) \in \mathbb{R}^n$, $u(t) \in \mathbb{R}^m$ and $y(t) \in \mathbb{R}^p$ are, respectively, the state vector, the input vector and the output vector at time t . The transfer function of the system is given by $G(s) = C(sI - A)^{-1}B$.

It is known that there exist nonsingular transformations T that will transform system (D.1) into the balanced state space representation

$$\dot{x}_b(t) = A_b x_b(t) + B_b u(t), \quad y(t) = C_b x_b(t) \quad (\text{D.2})$$

where $A_b = T^{-1}AT$, $B_b = T^{-1}B$, $C_b = CT$, and $x_b(t) = T^{-1}x(t)$. The controllability and observability gramians of the new system are given by

$$P_b = T^{-1}PT^{-T} \quad (\text{D.3})$$

$$Q_b = T^TQT \quad (\text{D.4})$$

Moreover, those gramians are equal and diagonal with special arrangement as follows:

$$P_b = Q_b = \Sigma = \text{diag}[\sigma_1, \sigma_2, \dots, \sigma_n] \quad (\text{D.5})$$

$$\sigma_1 \geq \sigma_2 \geq \dots \geq \sigma_n > 0 \quad (\text{D.6})$$

The σ_i called the Hankel singular values of the system are determined by

$$\sigma_i = (\lambda_i(PQ))^{\frac{1}{2}} \quad (\text{D.7})$$

where $\lambda_i(PQ)$ denotes the i^{th} eigen value of PQ , and P, Q are determined by the Lyapunov equations

$$PA^T + AP = -BB^T \quad (\text{D.8})$$

$$QA + A^T Q = -C^T C \quad (D.9)$$

An efficient algorithm for the computation of a balanced representation developed by Laub et. Al. is summarized as follows:

1. Use equations (D.8) and (D.9) to find the controllability and observability gramians.
2. Compute Cholesky factors of the gramians:

Let L_r and L_o denote the lower triangular Cholesky factors of gramians P and Q , i.e.,

$$P = L_r L_r^T, \quad Q = L_o L_o^T \quad (D.10)$$

3. Compute singular value decomposition of the product of the Cholesky factors:

$$L_o^T L_r = U \Sigma V^T \quad (D.11)$$

4. Form the balancing transformation

$$T = L_r V \Sigma^{-1/2} \quad (D.12)$$

5. Form the balanced state-space matrices

$$A_b = T^{-1} A T \quad (D.13)$$

$$B_b = T^{-1} B \quad (D.14)$$

$$C_b = C T \quad (D.15)$$

To obtain a reduced-order model, let the balanced system (D.2) be partitioned as

$$\begin{bmatrix} \dot{x}_{b1} \\ \dot{x}_{b2} \end{bmatrix} = \begin{pmatrix} A_{11} & A_{12} \\ A_{21} & A_{22} \end{pmatrix} \begin{bmatrix} x_{b1} \\ x_{b2} \end{bmatrix} + \begin{bmatrix} B_1 \\ B_2 \end{bmatrix} u \quad (D.16)$$

$$y = [C_1 \ C_2] \begin{bmatrix} x_{b1} \\ x_{b2} \end{bmatrix} \quad (D.17)$$

where the vector $x_{b1} \in \mathbb{R}^r$ contains the most controllable and observable states and the vector $x_{b2} \in \mathbb{R}^{n-r}$ contains the least controllable and observable states. Also, let Σ be partitioned in a similar way:

$$\Sigma = \begin{pmatrix} \Sigma_1 & 0 \\ 0 & \Sigma_2 \end{pmatrix} \quad (D.18)$$

where

$$\Sigma_1 = \text{diag}[\sigma_1, \dots, \sigma_r]$$

and

$$\Sigma_2 = \text{diag}[\sigma_{r+1}, \dots, \sigma_n]$$

if $\sigma_r / \sigma_{r+1} \gg 1$, then the subsystem

$$\dot{x}_{br}(t) = A_{11}x_{br}(t) + B_1u(t) \quad (D.19)$$

$$\hat{y}(t) = C_1x_{br}(t) \quad (D.20)$$

is the reduced-order model of the full-order balanced system which will contain only the most controllable and most observable parts of the system. If $\sigma_r \neq \sigma_{r+1}$, then the reduced-order balanced system (A_{11}, B_1, C_1) is stable, controllable and observable.

REFERENCES

- [1] G.W.Stagg and A.H.EL-abaid, “Computer methods in power systems (New york hills, 1968).
- [2] P.K. Padiyar,“ Power system stability and control” EPRI Power system series 1994.
- [3] P.M. Anderson and A.A.Fouad, “Power system control and stability”, Iowa state university press, 1980.
- [4] Kimbark, “ Power system stability” , vol. 1
- [5] Y.N. YU, “Electric power system dynamics”, Academic press 1983.
- [6] E.Lerch, D.Porh and L.XU, “Advanced SVC control for damping power system oscillations”, 1991.
- [7] N.Mithulananthan, C.A Canizares, J.Reeve and G.J.Rogers, “Comparison of PSS, SVC and STATCOM controllers for damping power system oscillations”. IEEE transactions on power systems, vol. 18, no.2, pp 786-792, May 2003.

- [8] A.M.Stankovic, P.C.Stefanov, G.Tadnor and D.J.Somajic, "Dissipativity as a unifying control design framework for suppression of low frequency oscillations in power systems". IEEE transaction on power system vol.14, no.1, pp 192-199 February 1999.
- [9] J.Chen, J.V.Milanovic, F.M.Huges, "Selection of auxiliary input signal and location of SVC for damping electro-mechanical oscillations". IEEE transactions on power system vol. pp 623-627 2001.
- [10] D.N.Koterev, C.W.Taylor and W.A.Mittlestadt, "Model validation for August 10, 1996 WSCC system outage". IEEE transactions on power systems vol. 14, pp 967-979, August 1999.
- [11] N.mithlananthan and S.C.Srivastva, "Investigation of voltage collapse in srilanka's power system network". In proc EMPD Singapore, pp 47-52, March 1995, IEEE catalog 98 EX 137.
- [12] Demello, P.J.Molan, T.F.Laskowski, J udrill, "Co-ordinated application of stabilizers in multi-machine systems". IEEE transaction on PAS, vol. PAS -99, pp 892-902, 1980.
- [13] Demello and C.Concordia, "Concepts of synchronous machine stability as affected by Excitation control". IEEE trans power APP and systems, vol. PAS 103, no 8, pp 1983-1989, 1984.
- [14] H.M.Al-Asooly, "Active and reactive power control of SMES units for power system Transient Improvement", A thesis submitted to university of Bahrain, 1995.

- [15] Laszlo Gyugi, "converter based facts controller", IEE colloquium on FACTS pages 1-11, November 23, 1998.
- [16] Y.H.Song, A.T.John, "Flexible A.C. transmission systems", IEE power energy series 30, 1999.
- [17] N.G.Hingoroni, "Flexible AC transmission system". Fifth IEE international conference on AC and DC transmission (IEE-pub. no 345), pp 1-7 September 1991.
- [18] N.G.Hingoroni, "Flexible AC transmission systems", IEEE spectrum (40-45) April 1993.
- [19] N.G.Hingoroni, "FACTS technology and opportunities IEEE colloquium". (Digest no. 1994/OCS) "FACTS the key to increased utilization of power system", pp 4/1-4/10, Jan 1994.
- [20] M.F.Kandlawala, "Investigation of dynamic behavior of power system installed with STATCOM", A thesis submitted to university of King Fahd University of Petroleum and Minerals, December 2001.
- [21] M.F.Kandlawala and A.H.M.A.Rahim, "Power system dynamic performance with STATCOM controller". 8th annual IEEE technical exchange meeting, April 2001.
- [22] A.H.M.A.Rahim, S.A.Al-Baiyat, F.M.Kandlawala, "A robust STATCOM controller for power system dynamic performance enhancement" IEEE PES Summer Meeting, Vancouver, pp.887-892, July 2001.
- [23] J. Machowski, "Power system dynamic and stability", John Wiley and Sons 1997.

- [24] K.V.Datil, J.Senthil, J.Jiang and R.M.Mathur, "Application of STATCOM for damping torsional oscillations in series compensated AC systems", IEEE transactions on energy conversion, vol. 13.no 3, pp 237-243, September 1998.
- [25] D.Shen, XU Liang and Y.Hani, "A modified per unit STATCOM model and analysis of open loop response time", IEEE proceedings pp 2624-2629, 2000.
- [26] C.A.Canizares, M.Pozzi and S.Corzi, "STATCOM modelling for voltage and angle stability studies", Electric power and energy systems, 2003.
- [27] K.R.Padiyar and A.M. Kulkarni, "Analysis and design of voltage control of static condenser", IEEE conference on power electronics, drives and energy systems for industrial growth 1, pp 393-398, 1996.
- [28] P.Petitclair, S.Bacha and J.Progon, Averaged modelling and non-linear control of an ASVC (advanced static var compensator). IEEE power electronics specialist conference 1, pp 753-758, 1996.
- [29] Y.YU, Chen, H.Yimgoduo, "STATCOM modelling and analysis in damping power system oscillations", Energy conversion engineering conference and exhibit, 2000. (IECEC) 35th intersociety volume 2, 24-28 July 2000, page(s) 756-762 vol.2.
- [30] M.J.Lanternberg, M.A.Pai and K.R.Padiyar, "Hopf bifunction control in power system with static var compensators", international journal of power energy system vol. 19, no 5, pp 339-347, 1997.

- [31] Z.Yao, P.Kesimar, N.lacchivin and V.rajagopalan, “Nonlinear control for STATCOM based on differential algebra”, IEEE specialist conference 1, pp 323-334, 1998.
- [32] Lichun, J.Qifong and Wang Zhongong, “Study of STATCOM control for power swings damping improvements”, IEEE transactions pp 535-540, 2000.
- [33] H.F.Wang and F.Li, “Design of STATCOM multivariable sampled regulator”, IEEE conference on electric utility deregulation and power technologies, April 2000.
- [34] Y.Ni and L.O.Mak, “Fuzzy logic damping controller for FACTS devices in interconnected power systems”. Proceedings of IEEE international symposium as circuits and systems, 5, pp 591-594, 1999.
- [35] B.K.Keshavan and M.Prabhu, “Damping of sub synchronous oscillations using STATCOM – A FACTS Device”, Transmission and Distribution conference and exposition, 2001 IEEE/PES volume 1, 28 Oct-2 Nov. 2001, page(s) 1-7. vol.1.
- [36] P.W.Lenh and M.R.IRavani, “Experimental evaluation of STATCOM closed loop dynamics”. IEEE transactions on power delivery, pp 1378-1384, October 1998.
- [37] Li Wang and Z Y Tsai, “Stabilization of generator oscillations using PID STATCOM Damping controllers and PID power system stabilizers”, IEEE Transactions on systems, man & cybernetics, part B volume 27, issue 1, Feb.1997 page(s):55-67.
- [38] T.Kando, A.Yokomaa, M.Goto , H.Konishi, M.Sekoguchi and Q.Liu, “ Power system transient stability enhancement by STATCOM with nonlinear control

- system”. International conference on power system technology, Proceedings POWERCON 2002. Volume 3, 13-17 oct.2002, page(s) 1908-1912 vol.3
- [39] H.F. Wang, “Selection of installing locations and feedback signals of FACTS based stabilizers in multimachine power system”, IEE proceeding in generation, transmission and distribution, vol. 144,no.3, may 1997.
- [40] Guohong Wu, A.Yokoyama, J.He and Y.Yu, “Allocation and control of FACTS devices for steady state stability enhancement of large scale power system”, pp 357-361, International conference on power system technology 1998, Proceedings. POWERCON ‘98’ volume 1, 18-21 Aug.1998 page(s) 357-361. vol. 1
- [41] M.Ishimarer, R.Yokoyama, G.Shirai and Kwang Y.Lee, “Allocation and design of robust TCSC controllers based on power system stability index”, Power engineering society winter meeting, 2002 IEEE, volume 1, 27-31 Jan. 2002, page(s) 573-578 vol.1
- [42] H.F.Wang, “Selection of robust installing location and feedback signals of FACTS based stabilizers in multimachine power systems”; IEEE transaction on power system, vol. 14, no.2, pp 6234-6242 May 1999.
- [43] A.R.Messina and M.Nayebzadeh, “An efficient algorithm of multiple controllers for damping power system oscillations”, Power engineering society summer meeting, IEEE volume 2, 18-22 July 1999, page(s) 1280-1285, vol.2
- [44] M.H.Haque, “Optimal location of shunt FACTS devices in long transmission lines”, IEE proceedings on generation, transmission and distribution, vol. 147, no.4, pp 679 – 686, July 2000.

- [45] S.N.Singh, "Location of FACTS devices for enhancing power systems security", pp 162-166, Large engineering systems conference on power engineering, 2001, LESCOPE 2001. 11-13 July 2001, page(s): 102-110.
- [46] S.Gerbex, R.Cherkauri and A.J.Germond, "Optimal location of multi-type FACTS devices in power system by means of genetic algorithm", IEEE transactions on power system, vol. 16, pp 537-544, August 2001.
- [47] L.Gyugi, "Dynamic compensation of AC transmission lines by solid state synchronous voltage sources", IEEE transactions on power delivery, vol. 9 no.2, April 1994, pp 904-911.
- [48] L.O.Mak, Y.X.Ni and C.M.Shen, "STATCOM with fuzzy controller for interconnected power systems", Electric power system research, August 1999, pp 87-95.
- [49] H.F.Wang, "Applications of damping torque analysis to STATCOM control". Electric power and energy systems 22, 2000, pp 197-204.
- [50] N.C.Sahoo, B.K.Panigrahi, P.K.Dash, G.Panda, "Application of multivariable feedback linearization scheme for STATCOM control", Electric power system research 62, 2002, pp 81-91.
- [51] E.V.Lausen, J.H.Chow, "Concepts for design of FACTS controllers to damp power swings", IEEE trans on power systems vol. 16, no.2, May 1995, pp 948-956
- [52] L.Chun, J.Qirong, W.Zhonghong, "Study of STATCOM control for power swings damping improvement", Power engineering society winter meeting, 2000 IEEE, volume 4, 23-27. Jan. 2000 page(s): 2630-2635.

- [53] F.liu, S.Mci, Q.Lu, Y.Ni, F.F.Wu, A.Yokoyama, "The non-linear internal control of STATCOM: theory and application", *Electric power and energy systems* 25, 2003, pp 421-430.
- [54] Q.Lu, F.Liu, S.Mei, M.Goto, "Non-linear disturbance attenuation control for statcom", *Power engineering society winter meeting, 2001, IEEE volume 3*, 28 Jan-1 Feb. 2001, page(s) 1323-1328, vol.3
- [55] Y.S.Lee, S.Y.Sun, "STATCOM controller design for power system stabilization with suboptimal control and strip pole assignment", *Electric power and energy systems* 24, 2002, pp 771-779.
- [56] S.Morris, P.K.Dash, K.P.Basu, "A fuzzy variable structure controller for STATCOM", *Electric power system research* 65, 2003, pp 23-34.
- [57] L.O.Malik , Y.X.Ni, C.M.Shen, "STATCOM with fuzzy controllers for interconnected power systems", *Electric power system research* 55, 2000 pp 87-95.
- [58] H.F.Wang, "Phillips-Hefron model of power systems installed with STATCOM and applications", *IEE proceedings on generation, transmission and distribution*, vol. 146, no.5, September 1999, pp 521-527.
- [59] K.Abdulla Tosh, "Development of robust control algorithms for static var compensators in multimode systems", A PhD thesis submitted to Washington state university, 1992.
- [60] K.R.Padiyar, V.Swayam Prakash, "Tuning and performance evaluation of damping controller for a STATCOM", *Electric power and energy systems* 25, 2003, pp 155-166.

- [61] Farasangi M.M, Song Y.H, Sun Y.Z, “Supplementary control design of SVC and STATCOM using H_{∞} optimal robust control” IEEE proceeding April 2000, pp 355-360.
- [62] Ammari.S, Besanger.Y, Hadjsaid.N, George.D, “Robust solutions for the interaction phenomena between dynamics loads and FACTS controllers”, IEEE power engineering society summer meeting, July 2000, pp 401-406.
- [63] Kennedy J. and Eberhart R, “ Particle swarm optimization”, IEEE international conference on neural networks, vol. 4, pp 1942-1948, 1995.
- [64] yuhui Shi, Russell C Eberhart, “ Emperical study of PSO”, Proceedings of the 2001 congress on Evolutionary computation, 2001. Volume 1, 27-30, May 2001 page(s): 81-86. vol. 1
- [65] Ali T. Al-Awami, “Design of robust PSS and FACTS-based controllers for stability enhancement of power systems”, A thesis submitted to University of King Fahd University of Petroleum and Minerals, June 2004.
- [66] L.B. Zhang, C.H.Zhou, X.U. Liu, Z.Q. Ma, M.Ma and Y.C.Liang, “Solving multiobjective optimization problems using particle swarm optimization”, The 2003 congress on evolutionary computation 2003, CEC '03. Volume 4, 8-12 Dec. 2003, page(s):2400-2405. vol.4
- [67] Kennedy J, “The particle swarm optimization: social adaptation of knowledge”, International conference of evolutionary computation, Indianopots April 1997, pp 303-308.

- [68] yuhui Shi, Russell C Eberhart, “ A modified particle swarm optimizer”, proceedings of IEEE international conference on evolutionary computation, Anchorage, May 1998, pp 69-73.
- [69] J.C. Doyle, B.A.Francis and A.R.Tannenbaum, “Feed back control theory”, Macmillan publishing Co. 1992.
- [70] Neil M.Cumbria “Robust controlled flux estimation for indirect field oriented control induction motor drives”, A thesis submitted to University of Calgary, Alberta Canada, April 1998.
- [71] S.A.Al – Baiyat and M. Bettayeb, “Application of recent model reduction techniques to nuclear reactors”, International journal of modeling and simulation, Vol. 14, No. 2, 1994.

Vitae

- Syed Faizullah Faisal
- Born in Hyderabad, India on 18th April 1978
- Received Bachelor of Technology in Electrical and Electronics Engineering from Jawaharlal Nehru Technological University, Hyderabad, India, June 2001
- Completed Master of Science in Electrical Engineering from King Fahd University of Petroleum and Minerals, Dhahran, Saudi Arabia, March 2005.

Publications

- S.F.Faizullah, Zakariya Al-Hamouz, “Application of particle swarm optimization for optimal reactive power planning”, accepted in international journal of control and artificial intelligence, March 2005.
- S.F.Faizullah , A.H.M.A. Rahim and J.M. Ba-Khashwain, “Robust STATCOM controller design using PSO based automatic loop-shaping procedure”, accepted in 2005 IEEE conference on control applications, Toronto Canada.
- S.F.Faizullah and A.H.M.A. Rahim, “A robust STATCOM controller for damping enhancement of multi-machine power system”, accepted in 7-th international power engineering conference IPEC 2005, Singapore.